



ISSN 1349-113X  
JAXA-SP-06-014

# 宇宙航空研究開発機構特別資料

## JAXA Special Publication

---

宇宙航空研究開発機構 情報・計算工学センター  
衛星環境プラズマ数値シミュレーションワークショップ  
報告書

情報・計算工学センター

2007年2月

宇宙航空研究開発機構  
Japan Aerospace Exploration Agency



JAXA-SP-06-014

宇宙航空研究開発機構特別資料

JAXA Special Publication

宇宙航空研究開発機構 情報・計算工学センター  
衛星環境プラズマ数値シミュレーションワークショップ  
報告書

JAXA/JEDI Workshop on  
Numerical Plasma Simulation for Spacecraft  
Environment

作成元 情報・計算工学センター

Prepared by

JAXA's Engineering Digital Innovation Center

2007年2月

February 2007

宇宙航空研究開発機構

Japan Aerospace Exploration Agency



## はじめに

平成 17 年度に JEDI(情報・計算工学センター)が発足し、これまで宇宙プラズマ物理解析に威力を発揮してきたプラズマシミュレーションを衛星機器の技術開発、衛星環境アセスメントなど工学的な分野に応用することが求められています。この要求に対し JEDI では、宇宙機と周辺宇宙プラズマの相互作用を模擬する「衛星環境プラズマ数値シミュレータ」の基礎開発を平成 18 年度から開始することになりました。本シミュレータでは、Particle-In-Cell(PIC)手法をプラズマ解法のコアエンジンとして採用し、これに衛星モデリングを組み合わせることによって衛星近傍でのプラズマ現象およびそれによる衛星環境への影響を定量的に解析することを目指します。特にイオン・電子ダイナミクスも含むプラズマの非定常過程の解析に本シミュレータは本領を発揮します。これを踏まえ、まず取り組むべき対象としては、小惑星探査衛星「はやぶさ」に搭載されて成功をおさめたイオン推進エンジンなど衛星からの能動的プラズマ噴射に関連した衛星環境アセスメントが考えられます。

そこで平成 18 年 10 月 2 日～3 日 JAXA 汐留分室にて、「衛星環境プラズマ数値シミュレータ」に期待される解析対象、取り込むべき技術などに関するワークショップを開催しました。まず初日には、米国バージニア工科大学から Joseph Wang 博士を迎え、イオンエンジンプラズマプルーム数値シミュレーション、コンタミ解析、イオン加速グリッド損耗解析などのこれまでの研究成果の紹介、現在の米国での研究動向、最新の数値手法などについて講演をいただきました。これに続き、本基礎開発プロジェクトの紹介、同じく本年度から開始される JEDI イオンエンジングリッド損耗解析ツール開発の紹介、衛星帯電解析ツール(MUSCAT)とプルーム解析への応用、最新のプラズマシミュレーション手法に関する講演をいただきました。2 日目は、新規宇宙航行システムとして検討が進められている磁気プラズマセイル(MPS)に関する数値シミュレーションに関連する講演を行っていただきました。

本ワークショップは、本基礎開発のキックオフ的な集まりであり、Wang 博士を含めお集まりいただいた関連研究者間で活発なご議論いただき、大変実りあるワークショップになりました。ここにご参加いただいた方々に感謝の意を表します。本基礎開発を発展させ、将来的には、イオンエンジン、プラズマコンタクターなどプラズマをアクティブに利用した推進系、帯電緩和技術などの技術開発、磁気プラズマセイルなど新規航行技術開発に関する大規模プラズマシミュレーションを本格的に行い、JAXA 宇宙プロジェクトの推進に貢献することをめざします。皆様方には今後とも引き続きご指導いただきたく思いますのでなにとぞよろしくお願い申し上げます。

最後に、お忙しい中、講演と報告書原稿をご準備いただいた各講演者の方々に、心より御礼申し上げます。

ワークショップ発起人

臼井英之(京都大学)

篠原育(JAXA)

上田裕子(JAXA)



## ワークショップ参加者

(順不同、敬称略)

Joseph Wang	Virginia Polytechnic Institute and State University, USA
百武 徹	岡山大
宮坂 武志	岐阜大
村中 嵩信	九工大
梶村 好宏	九州大
山川 宏	京大
三宅 洋平	京大
中本 成洋	京大
今里 康二郎	京大
南 祐一郎	京大
大津 広敬	静岡大
村岡 竹織	首都大学東京
石川 久	首都大学東京
佐高 大地	東大
横田 茂	東大
西田 浩之	東大
中野 正勝	都立航空高専
中村 匡	福井県立大
藤野 将生	リヴェールラボラトリ
大谷 洋	リヴェールラボラトリ
杉山 徹	JAMSTEC/ESC
船木 一幸	JAXA/ISAS
国中 均	JAXA/ISAS
大川 恭志	JAXA/ISAS
真志取 秀人	JAXA/総研
仁田 工美	JAXA/総研
清水 和弥	JAXA/JEDI
臼井 英之	京大
篠原 育	JAXA/ISAS
上田 裕子	JAXA/JEDI





## 目次

Particle-in-Cell Simulations for Ion Propulsion Applications	...1
J. Wang (Virginia Polytechnic Institute and State University, USA)	
JAXA/JEDI Project on the Development of Plasma Simulator for Spacecraft Environment	...28
H. Usui (Kyoto Univ.), I. Shinohara (JAXA/ISAS), H. O. Ueda (JAXA) and M. Okada (NIPR)	
Development of Grid-Life Evaluation Tool for Ion Engines	...35
H. Kuninaka (JAXA/ISAS)	
Numerical Simulations of Ion Beam Optics and Grid Erosion for Ion Engine Systems	...45
M. Nakano (Tokyo Metropolitan College of Aeronautical Engineering)	
MUSCAT Project and its Application to Plasma Plume Analysis	...55
T. Muranaka, S. Hatta, J. Kim, S. Hosoda, M. Cho(Kyusyu Institute of Technology), H. O. Ueda, K. Koga and T. Goka(JAXA)	
Development of Macro-Micro Interlocked Simulation Algorithm	...78
T. Sugiyama and K. Kusano(Earth Simulator Center)	
Microscopic Plasma Simulation using Numerical Calculation Accelerator "GRAPE-6"	...89
M. Fujino, H. Otani (Reveal Laboratory, Inc.), I. Shinohara (JAXA/ISAS), H. Usui (Kyoto Univ.)	
Research of Magneto Plasma Sail (MPS) : A Quick Review	...100
I. Funaki and H. Yamakawa (JAXA/ISAS)	
MHD Study on Pure Magnetic Sail	...111
H. Nishida (U. of Tokyo)	
Current Status of MHD Simulation for Magneto Plasma Sail	...122
H. Otsu (Shizuoka Univ.)	
Numerical Simulation of Magneto Plasma Sail by using 3D Hybrid Code	...134
Y. Kajimura (Kyushu Univ.)	



## Particle-in-Cell Simulations for Ion Propulsion Applications

Joseph Wang

Department of Aerospace & Ocean Engineering  
Virginia Polytechnic Institute and State University  
Blacksburg, VA 24061-0203  
jowang@vt.edu

This paper presents an overview on some recent advances in particle simulation modeling of ion propulsion. We first discuss two new particle simulation algorithms designed to handle complex boundary conditions accurately while maintaining the computational speed of the standard PIC code.

The first is the parallel, three-dimensional immersed-finite-element particle-in-cell (IFE-PIC) algorithm. Domain decomposition is used in both field solve and particle push to divide the computation among processors. It is shown that the parallel IFE-PIC achieves a high parallel efficiency of >90%. The second is the hybrid IFE-PIC (HG-IFE-PIC) algorithm, extended from IFE-PIC to further reduce the computation time and memory requirement for simulations involving non-uniform plasmas. In HG-IFE-PIC, the meshes used by the IFE field solve and PIC are decoupled and the IFE mesh is stretched according to local potential gradient and plasma density. It is shown that the HG-IFE-PIC can achieve approximately the same accuracy as IFE-PIC. Both the parallel IFE-PIC and HG-IFE-PIC are applied for ion thruster plume modeling and ion optics plasma flow modeling. We next present two simulation studies. The first concerns multiple ion thruster plume interactions for a realistic spacecraft and plume contamination on solar array. The second concerns the simulation of whole sub-scale ion optics gridlet and accelerator grid impingement current. Finally, we present an ongoing research on the development of simulation based design tool. The unsolved issues and future directions in ion propulsion modeling are also discussed.



---

# Particle-in-Cell Simulations for Ion Propulsion Applications

**Joseph Wang**

**Department of Aerospace and Ocean Engineering  
Virginia Polytechnic Institute and State University**



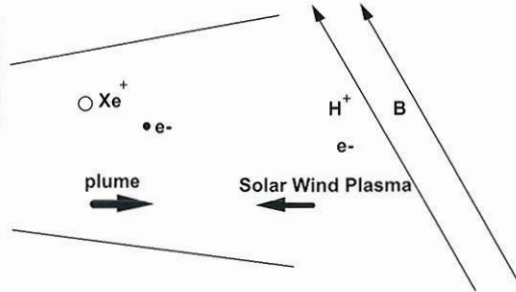
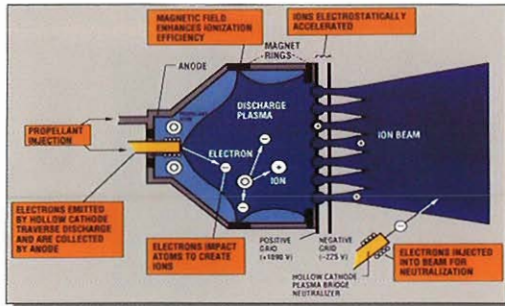
## Outline

---

- **I. Introduction and Background**
- **II. Simulation Approach**
- **III. Ion Thruster Plume Modeling**
- **IV. Ion Optics Modeling**
- **V. Simulation Based Design Tool**
- **VI. Summary and Conclusions**



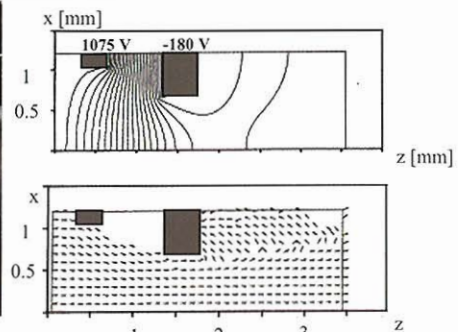
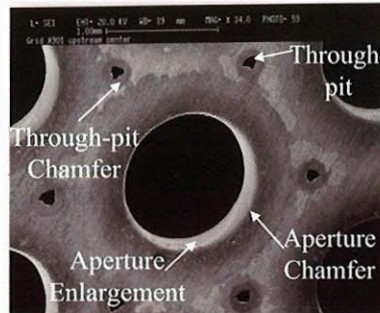
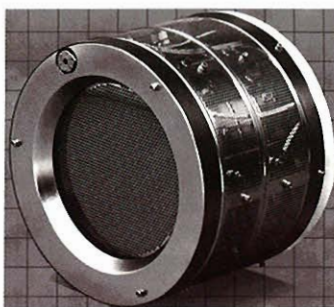
# I. Introduction and Background



- Flow Species: (IPS ionizes 80% to 90% of xenon in discharge chamber)
  - beam ions:  $O(10^3)eV$ ; un-ionized neutrals:  $O(0.01)eV$ ; electrons:  $O(1)eV$
  - charge-exchange xenon ions:  $O(0.01)eV$
$$Xe^+_{beam} + Xe^0_{thermal} \longrightarrow Xe^0_{beam} + Xe^+_{CEX}$$
  - sputtered grid material
- Flow Characteristics:
  - inside optics/near spacecraft: **electrostatic, “space-charge” flow**
  - far from spacecraft: **electromagnetic, quasi-neutral flow**
  - ion flow **“collisionless”**



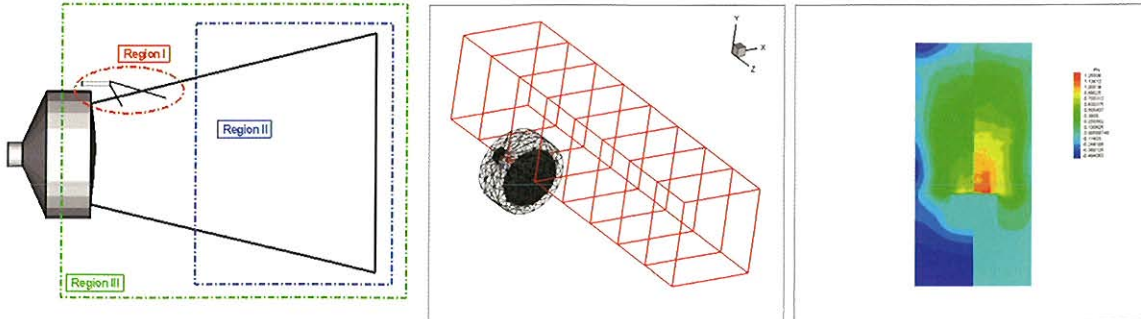
## Plasma Interaction Problem I: Ion Optics Plasma Flow & Grid Erosion



- The behavior of the accel grid current defines the operation envelop of an ion optics system
- Impingement of beam ions and CEX ions cause grid erosion, the primary factor that limits the service life of an thruster
  - Structural failure due to grid erosion from CEX ions
  - Electron backstreaming due to enlargement of grid holes from erosion
- Current modeling status:
  - Many ion optics models (designed for “local” aperture simulations) exist
  - An ion optics model designed for whole grid simulation was also developed recently (Kafafy and Wang, 2006)



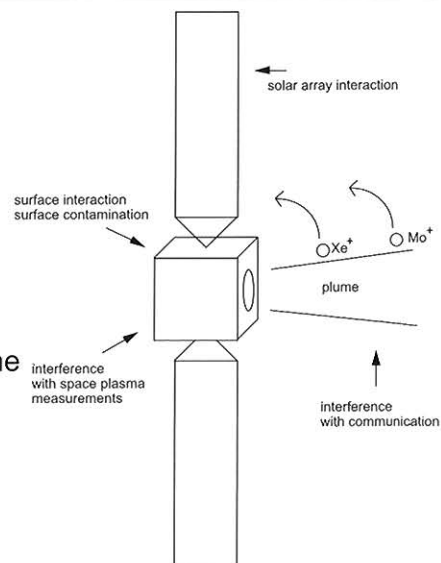
### Plasma Interaction Problem II: Near-Thruster Beam Interactions



- While ion beam neutralization is readily achieved in experiments, the detailed physics in the near thruster region is still not well understood.
- Current modeling status:
  - Few simulation model exists for near-thruster interaction
    - Full particle PIC simulations using realistic ion/electron mass ratio were carried out for scaled-down thruster models (Wang et al., 2005)
  - Near-thruster simulation remains a significant challenge



### Plasma Interaction Problem III: Plume-Spacecraft Interactions

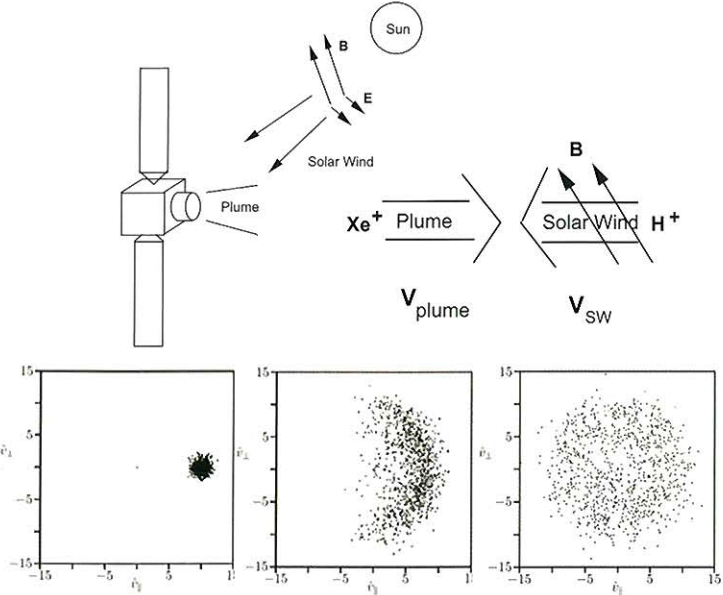


- Low energy ions ( $Xe^+$  and  $Mo^+$ ) produced in the plume can backflow to interact with spacecraft
  - $Xe^+$  plasma dominates local plasma environment, affects spacecraft charging and plasma measurements
  - $Mo^+$  contaminates spacecraft surface
- Current modeling status:
  - Many ion thruster plume models (most designed for simplified spacecraft) exist
  - New simulation algorithms and parallel computing techniques are being applied to perform more realistic simulation (Wang et al., 2006)



### Plasma Interaction Problem IV: Plume-Solar Wind Coupling

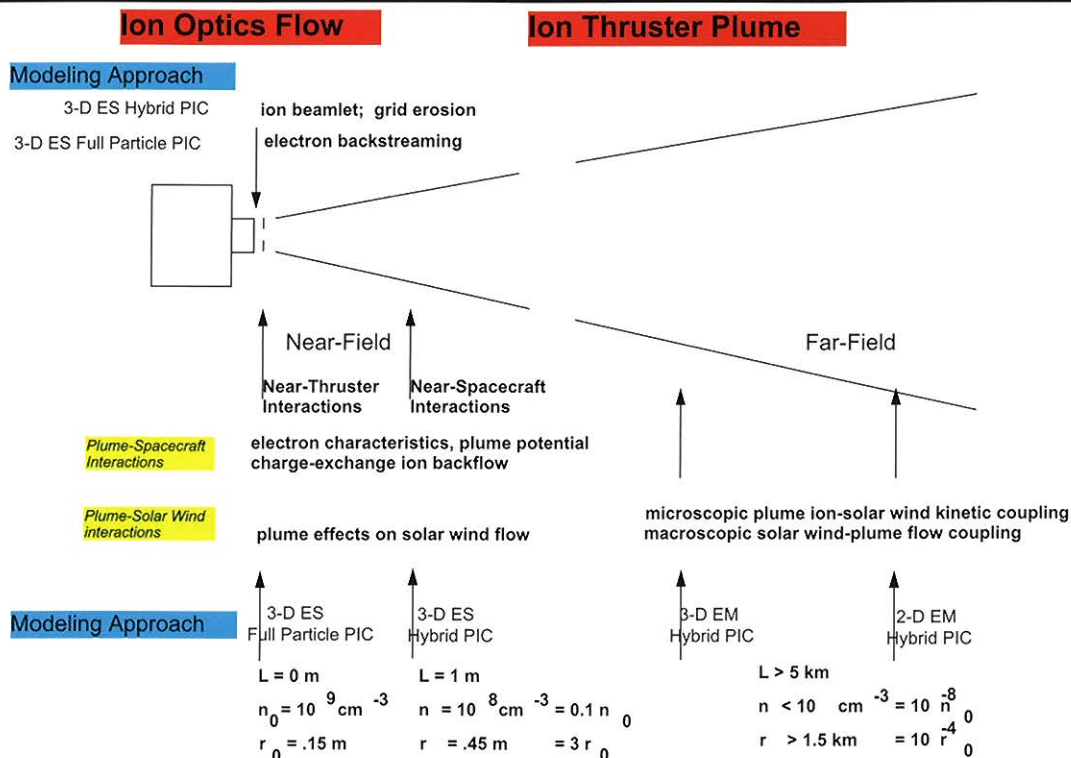
- Thruster produced ions may couple with the solar wind plasma via several mechanisms:
  - Particle/particle coulomb collisions (negligible)
  - Cyclotron pickup
  - Wave particle interactions
- Current modeling status:
  - Hybrid simulations were carried out on coupling by wave-particle interactions (Wang et al., 1999)
  - This problem is primarily of theoretical interest



Solar wind proton pickup through electromagnetic heavy ion-proton instabilities



### Overview of EP Interaction Modeling at Virginia Tech





## II. Particle Simulation Approach

---

- There have been significant progress in ion propulsion modeling and simulation in recent years
  - Particle-in-cell has become standard modeling algorithm
  - Numerous PIC based models have been developed for ion thruster plume and ion optics
- **Status:** Computational time/cost & computer memory restrict the application of particle simulation to small scale problems and simplified spacecraft model
  - Plume simulations typically use simplified spacecraft configuration
  - optics simulations concern single aperture
  - most use simplified model for electrons
  - almost all use small domain...etc
- **Challenge:** Accuracy and computational speed present conflicting requirements for large-scale PIC simulations involving complex object boundary
  - Accuracy requires the use of tetrahedral cell based or unstructured mesh to body fit the boundary to solve the electric field
    - Very expensive for particle push
  - Computing speed requires the use of structured, preferably Cartesian, mesh to push particles
    - May lose accuracy in field solve in the vicinity of boundary



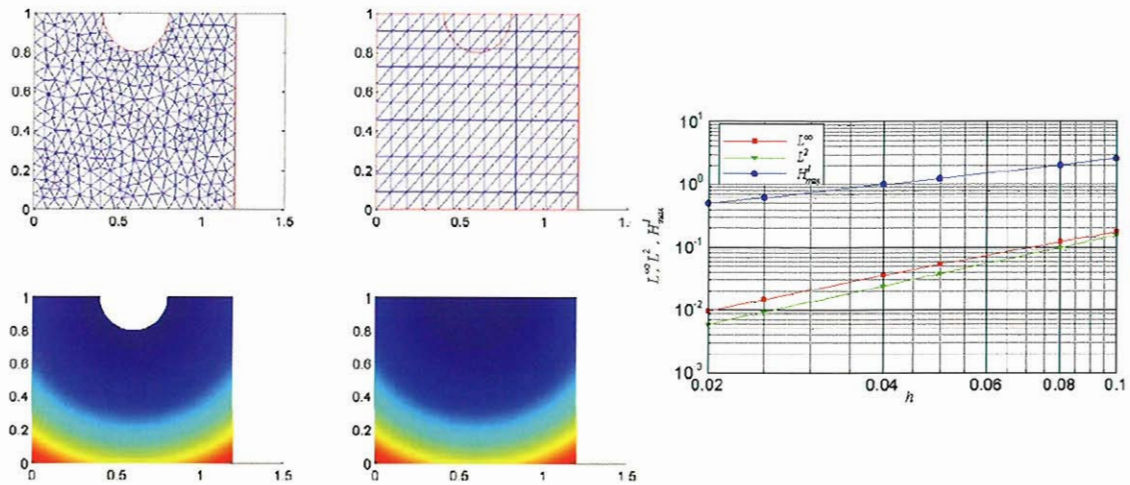
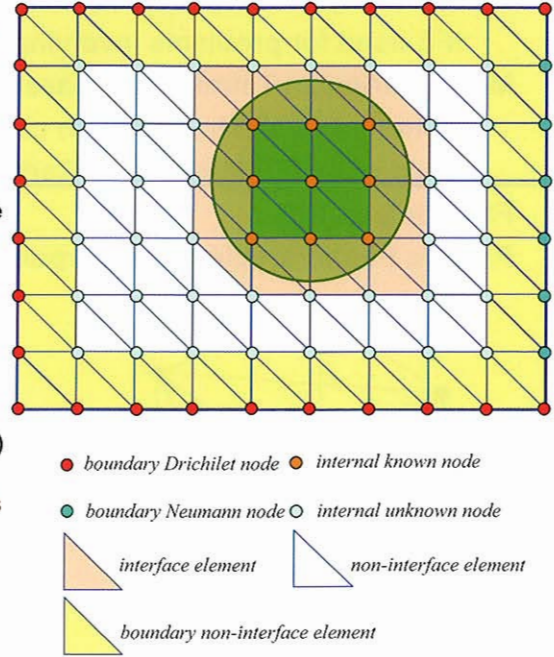
- 
- Existing parallel PIC algorithms:
    - All use domain decomposition
    - Most use either fast Fourier transform (FFT) or a local, non-iterative method (such as finite-difference time-domain or discrete-volume time-domain)
    - Efficient parallel PIC codes have been developed using FFT or local, non-iterative field solve methods for problems involving simple boundary conditions
    - Few parallel PIC codes exists using global, iterative field solve methods for problems involving complex boundary conditions
  - **Our Recent Research:**
    - A new class of ES PIC algorithm is developed using the immersed finite element formulation
    - IFE is designed to accurately resolve boundary effects while maintaining computational speed associated with standard PIC code





## Immersed Finite Element Formulation for PIC Code

- Major features of IFE (Kafafy et al, 2005):
  - Mesh independent of object boundary: Allows the use of Cartesian mesh for complex geometric interface and/or time-varying interface with the approximation capability as the body-fit mesh
    - Accuracy: 2<sup>nd</sup> order convergence
  - Electric field solved for both inside and outside the object if needed: material property effects explicitly included
  - Trial functions satisfy the jump conditions imposed by material properties at interface : Physics maintained at object interface
  - Based on finite element formulation: Nice mathematical properties (e.g. algebraic systems are symmetric & positive definite, etc.)
  - Cartesian mesh for PIC: maintains standard particle search and particle push in PIC; avoids numerical diffusion associated with particle shape change

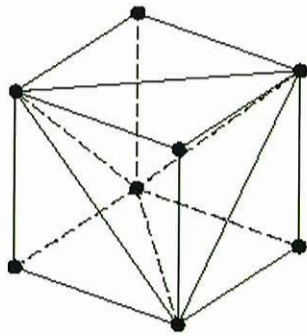


- IFE allows the use of standard Cartesian mesh based PIC algorithm for problems involving complex boundary conditions
  - Possibility to maintain standard PIC speed without losing accuracy
  - Easy parallel implementation

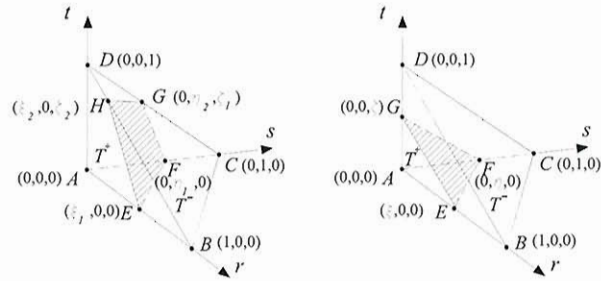


## Immersed-Finite-Element PIC (IFE-PIC)

- **IFE-PIC:** A hybrid finite-difference finite element PIC
  - IFE used for problems involving complex geometric boundary
- **Mesh:** Cartesian Tetrahedron-Based Structured Mesh
  - Primary PIC Mesh: Cartesian cells
  - Secondary IFE Mesh: each Cartesian cell is divided into 5 tetrahedrons.
- **Field Solver:** IFE
- **Particle Push/Particle-Grid Interpolation:** standard PIC



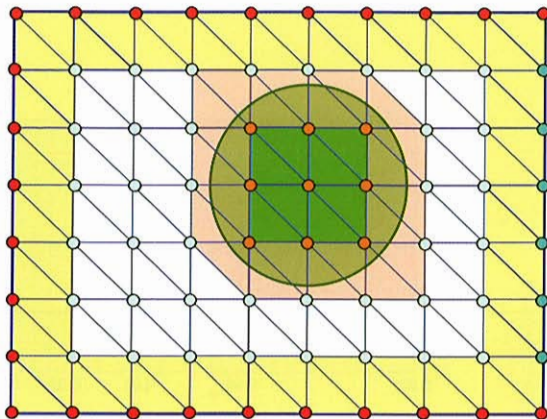
IFE-PIC cell



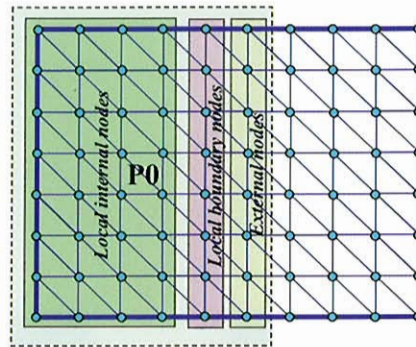
Intersection of boundary with IFE cell



## Parallel IFE-PIC



- boundary Dirichlet node    ● internal known node
- boundary Neumann node    ○ internal unknown node
- interface element    non-interface element
- boundary non-interface element

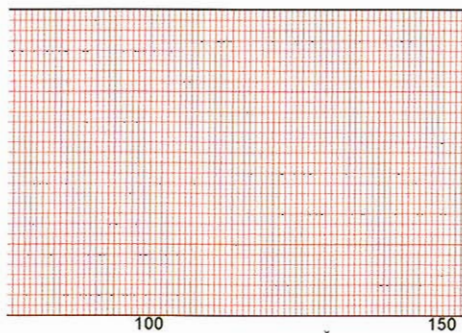


- **IFE Sub-domain Mesh**
  - Sub-domain IFE mesh includes local and external nodes
  - Pointers are used to local internal, local boundary, and external nodes
  - Boundary conditions are copied from global Mesh definition

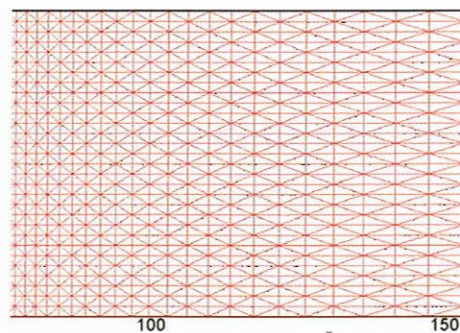


## Hybrid-Grid IFE-PIC (HG-IFE-PIC)

- **HG-IFE-PIC:** Designed for problems involving **complex geometric boundary and non-uniform plasma in a large domain**
  - In the hybrid-grid version of the IFE-PIC code, the PIC and IFE meshes are further made independent of each other.
    - PIC mesh: **Uniform Cartesian mesh**
    - IFE mesh: **Stretched Cartesian-based tetrahedral mesh**
  - Stretched IFE mesh is used for problems involving non-uniform plasmas in large simulation domain.
  - Mesh stretching follows potential gradients and local plasma conditions.



PIC mesh  
(uniform Cartesian)

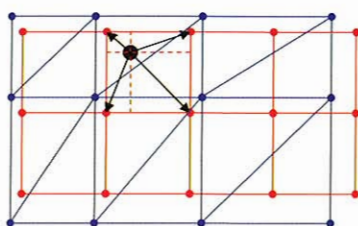


IFE mesh  
(Cartesian-based, tetrahedral stretched mesh)

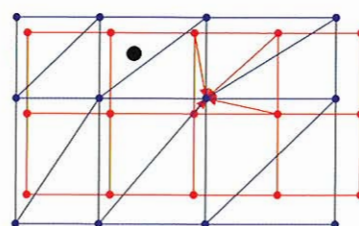


## HG-IFE-PIC Details:

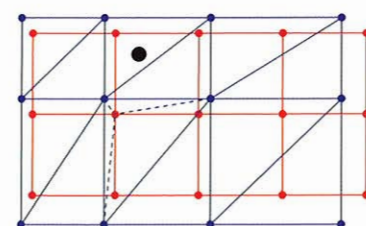
- IFE-PIC-Particle Interpolation Procedure
  - Physical quantities need to be appropriately traded among particle locations, PIC mesh nodes and IFE mesh nodes.
  - Particle charges are deposited onto PIC mesh nodes using linear weighting.
  - Charge densities are linearly interpolated from PIC mesh nodes into IFE mesh nodes.
  - After field solution, field quantities are interpolated from IFE mesh nodes into PIC mesh nodes using the IFE *linear basis functions*.



a) Particle-PIC Deposition



b) PIC-IFE Interpolation



c) IFE-PIC Interpolation

IFE-PIC-Particle Interpolation Process  
Particle [black], PIC mesh [red], IFE mesh [blue]



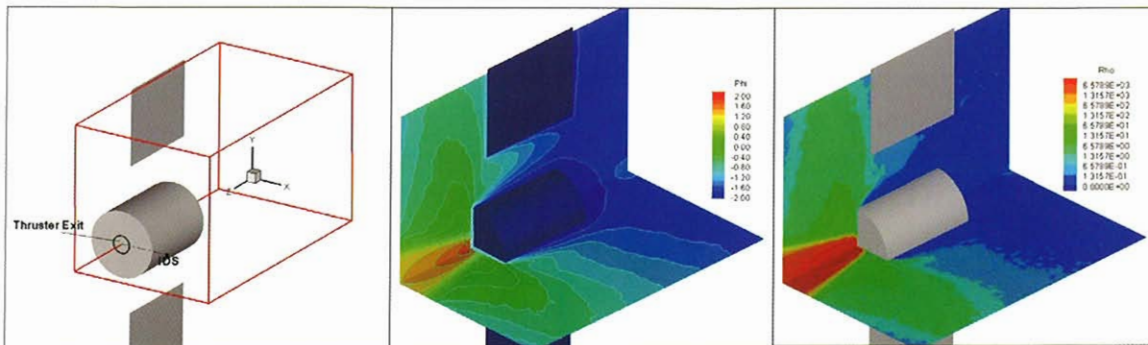
### III. Ion Thruster Plume Modeling

- Previous Study (Wang et al., JSR, 2001):
  - A 3-D simulation model developed for the Deep Space 1
  - Results in excellent agreement with DS1 in-flight measurements
- This study (Wang et al., IEEE Trans. Plasma Science, 2006):
  - Simulation of more complex spacecraft configuration with multiple ion thrusters
  - Parallel IFE-PIC simulation using parallel computer
  - HG-IFE-PIC simulation using PC
  - Predict plume contamination for DAWN spacecraft



### Simulation Model

- Model based on the same physics formulation of our previously developed Deep Space 1 ion thruster plume model (Wang et al., JSR, 38(3), 2001)
- Model validation using Deep Space 1 in-flight data:



#### NSTAR thruster operating condition ML83:

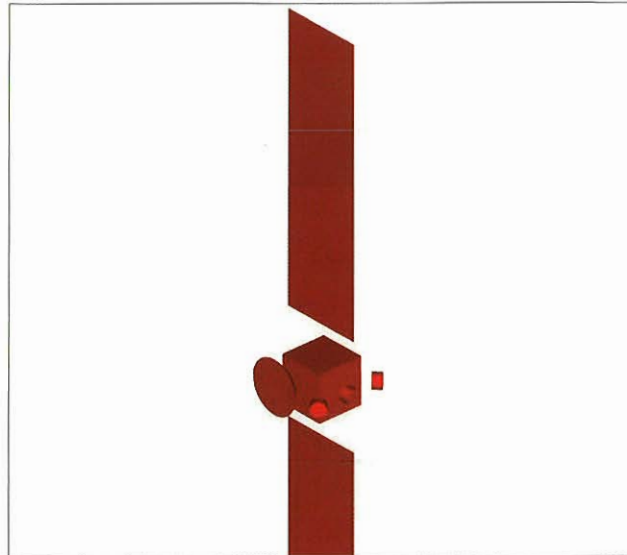
IDS measurement: IDS potential – center potential: -15V; CEX ion density:  $1.2E6\text{cm}^{-3}$

Simulation: IDS potential – center potential: -13V; CEX ion density:  $1.1E6\text{cm}^{-3}$

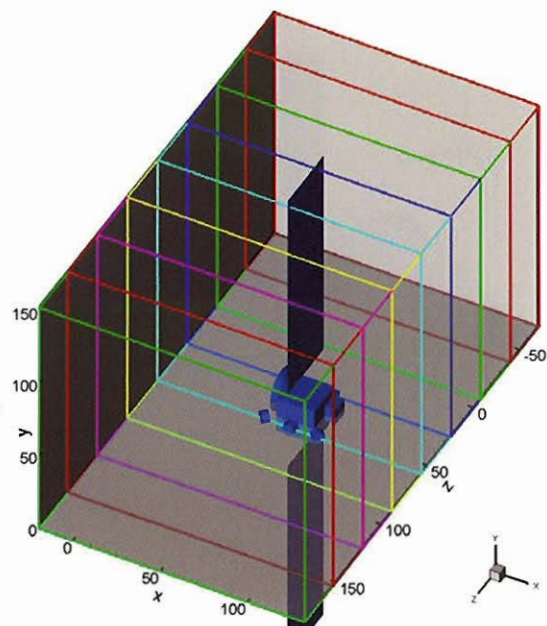


## High Resolution IFE-PIC Simulations of Multiple Ion Thruster Plume Interactions

- **Objective:**
  - multiple ion thruster plume interactions with a realistic spacecraft
  - CEX plasma distribution on solar array surface and payload
- **Domain:**
  - encloses the entire solar array panel: 9.3mx9.3mx15.4m
- **Resolution:**
  - resolves the CEX plasma Debye length in the entire domain
  - CEX plasma resolution: 5cm
  - Electric field resolution: 1cm

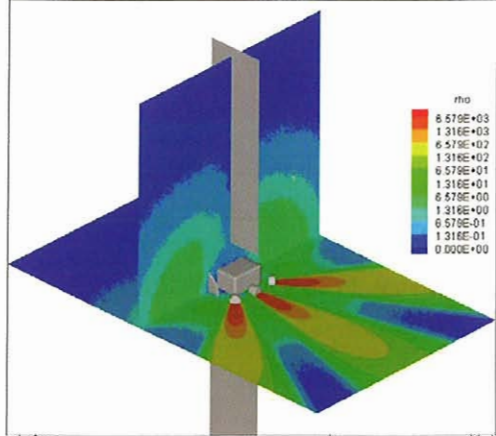
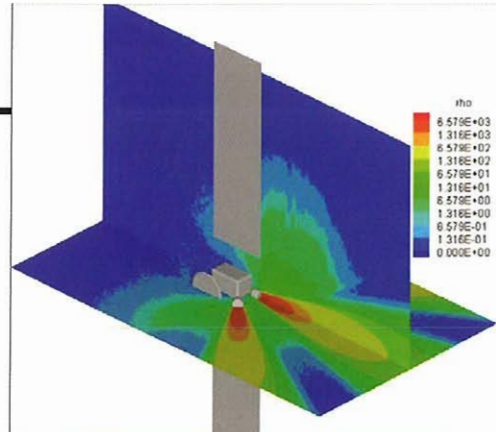
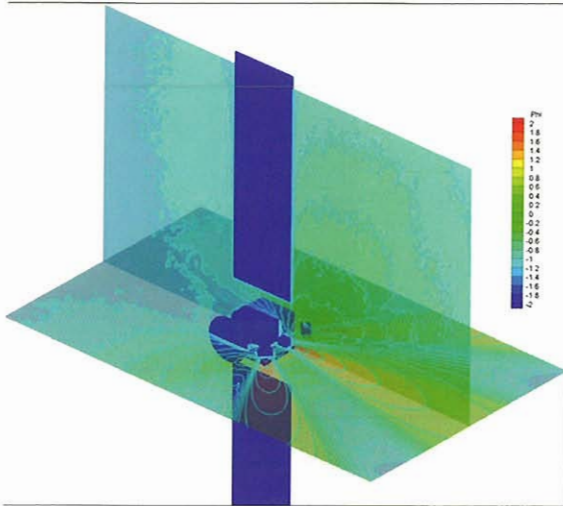


- **Simulation Parameters:**
  - Particles at steady state: 125 million
  - PIC cells: 155x155x256 (>6.15 million)
  - Tetrahedral elements: 30.8 million
- **Typical Computation Time:**
  - Full transient to steady state simulation: 10 hrs on 64 processors of Dell cluster for 1000 PIC steps
  - Steady state only simulation: 2 hrs on 64 processors

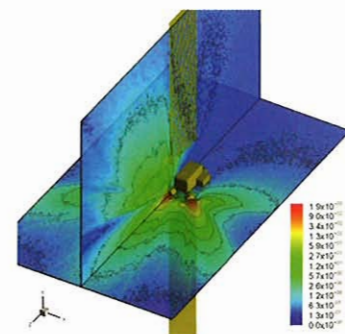
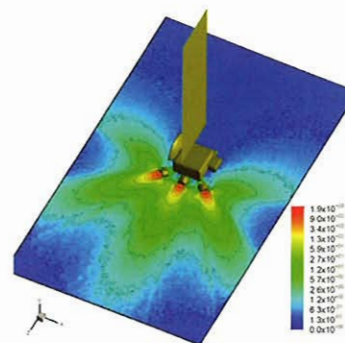
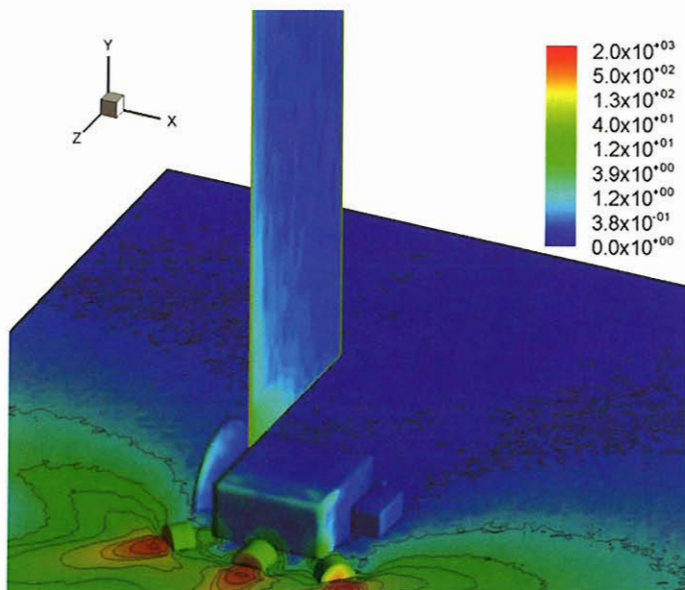


Domain Decomposition

Virginia Tech

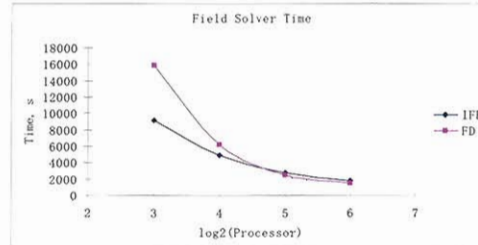
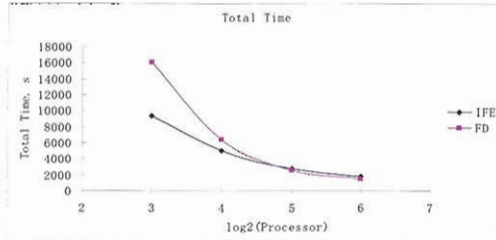


Virginia Tech





## Computational Time: IFE-PIC vs. FD-PIC

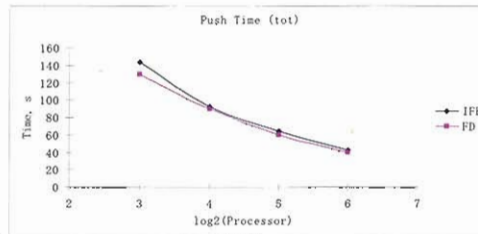


**Code speed on 64 processors of the Dell Xenon cluster:**

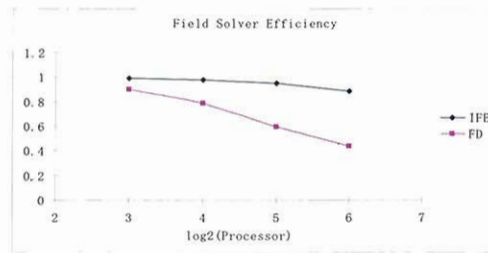
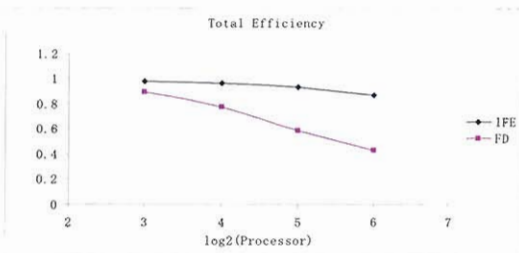
**steady state: 125 million particles and 30million tetrahedral elements**

**IFE-PIC loop time = 38s/step  
Particle push time = 21.2 ns/particle/step**

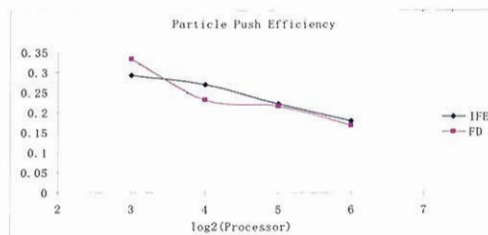
**IFE field solve time = 4986 ns/cell/step (997 ns/element/step)**



## Parallel Efficiency: IFE-PIC vs. FD-PIC



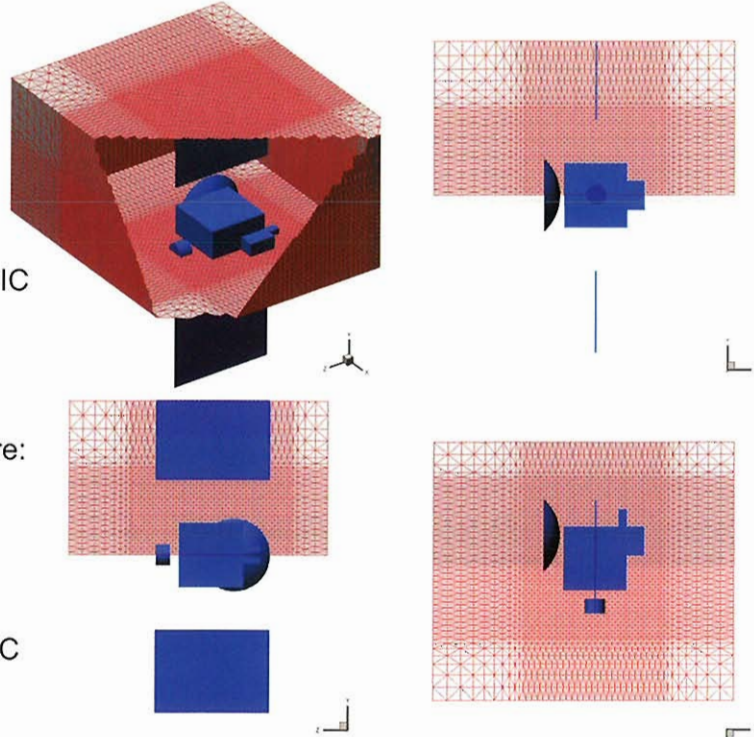
**Parallel efficiency for IFE-PIC at steady state on 64 processors: ~ 90%**



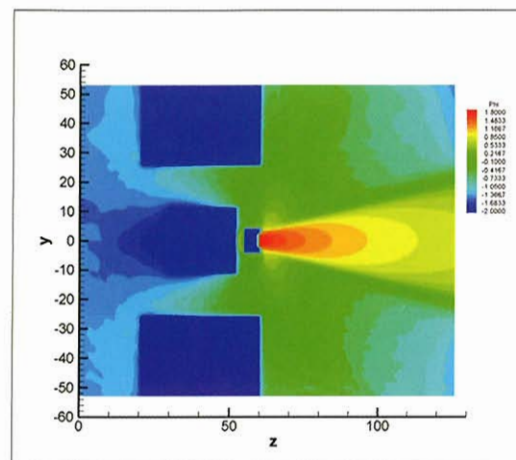


## Hybrid Grid IFE-PIC Simulations of Multiple Ion Thruster Plume Interactions

- **Objective:**
  - To further reduce computation time and memory requirement
- **Domain:**
  - 2-zone mesh
  - Inner zone uses IFE-PIC
  - Outer zone uses HG-IFE-PIC
- **Resolution:**
  - PIC cell same as before: 5cm
  - IFE cell:
    - Inner zone: 5cm
    - Outer zone:  $V_{cell\_IFE}/V_{cell\_PIC} = 1$  to  $\sim 7$

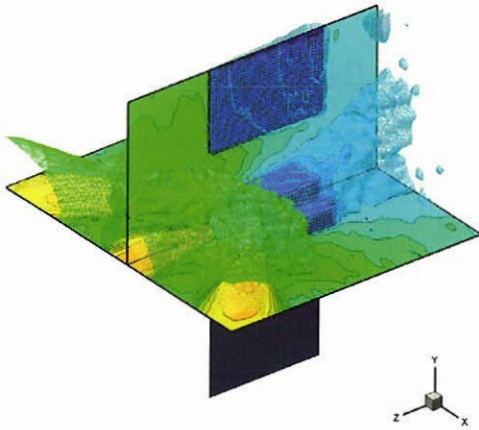


- **Simulation Parameters:**
  - Particles at steady state: 6 million
  - PIC cells: 105x54x90
  - Tetrahedral elements: 0.83 million
- **Typical Computation Time:**
  - Steady state only simulation:  $\sim 3$  to  $5$  hours on P4 @ 2.2 GHz

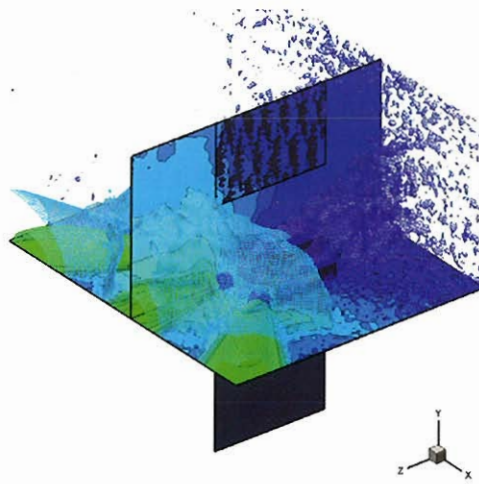


Comparison of  
IFE-PIC and HG-IFE-PIC

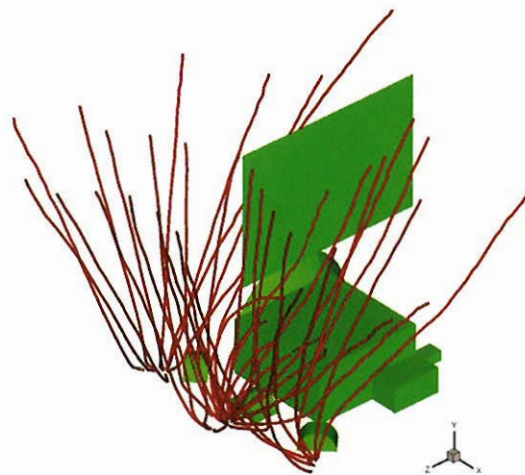
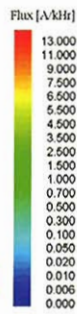
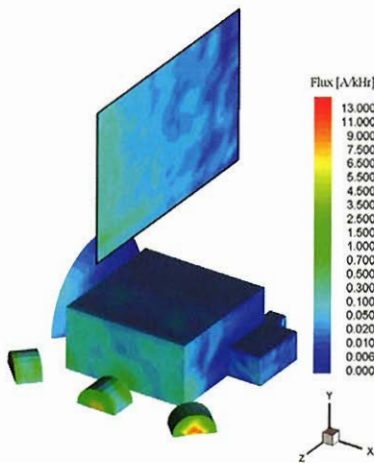




Electric Potential



Ion density





## Prediction of Plume Contamination on Solar Array

- A primary concern for space missions using solar electric propulsion is plume induced contamination on solar cell
  - power loss; temperature change; catastrophic shorting
- Deposition of contaminants is calculated by tracing Mo<sup>+</sup> particles from plume to solar array surface
- For an ion thruster similar to the NSTAR thruster, the contamination effect on the solar array is very moderate for DAWN configuration
- For multiple ion thruster plumes, deposition on solar array in general is NOT the sum of the contamination produced by individual thrusters

	Cases	1	2-A	2-B	2-C	3
Solar	Ave. (A/kHr)	0.014	0.014	0.018	0.0501	0.0704
Array	Max. (A/kHr)	0.2513	0.216	0.0357	0.4085	0.4717



## IV. Ion Optics Modeling

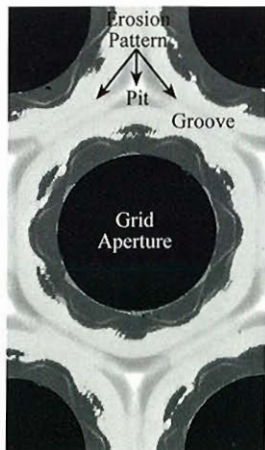
- Previous Study (Wang et al., JPP, 2003):
  - A 3-D “local” simulation model developed for NSTAR ion optics
  - Results in excellent agreement with measured erosion pattern and erosion depth
- This study (Wang et al., 2006):
  - Simulation of a whole ion optics gridlet
    - new model explicitly includes apertures located at the edge and fully accounts for the effects of geometric asymmetry
  - HG-IFE-PIC simulation using PC
  - Predict erosion from direct impingement at cross-over for CSU subscale ion optics



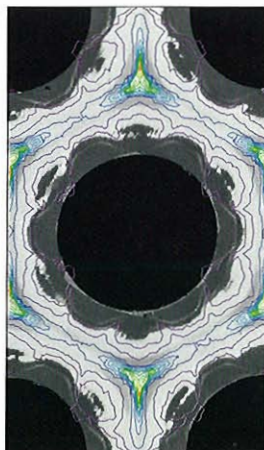
- The behavior of the accel grid current defines the operation envelop of an ion optics system.
- Accurate prediction of the cross-over and preveance limit is essential to ensure long-term ion thruster operation.
- Model predictions of ion impingement limits are currently based on extrapolations of single beamlet simulations
  - Existing ion optics models are either axi-symmetric or 3-D with symmetric boundaries.
  - The geometric asymmetry associated with the edge apertures are not resolved.
- Previous simulations of CBIO gridlet were not able to accurately predict the cross-over limit
- Both the disagreement between simulation and experiment and ongoing experimental studies suggest that the effects of geometry asymmetry and sheath interaction between adjacent holes may have a significant influence on the cross-over limit



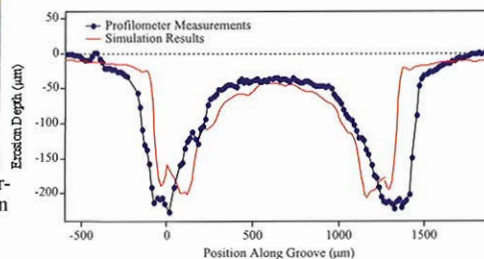
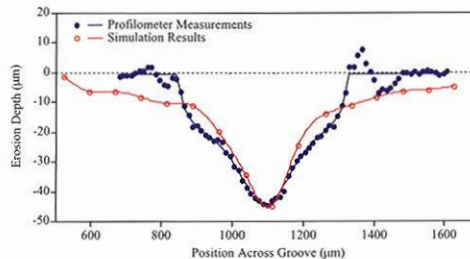
- “Local” optics simulation of grid erosion for normal operation condition (Wang et al., J. Propulsion & Power, 2003)



Downstream face of accelerator grid after 8200 hours at 2.3 kW

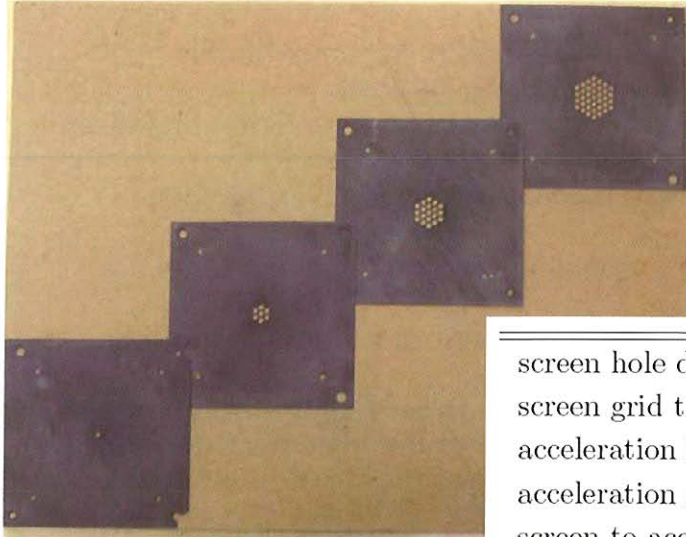


Simulated erosion contours overlaid on measured erosion pattern





### CSU Subscale Gridlet



screen hole diameter, $d_s$	2.305 mm
screen grid thickness, $t_s$	0.461 mm
acceleration hole diameter, $d_a$	1.396 mm
acceleration grid thickness, $t_a$	1.016 mm
screen to acceleration grid gap, $l_g$	0.810 mm
center-to-center hole spacing, $l_{cc}$	2.674 mm

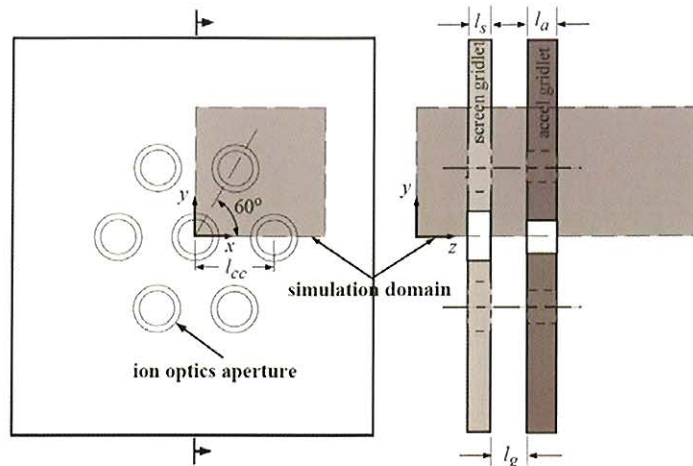
Sub-scale CBIO-style Poco graphite grids.



### Simulation Model

- Simulation model are based on the HG-IFE-PIC algorithm (Kafafy and Wang, JPP, 2006)
  - Explicitly includes apertures located at the edge
  - Fully accounts for the effects of multiple ion beamlets and geometric asymmetry

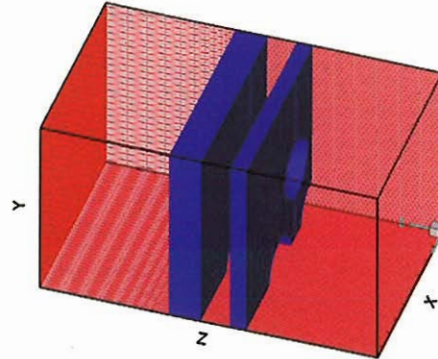
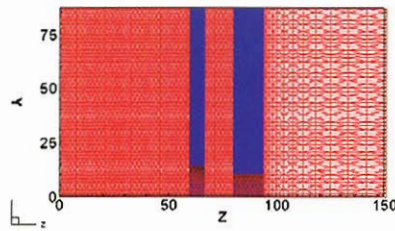
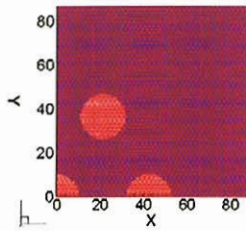
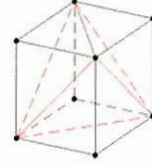
**7-hole gridlet model:**  
Assume uniform upstream plasma density





### Simulation Mesh and Simulation Parameter

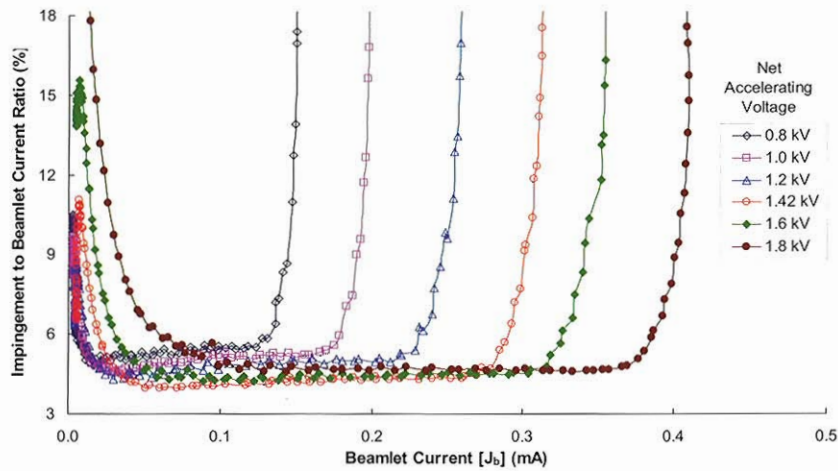
- PIC Mesh:
  - Uniform Cartesian
- IFE Mesh:
  - Multi-zone stretched Cartesian-based tetrahedral mesh



- Simulation Parameters:
  - PIC mesh: 90X52X281
  - IFE mesh: 90X52X280 (4,704,400 elements)
  - Upstream resolution:  $h=5.2E-5m$
  - ~ 117,000 streamlines per simulation loop.



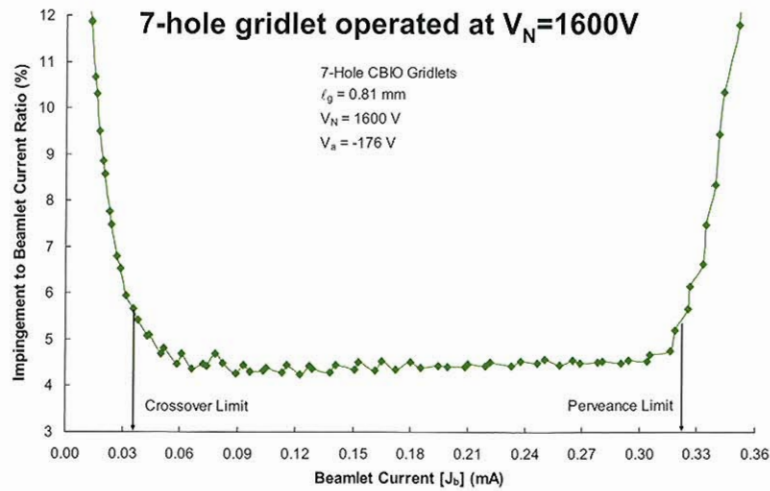
### Experimental Results: Accel Grid Impingement Current for 7-hole Gridlet



net acceleration $V_N$	screen grid voltage $V_s$	accel grid voltage $V_a$
800V	770V	-140V
1000 V	970V	-150 V
1200 V	1170V	-166 V
1420 V	1390V	-170 V
1600 V	1570V	-176 V



### Experimental Results: Cross-over and Preveance Limit Definition

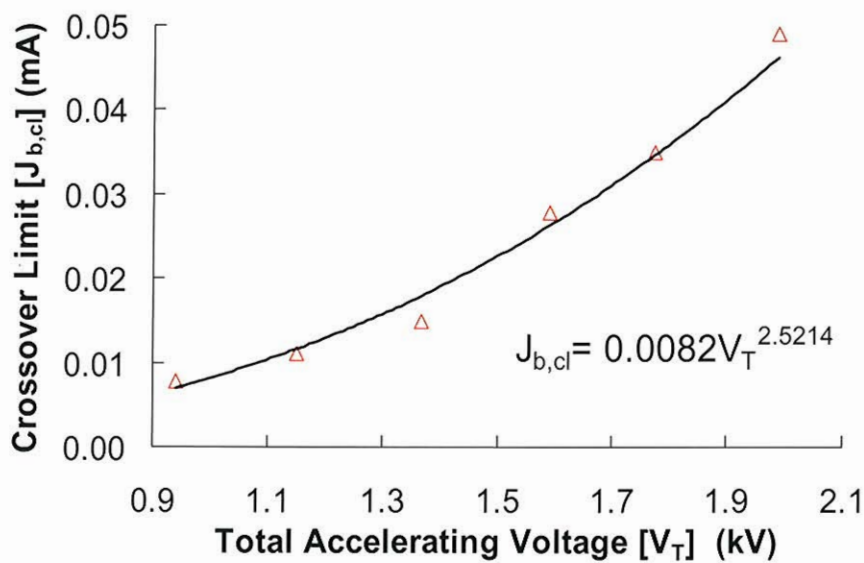


$$J_a = J_{imp} + J_{cex} + J_{leakage} \quad J_{cex} \sim 4.5\%J_b$$

**Cross-Over and Preveance Limit is defined at  $J_a/J_b=5.5\%$**

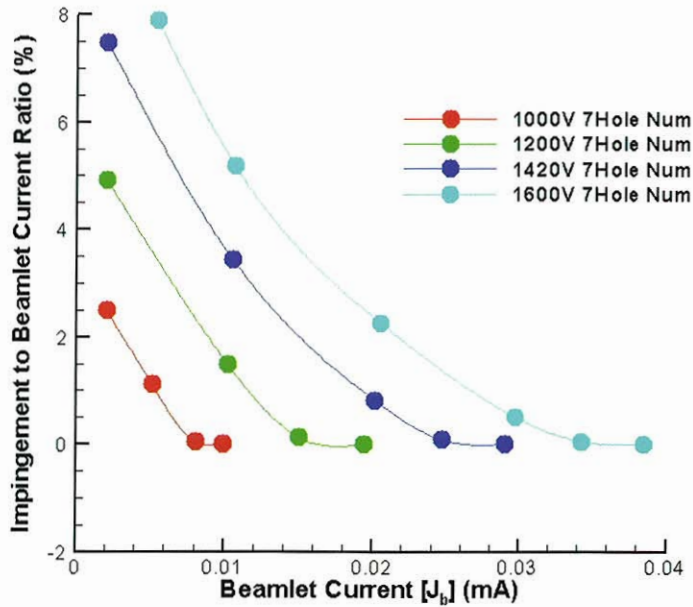


### Experimental Results: Cross-Over Limit Behavior for 7-hole Gridlet





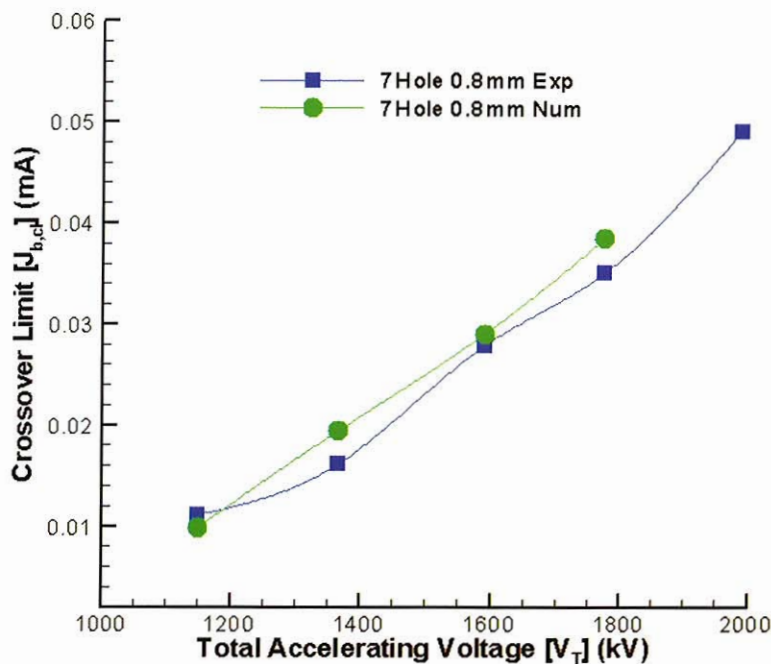
### Simulation Results: Accel Grid Impingement Current for 7-hole Gridlet



Simulations do not include CEX ions and leakage current



### Simulation vs. Experiment: Cross-Over Limit Behavior for 7-hole Gridlet



Cross-over limit in experiment:

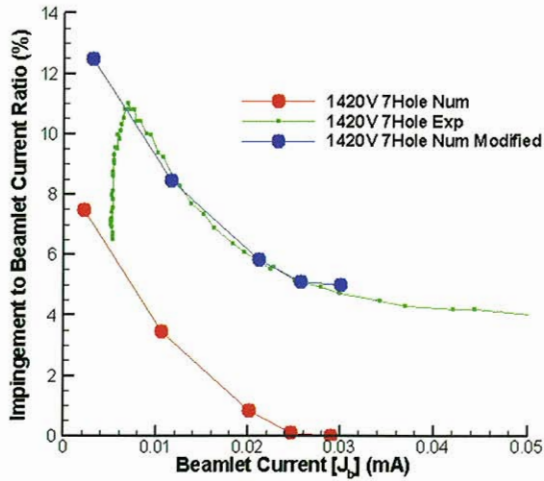
$$J_a - J_{cex} = 1\% J_b$$

Cross-over limit in simulation:

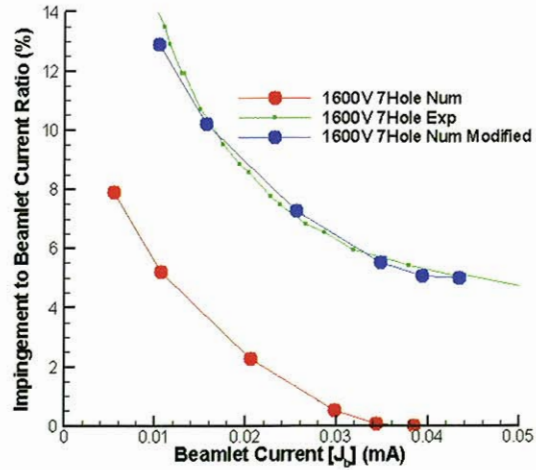
$$J_a \geq 0$$



### Simulation vs. Experiment: Accel Grid Impingement Current for 7-hole Gridlet



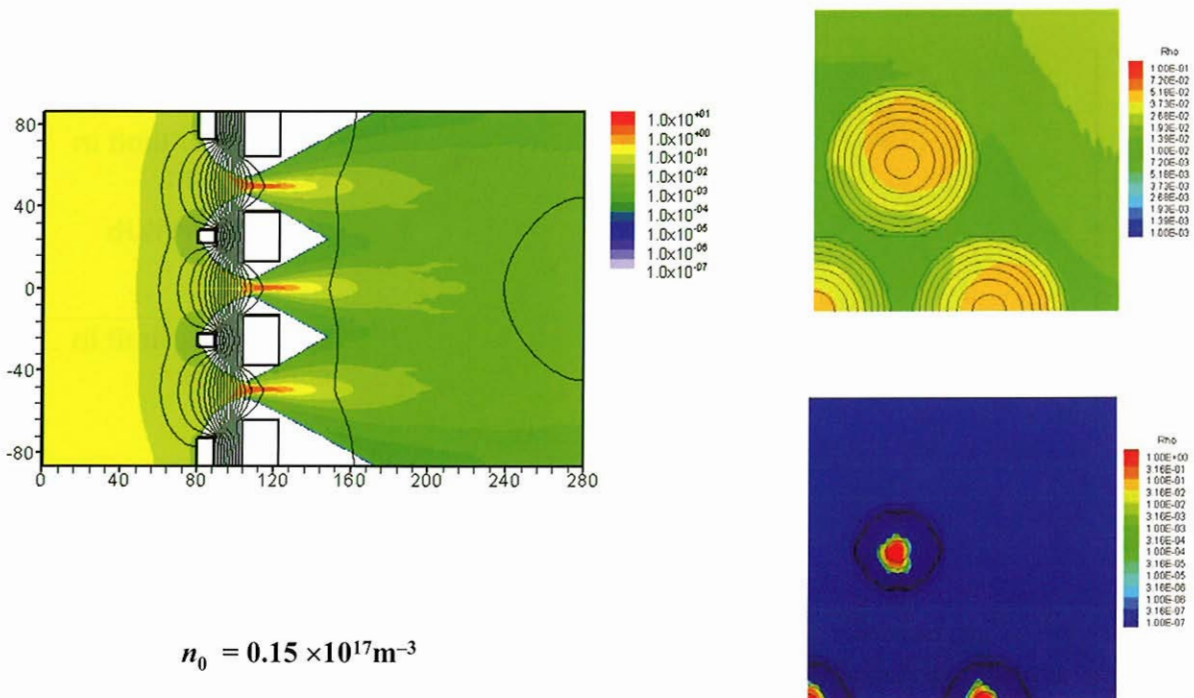
Blue line: origin of the simulation curve shifted from (0,0) to (0.001,4.5)



Blue line: origin of the simulation curve shifted from (0,0) to (0.005,4.5)



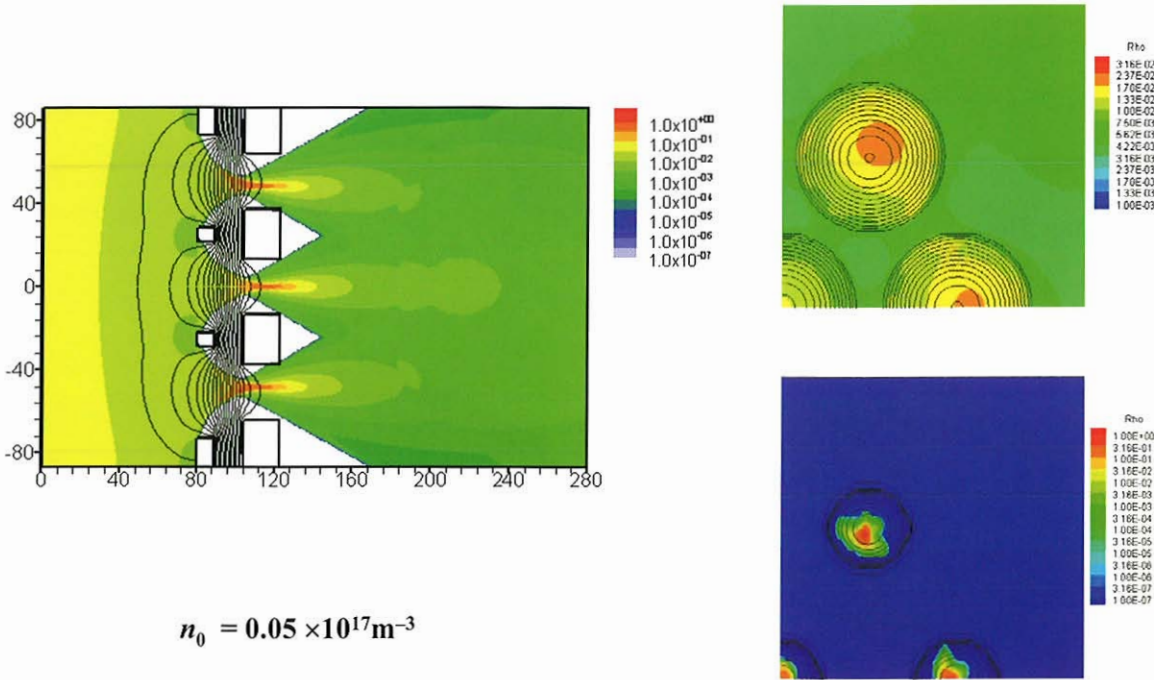
### Simulation Results: Beamlet Profile at Cross-Over



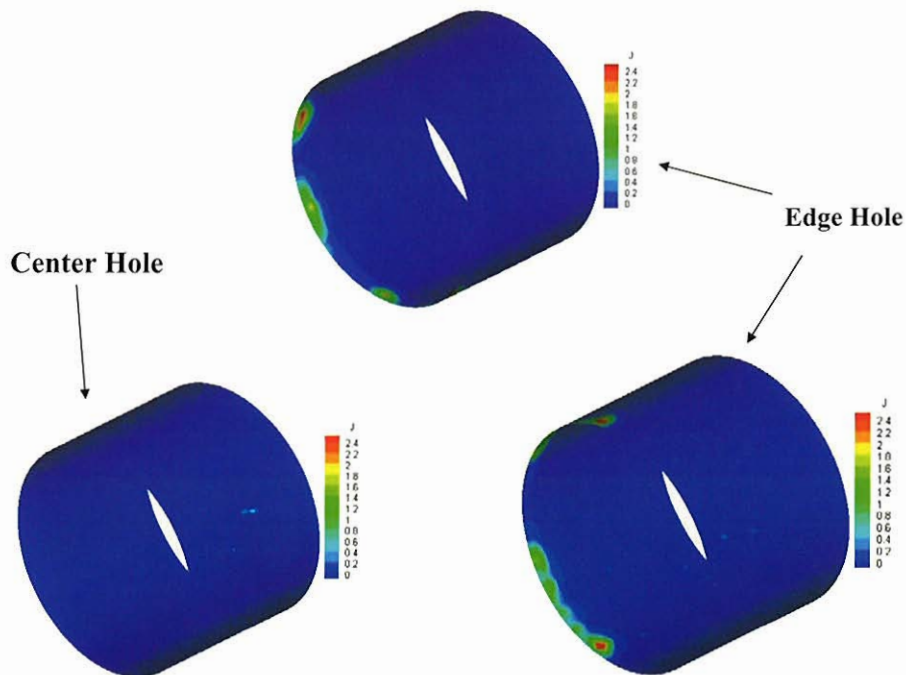




### Simulation Results: Beamlet Profile beyond Cross-Over

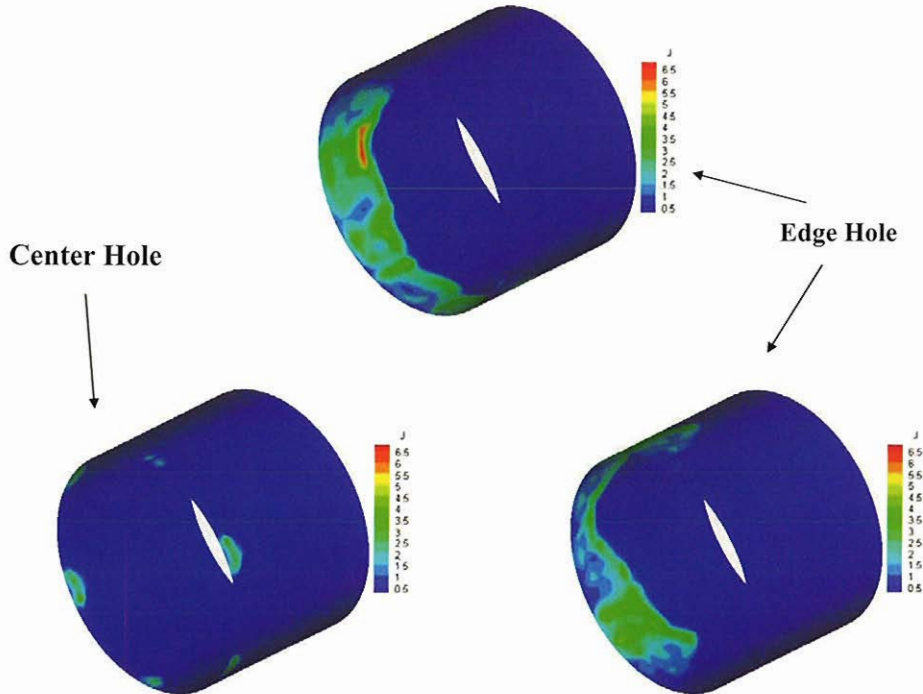


### Simulation Results: Ion Impingement Distribution at Cross-Over





## Simulation Results: Ion Impingement Distribution beyond Cross-Over



## Prediction of Cross-Over for CSU Ion Optics Gridlet

- **Cross-Over onset starts at edge apertures!**
  - Cross-over occurs at higher  $J_b$  than the center aperture
- Beamlet profile is asymmetric for edge apertures
  - Ion beamlets focused more towards the gridlet center due to the asymmetry in E field near grid surface
- Ion impingement distribution is asymmetric for edge apertures
  - Direct impingement concentrated on the aperture side oriented towards the gridlet center
- Ion impingement distribution has a hexagonal pattern for the center aperture
- Edge apertures will experience significant more sputtering erosion than the center aperture.

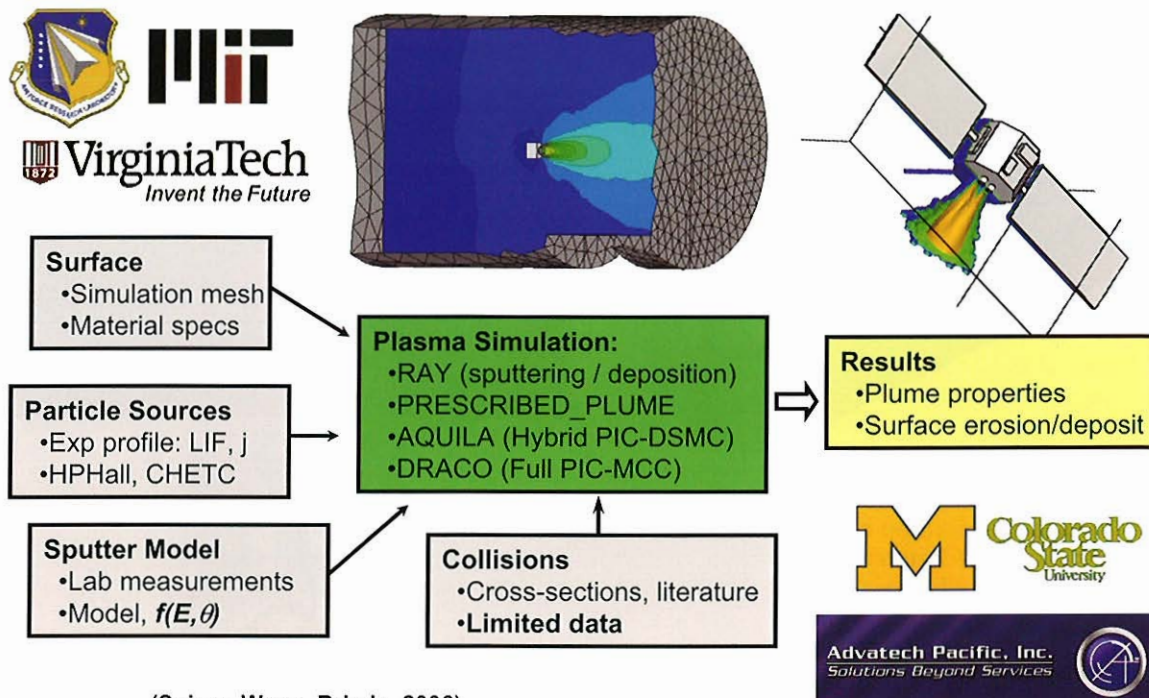


## V. Simulation Based Design Tool

- Modeling and simulation are playing an ever more important role in electric propulsion and spacecraft interactions research
- The sophistication of the models and the capability of supercomputers have reached such a level that it is becoming feasible to use computer simulations as “virtual” experiments in place of real experiments for many applications
- **Objective:**
  - To develop a simulation based design tool for spacecraft using electric propulsion



## COLISEUM framework

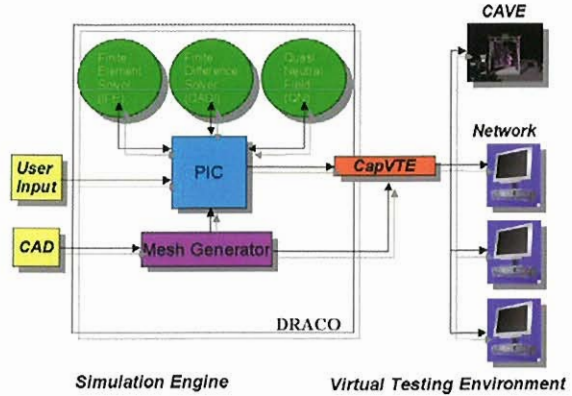


(Spicer, Wang, Brieda, 2006)

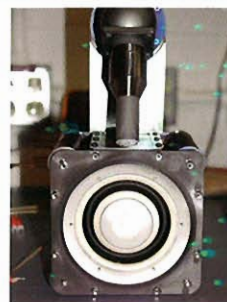
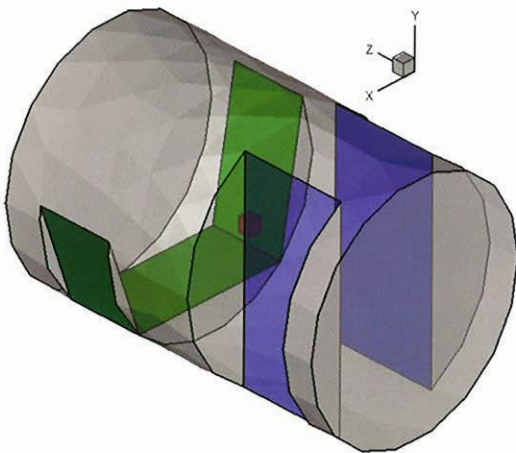


## DRACO

- A set of multi-purpose 3-D electrostatic PIC codes developed at VT and AFRL
  - **QN-PIC:**
    - Quasi-neutral plasma with Boltzmann electrons
  - **FD-PIC:**
    - Full particle/hybrid PIC
    - Standard finite-difference field solver
  - **IFE-PIC**
    - Full particle/hybrid PIC
    - Hybrid finite element/finite difference formulation
    - Immersed finite element field solver
  - **Mesh-Object Intersection (VOLCAR)**
    - Interface between PIC and CAD defined spacecraft model



## Ongoing Work: Simulation of EP Ground Experiment



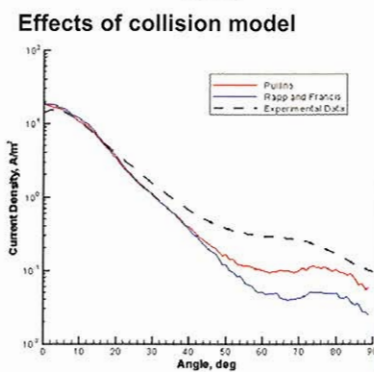
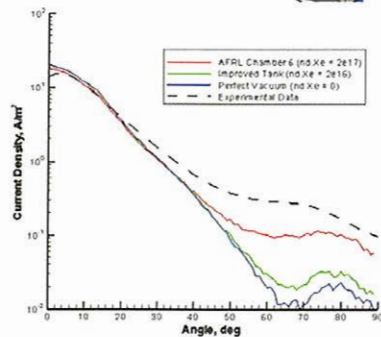
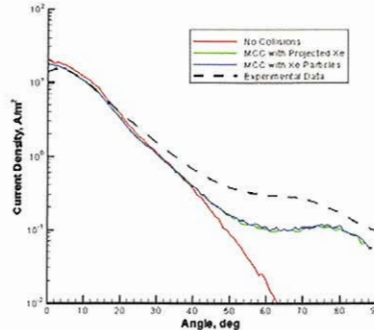
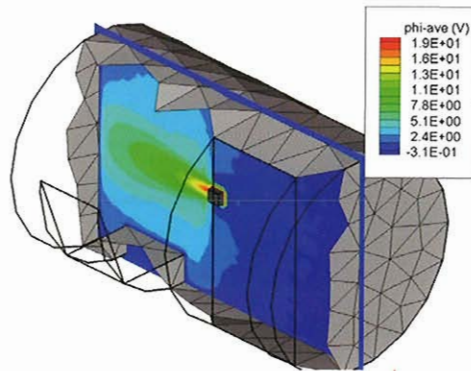
### DRACO Simulation set-up:

- Model generated by Solidworks /Hypermesh
- Red = Thruster
- Blue = Pump
- Grey = Tank Walls
- Green = Graphite

Comparison with experimental current density sweep at 0.6m



## Preliminary Results



Effects of neutral plume density

Effects of collision cross section data

(Spicer, Wang, Brieda, 2006)



## VI. Summary and Conclusions

- Significant progresses have been made on developing particle simulation models for ion propulsion
  - Such models are *beginning* to meet user's requirements in *sophistication* (all physics included), *computational speed* (3-D simulations performed routinely), and *accuracy* (agreement with experimental data)
  - Particle simulation models are increasingly being used as engineering design tool in development of new thrusters and in preflight predictions of plume effects
- However, many challenging issues still remain to be solved
  - How to accurately incorporate the many "engineering details" of real spacecraft (or thruster) into the model?
    - surface material properties, surface interactions, detailed device configuration, detailed plume characteristics, detailed experimental setup... etc, etc
  - How to account for uncertainties in experimental data?
  - How to avoid mis-interpreting the physics?
  - How to continuously overcome the computation limitation?

## JAXA/JEDI project on the development of plasma simulator for spacecraft environment

臼井 英之

京都大学 生存圏研究所

E-mail: usui@rishi.kyoto-u.ac.jp

篠原 育

宇宙航空研究開発機構 宇宙科学研究本部 宇宙科学情報解析センター

E-mail: iku@stp.isas.jaxa.jp

上田 裕子

宇宙航空研究開発機構 情報・計算工学センター

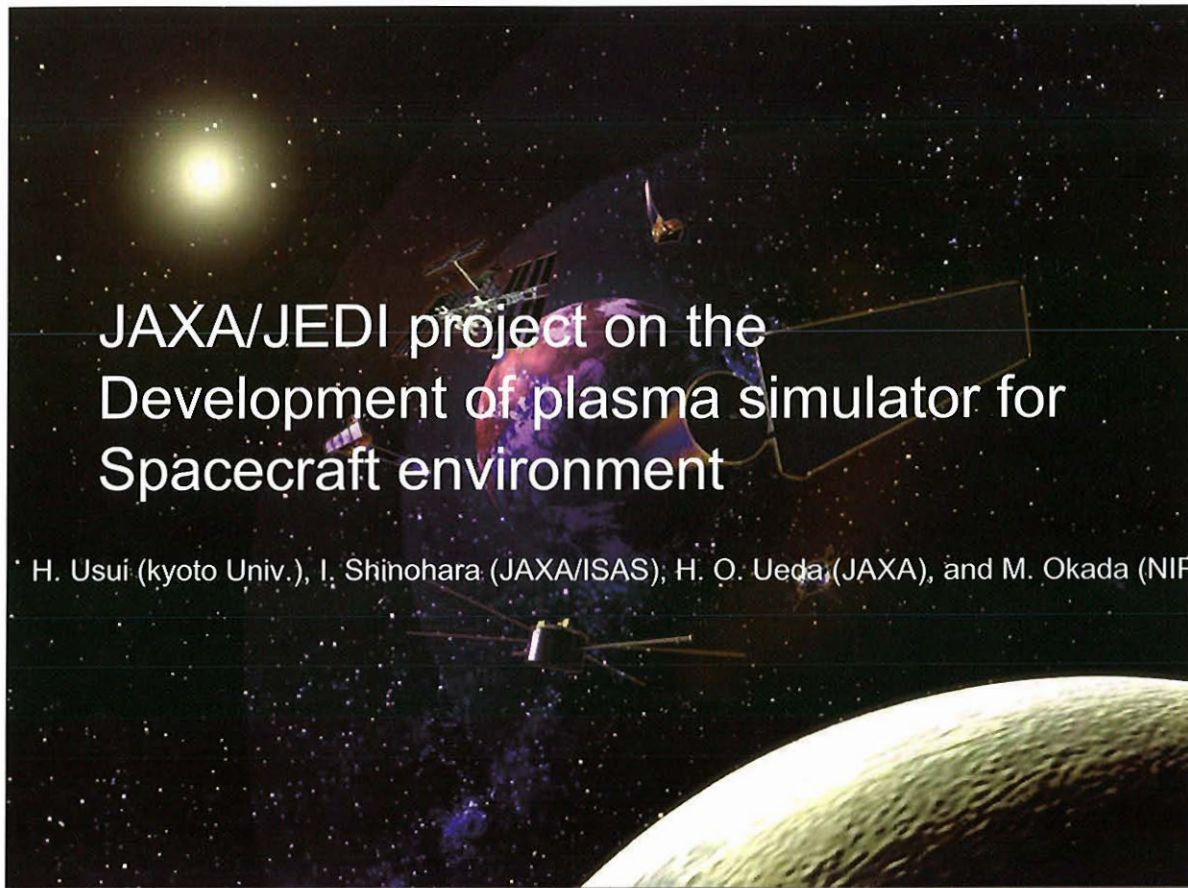
E-mail: ueda.hiroko@jaxa.jp

岡田 雅樹

国立極地研究所

E-mail: okada.masaki@nipr.ac.jp

平成 17 年度に JAXA 情報・計算工学センター (JEDI) が発足し、これまで行われた宇宙プラズマ物理解析のプラズマシミュレーションを衛星機器の技術開発、衛星環境アセスメントなど工学的な分野に応用することが求められている。この要求に対し、JEDI では、宇宙機と周辺宇宙プラズマの相互作用を模擬する JAXA 衛星環境プラズマ数値シミュレータの基礎開発を平成 18 年度から開始する。この衛星環境プラズマシミュレータは、これまで宇宙プラズマ現象の解析に用いられてきた Particle-In-Cell (PIC) プラズマシミュレーションをコアエンジンとし、これに、現在 JAXA/九州工業大学で開発が進められている衛星帯電解析ツール (MUSCAT) で開発された高分解能衛星モデリング機能を付加することにより、宇宙プラズマによる衛星環境への影響について定量解析を行う数値シミュレーションツールである。特に、MUSCAT では解析することが困難なプラズマ非定常過程や電子ダイナミクスが関与する現象について、JAXA スーパーコンピュータを最大限に駆使して大規模数値シミュレーションを行うことによって解析を進める。具体的には、衛星からの能動的プラズマ放出による衛星環境への影響に着目し、将来的には、イオンエンジン、プラズマコンタクター、などプラズマをアクティブに利用した推進系、帯電緩和技術などの技術開発、磁気プラズマセイルなど新規航行技術開発に貢献することをめざしている。平成 18,19 年度は、シミュレータの基礎開発として、PIC シミュレータの JAXA スーパーコンピュータへの移植、MUSCAT 衛星モデリングとのリンク、衛星からの能動的プラズマ放出を模擬できるルーチンの開発とその動作テストを行い、平成 20 年度以降のシミュレータの本格的開発への準備を行う。



## Background

- JAXA/JEDI (JAXA's Engineering Digital Innovation Center): Importance of plasma simulation
- They need plasma simulations useful for spacecraft design and space projects (engineering aspects)
- In FY2006 and 2007, feasibility studies on
  - \* Numerical tool for grid-life estimate of ion propulsion engine
  - \* Plasma numerical simulator for spacecraft environment
- Combination with MUSCAT (Multi-utility spacecraft charging analysis tool)

## Objectives

- To develop a numerical plasma simulator with which we can examine various interactions between spacecraft and spaceplasma.
- To investigate active plasma emission such as electric propulsion and plasma contactor and its interactions to the spacecraft environment
- To contribute to the development of the associated technology

## What MUSCAT can do or cannot do ?

- Approximated steady state values of S/C surface potential
- High-resolution S/C modeling

### Difficult to treat

- Active plasma emission from S/C and its effect on the plasma environment
- Time-dependent, transient phenomena



# Numerical plasma simulator

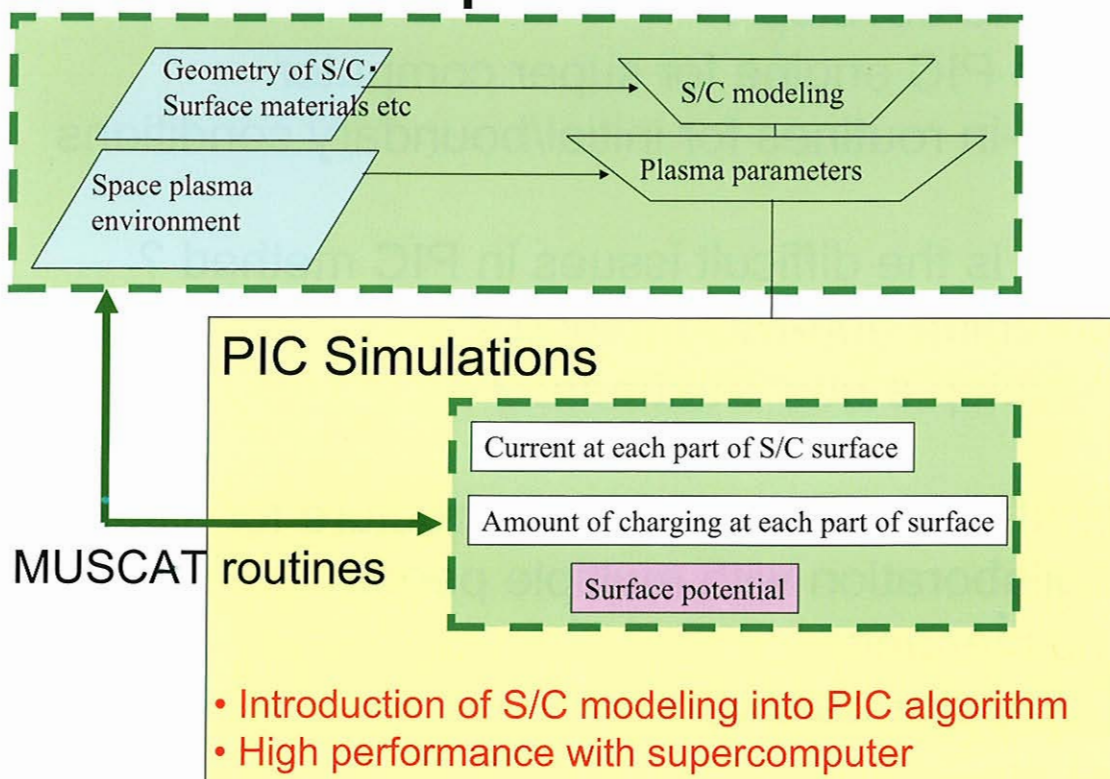
So far, almost no full PIC simulations with complex spacecraft modeling

High-resolution S/C modeling developed for MUSCAT

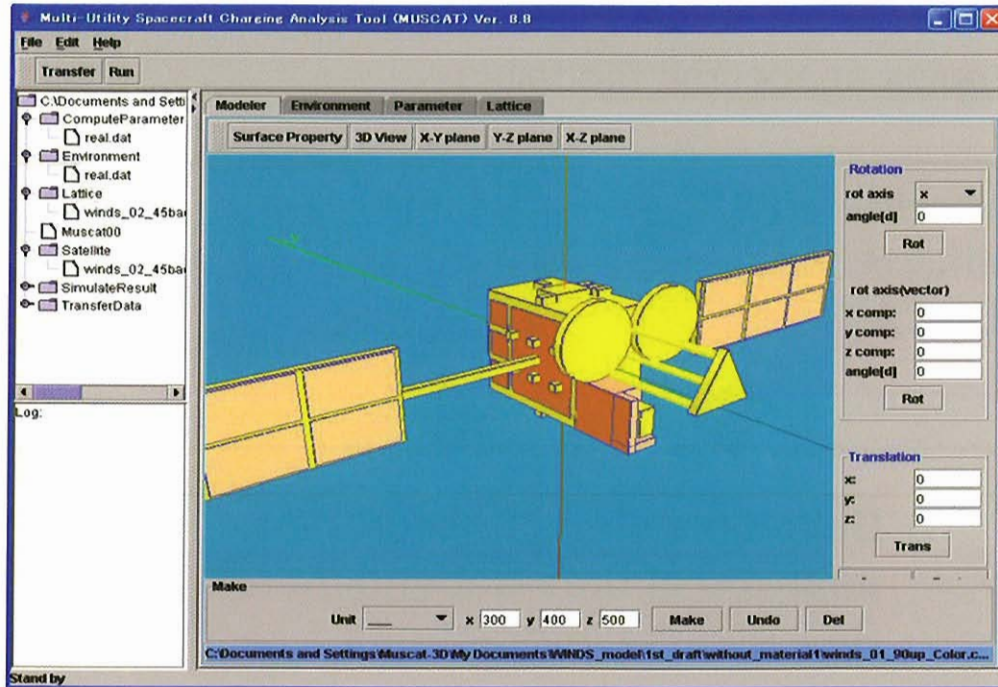
Domain decomposition model PIC code developed for massive parallel super computers

Develop a simulator for the analysis of time-dependent S/C- plasma interactions

## In numerical plasma simulator...



## An example of MUSCAT S/C modeling – WINDS satellite-



What to develop ?

- Core PIC engine for super computer
- Plug-in routines for initial/boundary conditions

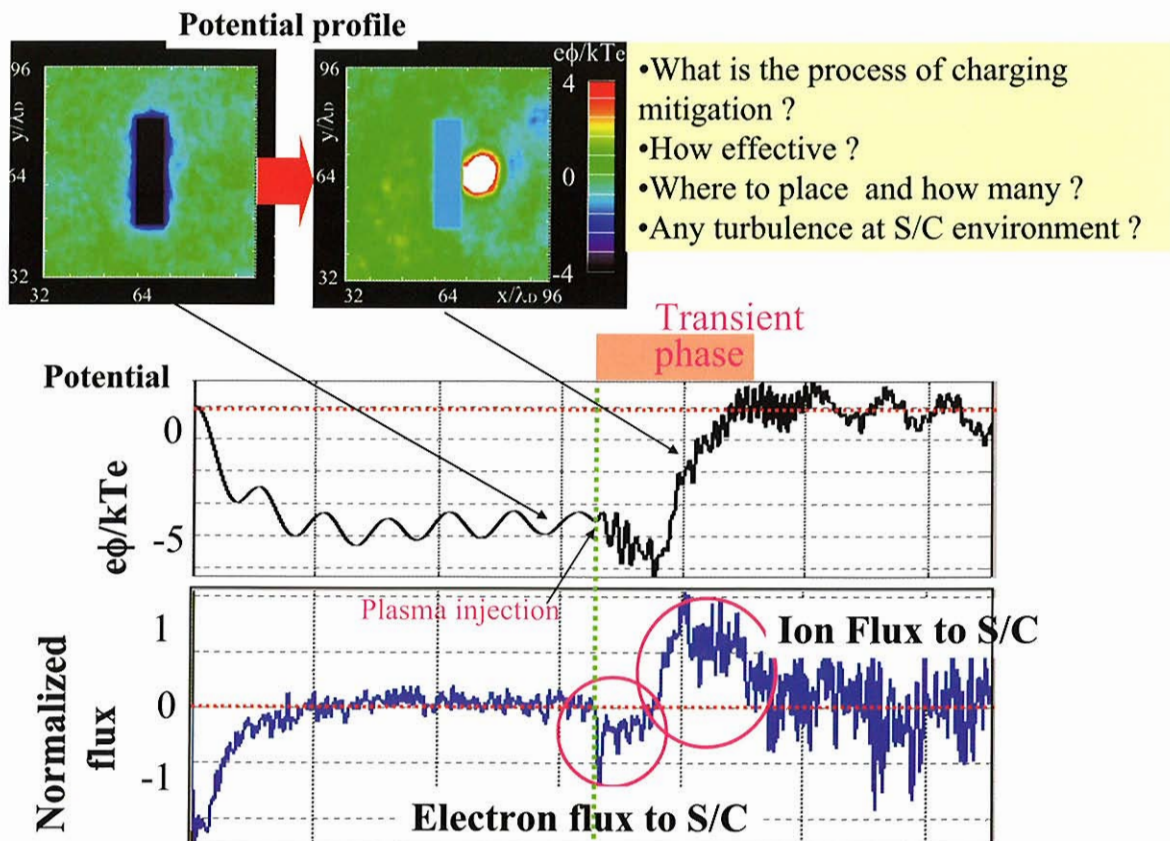
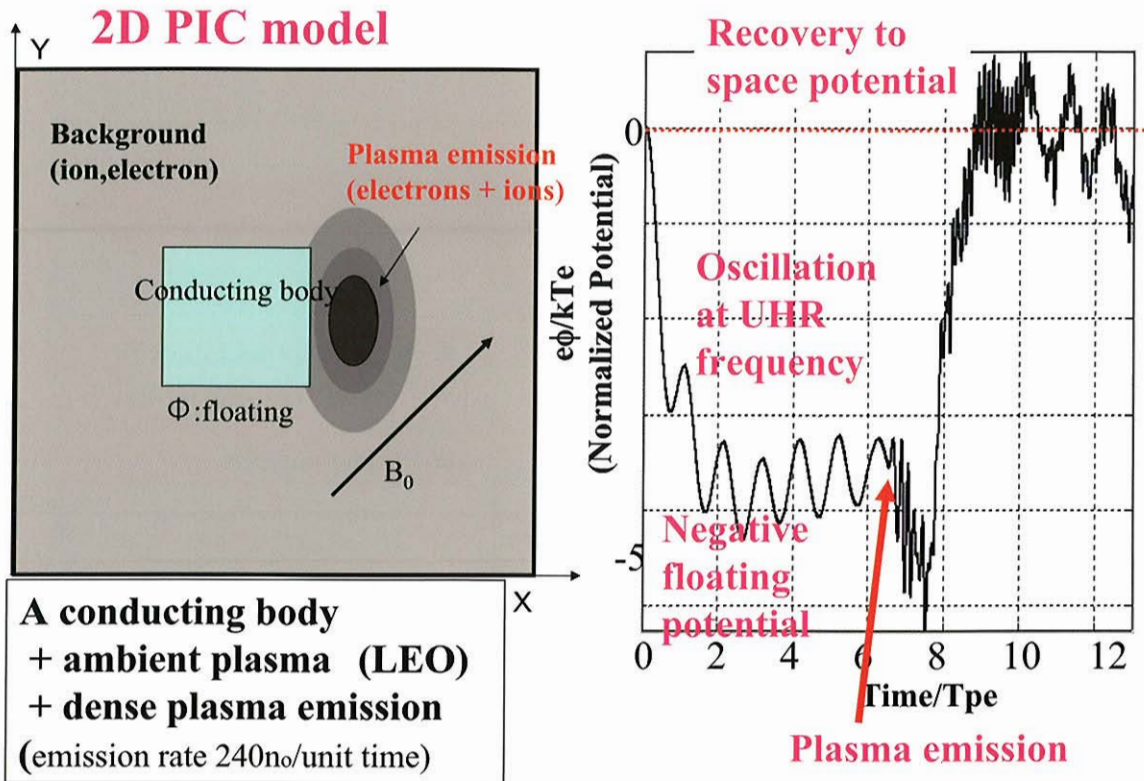
What is the difficult issues in PIC method ?

- Combine non-PIC method ?
- Develop a new treatment ?

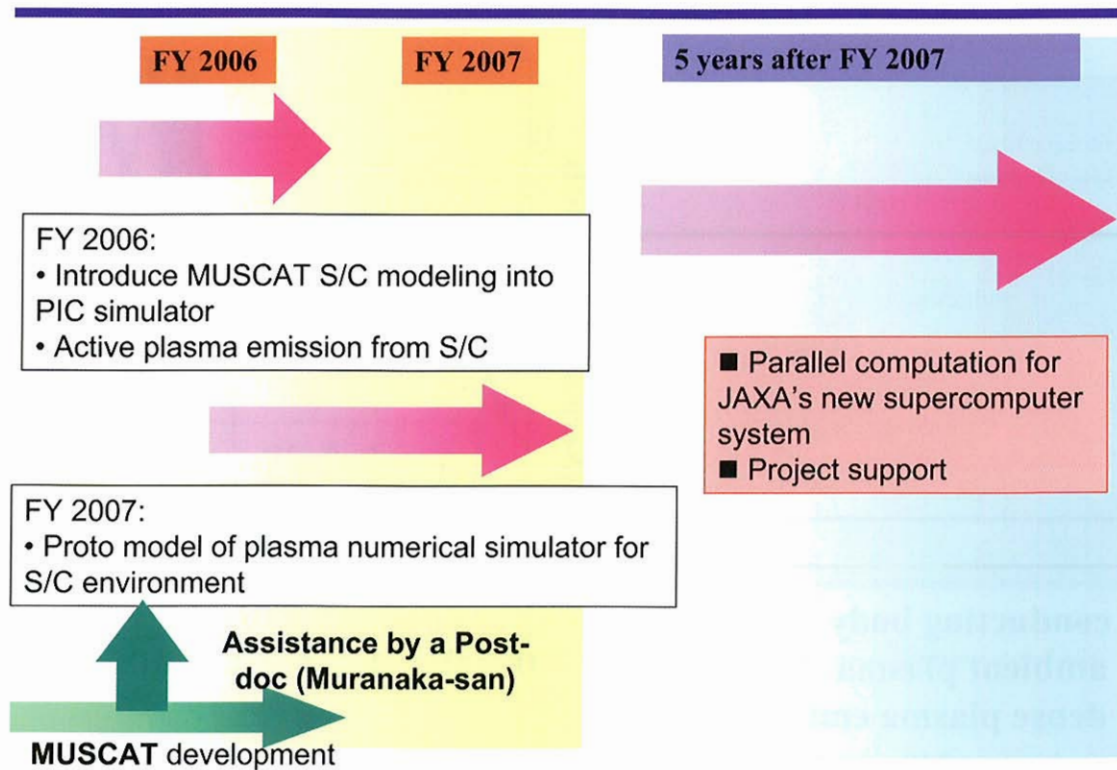
What kind of framework or structure for simulator ?

- Collaboration with multiple people
- Maintenance
- Computer hardware

# Simple model of plasma contactor



## Roadmap



## イオンエンジンのグリッド耐久認定用数値解析ツールの研究開発

### Development of Grid-Life Evaluation Tool for Ion Engines

國中 均

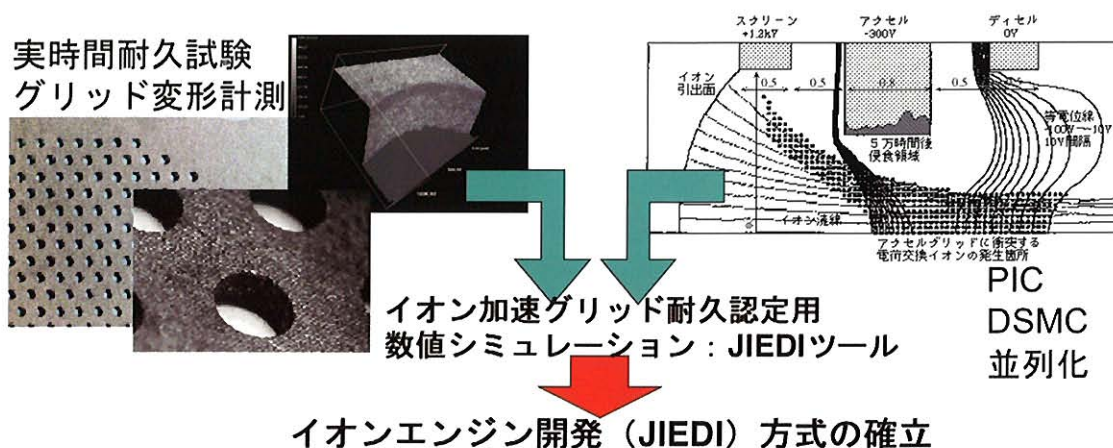
ISAS/JAXA

E-mail: kuninaka@isas.jaxa.jp

ETS-III、ETS-VI、COMETSを経て、ETS-VIIIにて静止衛星へ本格的なイオンエンジン利用が始まろうとしています。地球周辺に留まらず、はやぶさ小惑星探査機の深宇宙動力航行により、新しい宇宙観が開拓されました。地上にあつては、次期の宇宙ミッションを睨み、35cmエンジン・ $\mu 20$ ・ $\mu 10$ HIsp等へ研究開発努力が費やされています。

イオンエンジンのフライトモデル開発に当っては、これまで耐久認定のために実時間で数万時間級の寿命試験を実施してきました。耐久性が向上し、また要求寿命の進展に伴い、このような旧態然とした開発方式では、時機を得た宇宙機の実現がもはや実施不可能になっています。

イオンエンジンの数値解析に関する国内研究意欲は旺盛で、これまで世界に広く貢献して参りました。特に、90年台初頭に東京大学で開発されたイオン軌道解析ツールは、隠れた世界スタンダードであり、 $\mu 10$ イオンエンジングリッド開発に深く貢献しました。この国内蓄積に立脚し、電気推進技術をさらに発展させるために、国内の識者・研究者の英知を結集し、JIEDI(JAXA Ion Engine Development Initiatives)ツールの研究開発に着手しました。これは、イオン・オプティクス数学モデルを実作動試験結果により校正した後、数値解析により積算作動数万時間後、または特定の作動履歴後の寿命評価を実施するものです。JIEDI方式耐久認定により、世界競争力のあるイオンエンジン技術を国内に担保し、近宇宙・深宇宙への橋頭保(foothold in space)を確保することができるでしょう。



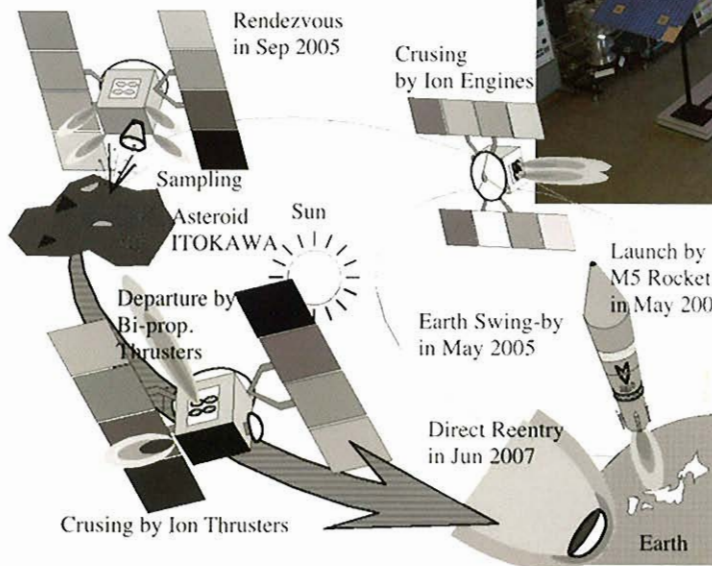
# Development of Grid-Life Evaluation Tool for Ion Engines

## JIEDI(JAXA Ion Engine Development Initiatives)



1

### Asteroid Explorer "HAYABUSA"



Dimensions : 1.0m x 1.6m x 1.1m

Weight : 380kg(Dry)

Chemical Fuel 70kg

Xe Propellant 60kg

Total 510kg

Electric Power : 2.6kW@Earth

Communication : X band

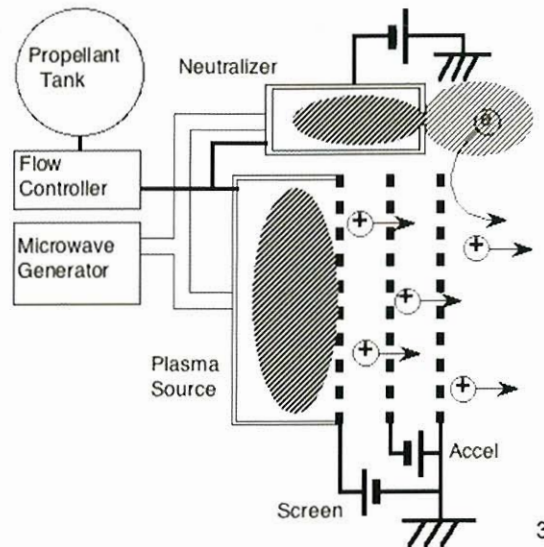
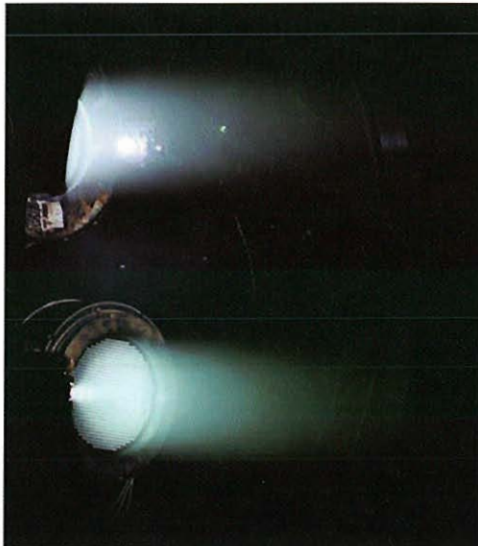
2

## Microwave Discharge Ion Engine

Single microwave (4.25 GHz) generator drives Ion Source and Neutralizer without hollow cathodes.

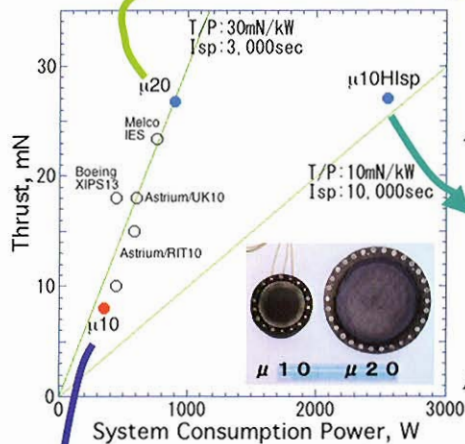
No time limitation for air exposure.

C-C composite material grids are used instead of Molybdenum.



3

## Microwave Discharge Ion Engines $\mu$ family



Achieve 30mN thrust in 2005



Multistage Return



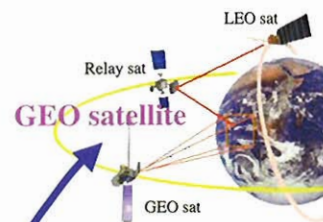
Achieve 10,000sec Isp in 2005



Solar Electric Sail

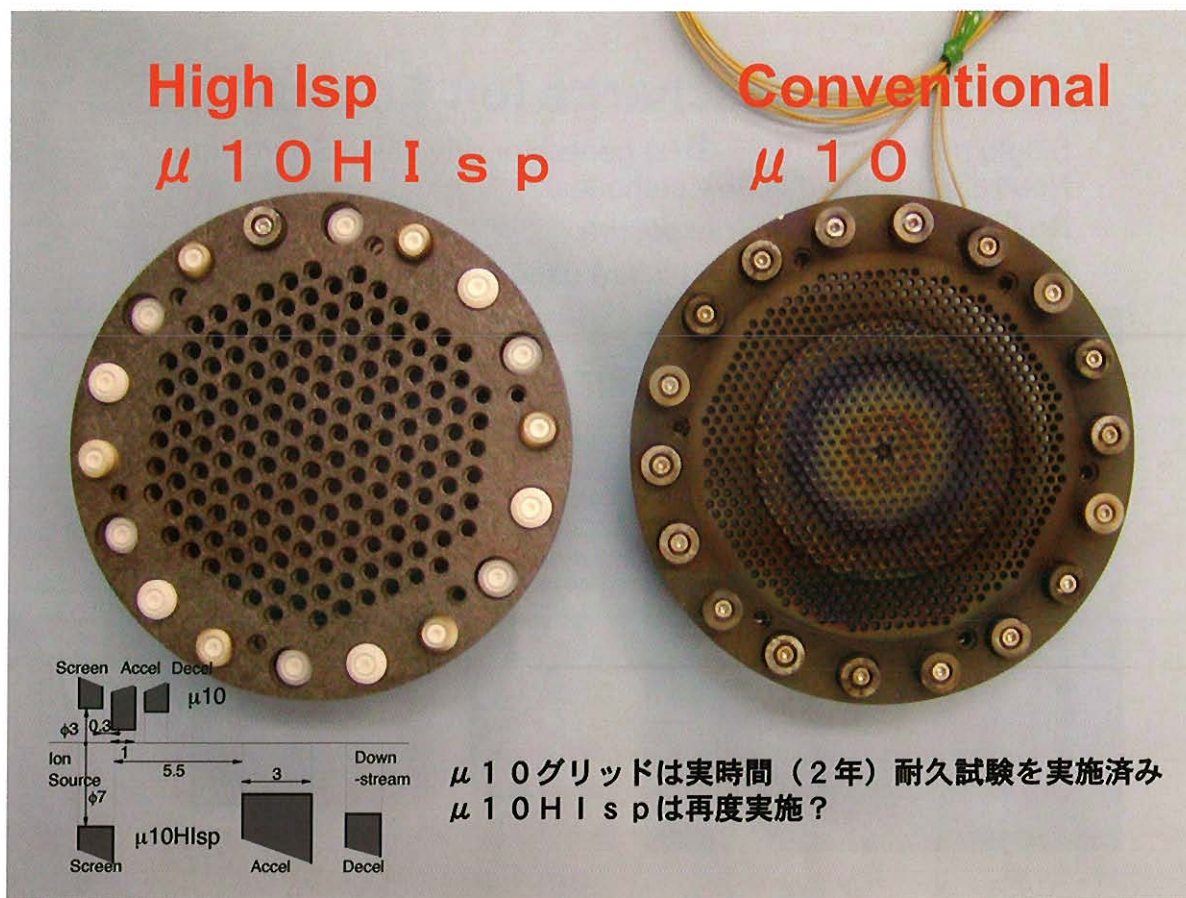


Achieve 26,000hours space operation in 2005



GEO satellite

HAYABUSA Next

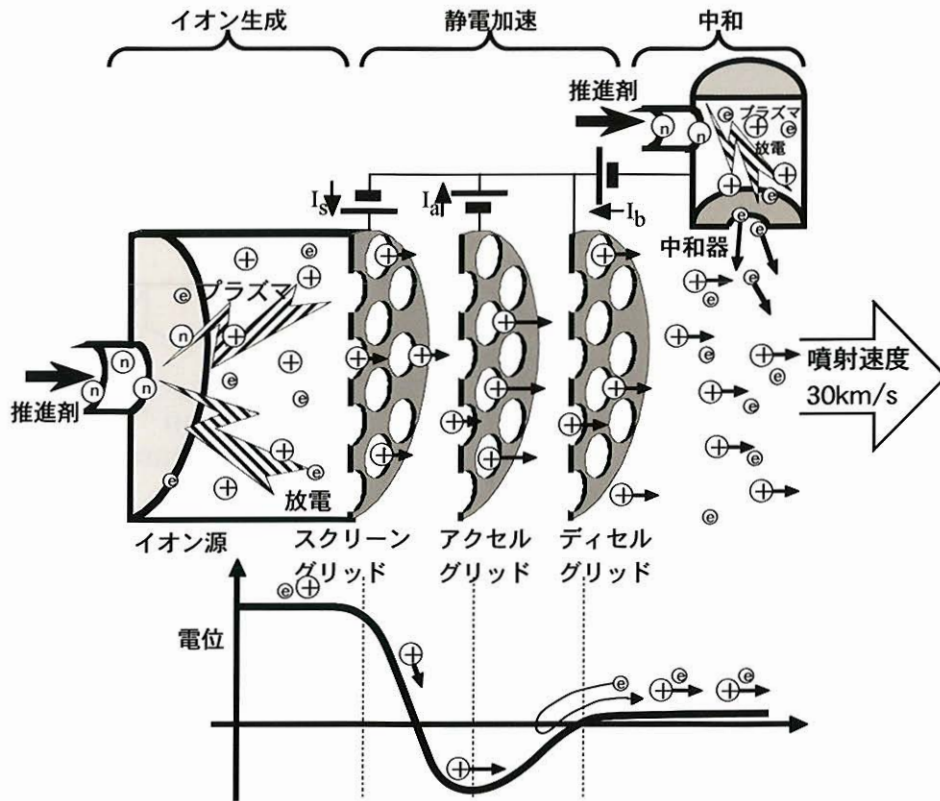


## Failure modes on DC discharge ion engines

- (a) Flakes on screen grid disturb ion acceleration and causes direct impingement to accel grid and resultant structural break.
- (b) Flakes between grids cause electrical short or degrade electrical isolation.
- (c) CEX ions cause structural break of accel grid.
- (d) Enlargement of accel grid hole leads electron back flow.
- (e) Heater snapping of hollow cathodes.
- (f) Erosion of hollow cathode due to plasma impingement in ion source.
- (g) Erosion of screen grid due to plasma in ion source.

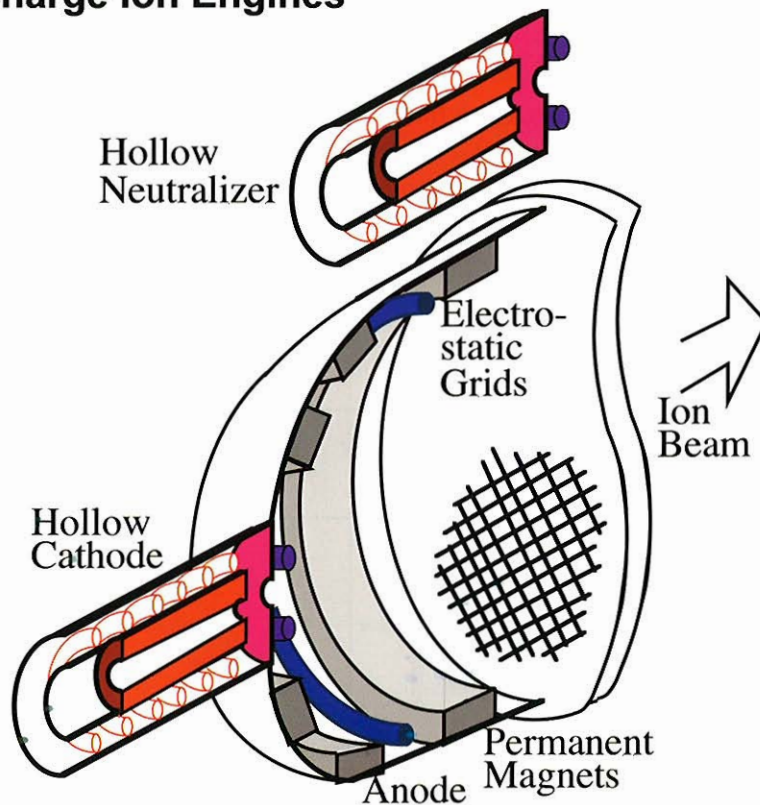
J.R. Brophy, J.E. Polk and V.K. Rowlin, "Ion Engine Service Life Validation by Analysis and Testing", AIAA-96-2715, 1996





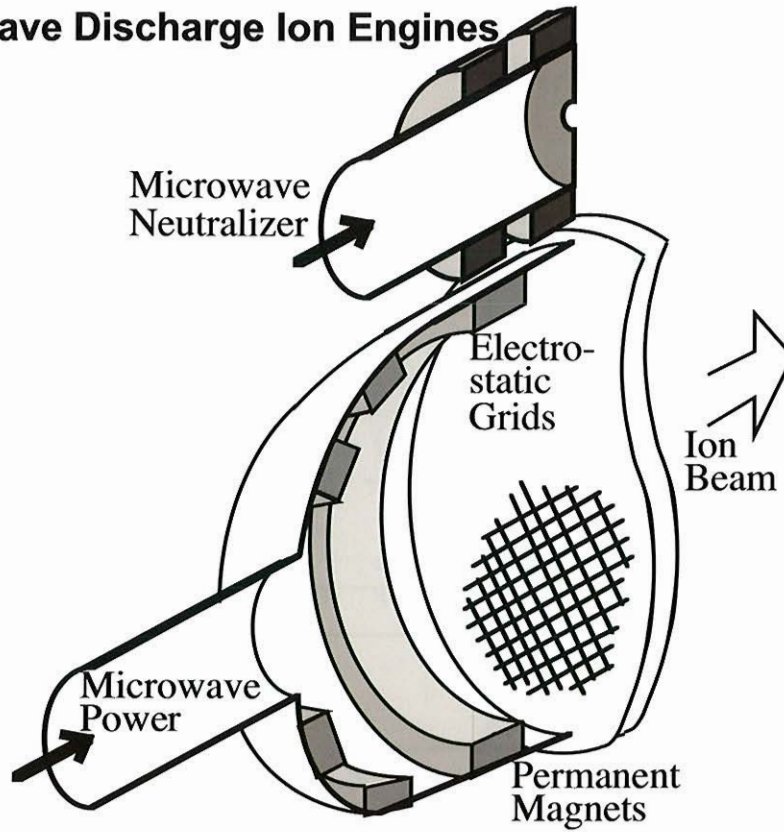
7

## DC Discharge Ion Engines



8

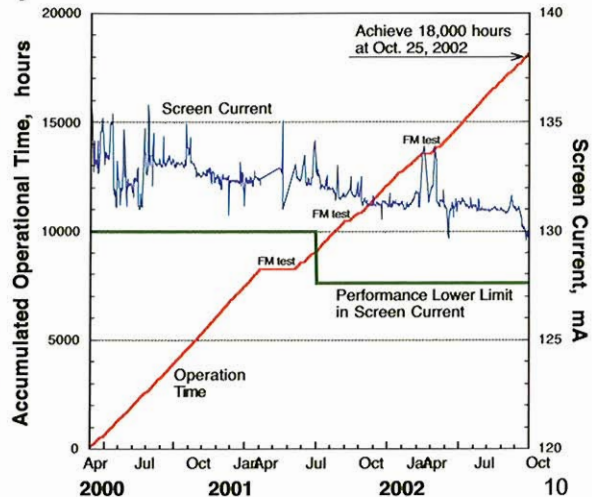
### Microwave Discharge Ion Engines



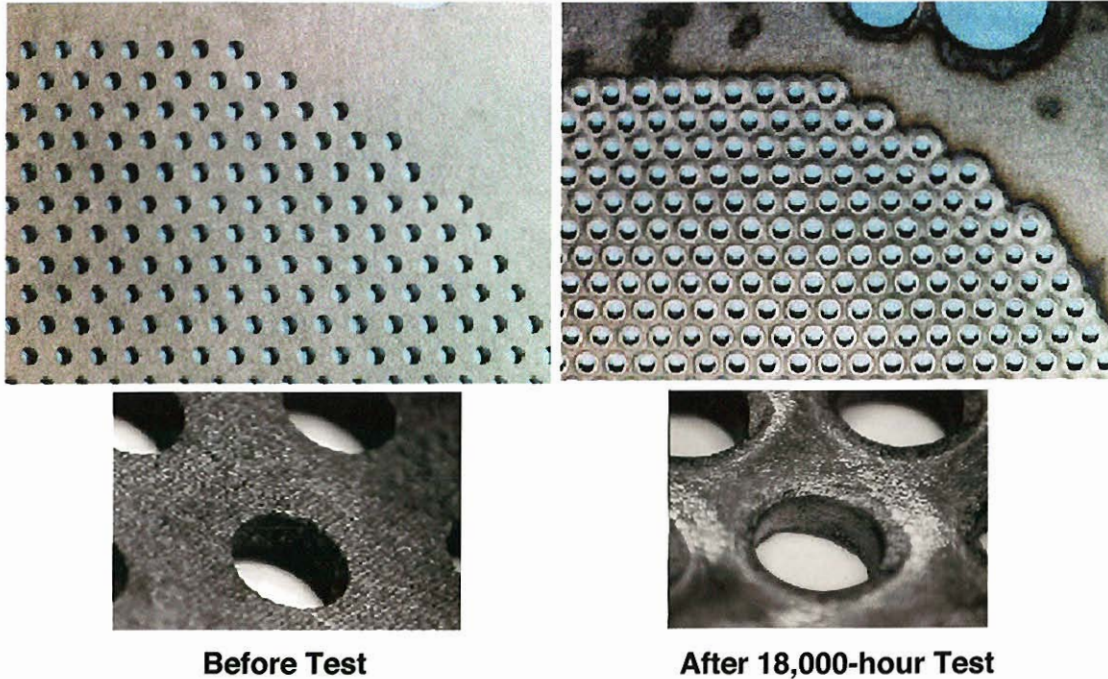
9

### PM-Phase Endurance Test History

PM-phase endurance test achieved 20,000 hours at end of 2002. Whole PM ion thruster head with neutralizer has generated screen current enough to I/F performance during test. There was no interruption except FM performance test and maintenance of test facility.



## Accel Grid Erosion on EM endurance test



11

## Objectives

Construction of Development Scheme of Ion Engine System  
JAXA Ion Engine Development Initiative (JIEDI)  
Development of Grid-Life Evaluation Tool

## Grid-Life Approval Method

JIEDI Tool + Long Term Operation

## Development Scheme

Workshop 2006-2007

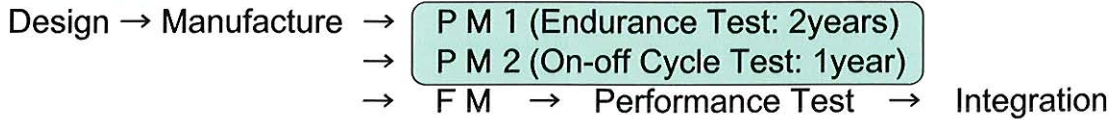
Preliminary Version will be applied to HAYABUSA2

Tool Development 2008-2009

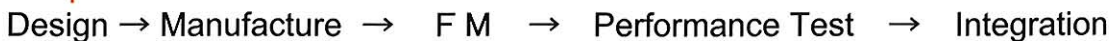
12

# JAXA Ion Engine Development Initiatives (JIEDI) Endurance Qualification Scheme

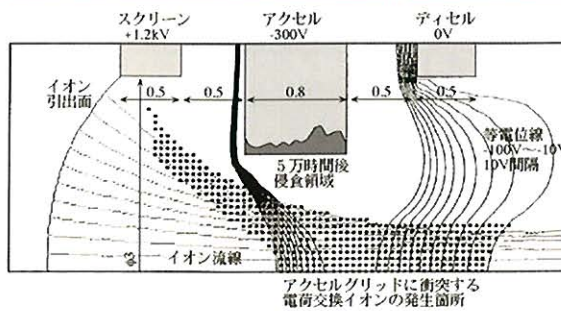
## Old Method



## Proposed Method

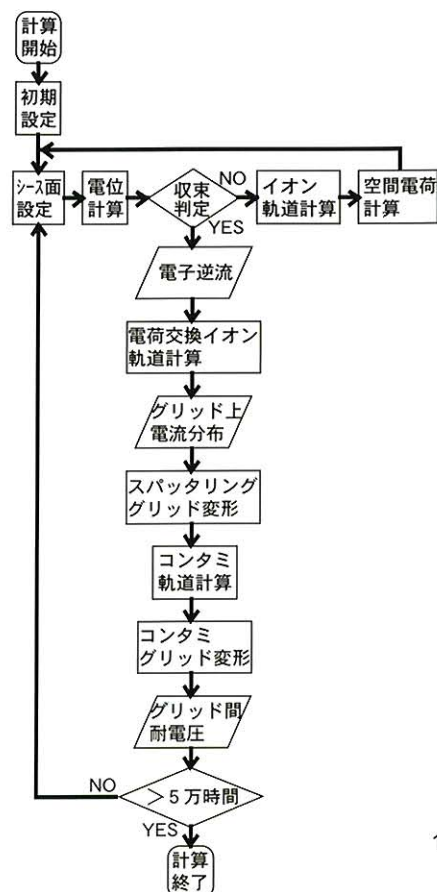
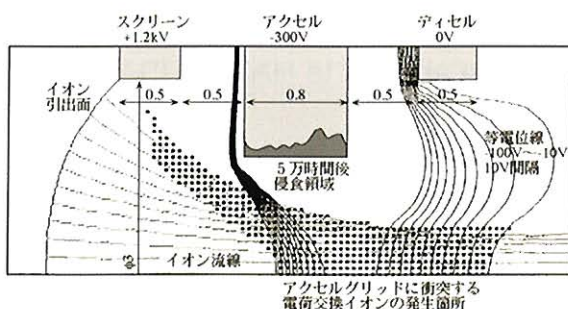


### Endurance Qualification by JIEDI Tool

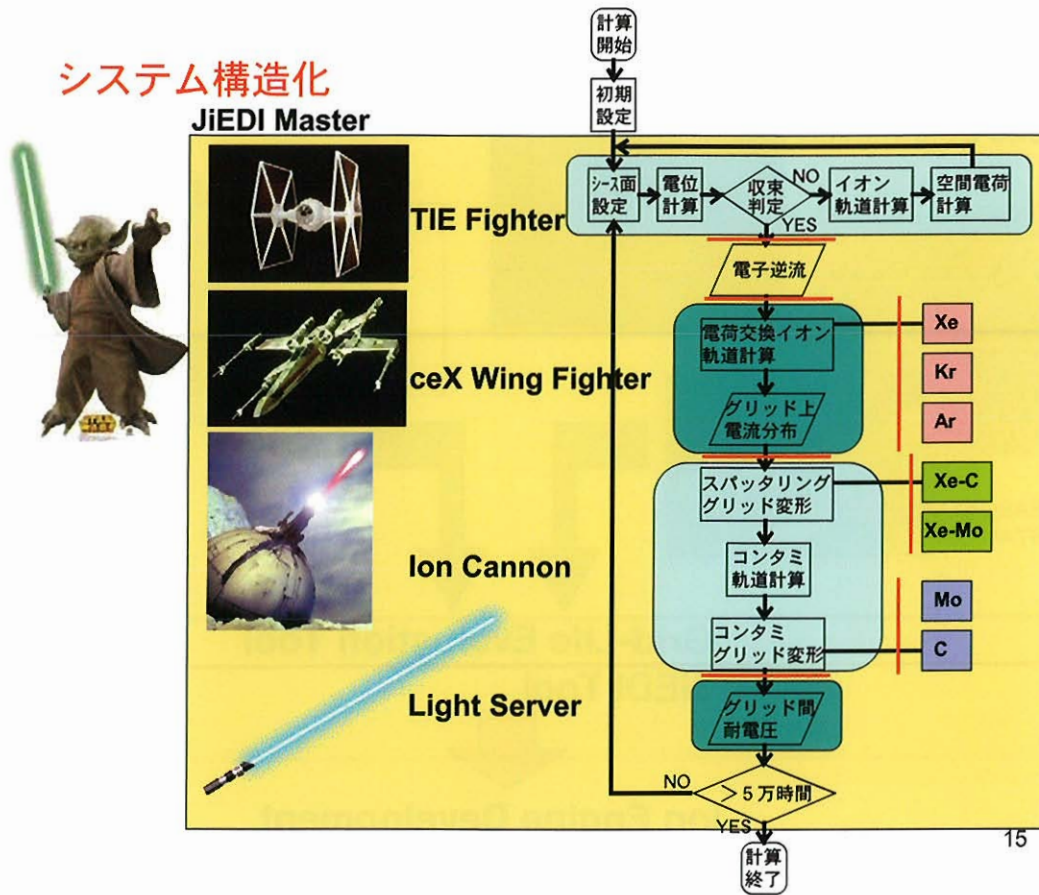


## Outlines of JIEDI Tool

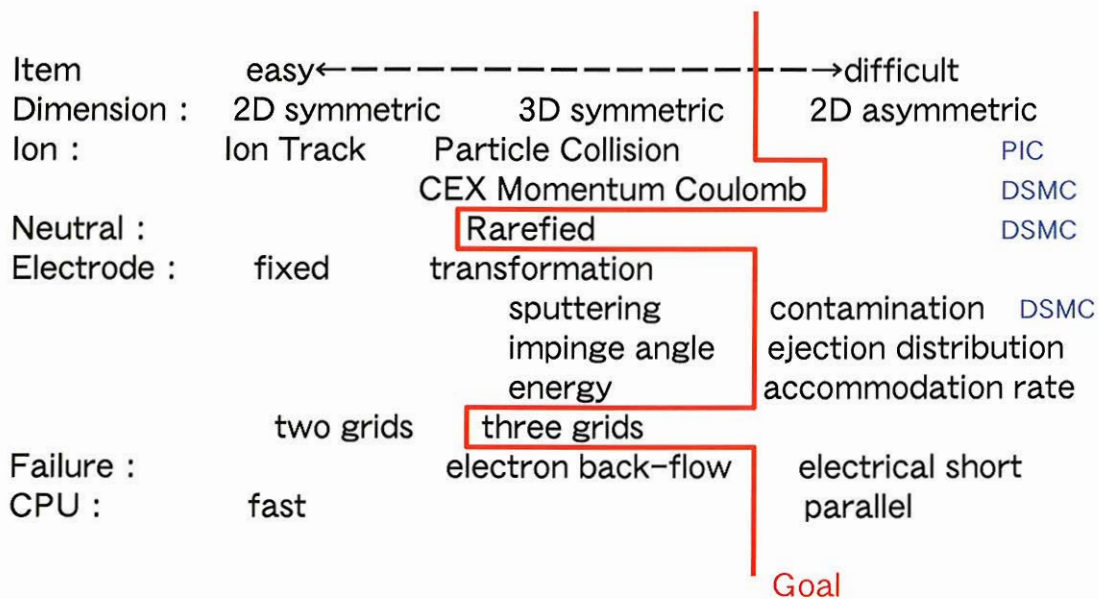
- (1) Three dimensional and asymmetric
- (2) Constant and Time-dependent Bias
- (3) Collision between ions and neutrals
- (4) Grid deformation due to sputtering and contamination
- (5) Failure modes:
  - Electron back-stream
  - Electrical isolation between grids



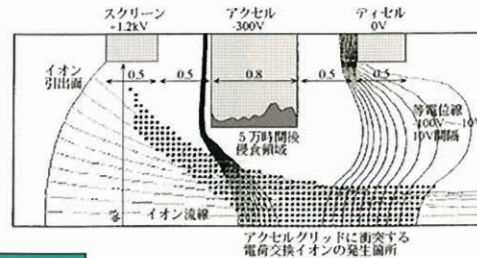
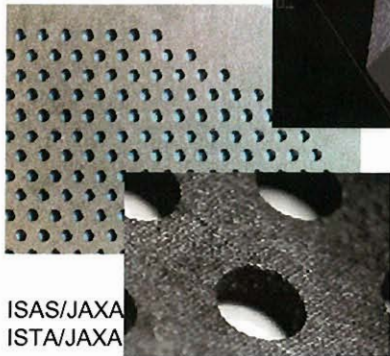
システム構造化



Technologies for JIEDI Tool



Real Time Endurance Test  
Grid Deformation



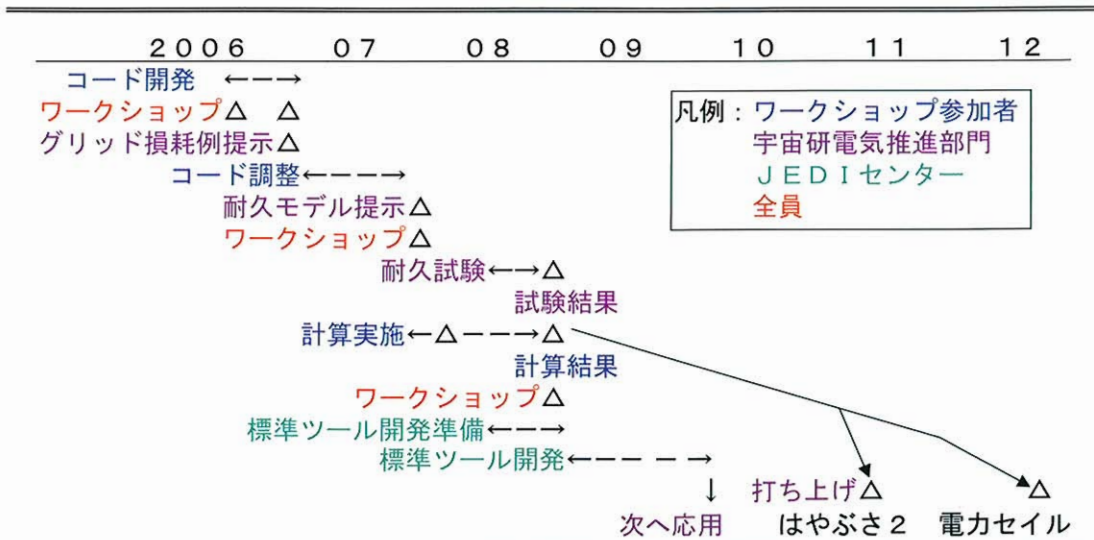
PIC  
DSMC  
並列化

Grid-Life Evaluation Tool  
JIEDI Tool

Ion Engine Development

17

イオン加速グリッド耐久性評価用  
数値ツール(JIEDI)の開発



18年度・19年度：ワークショップ方式（大学系研究者の参画）  
 リファレンス：PM耐久2万時間試験後のグリッドデータ  
 アウトプット：直近ミッション用グリッドの1千時間及び3万時間耐久試験結果予測  
 JAXA研究報告として出版  
 20年度以降：標準ツールの開発

18

## Numerical Simulations of Ion Beam Optics and Grid Erosion for Ion Engine Systems

中野 正勝

東京都立産業技術高等専門学校 ものづくり工学科

E-mail: mnakano@kouku-k.ac.jp

イオンエンジンの研究・開発においてシミュレーションが果たしている役割を紹介するとともに、加速グリッド系の損耗評価の研究例を紹介する。イオンエンジンは推進剤をプラズマ化することによりイオンを作り出し、電位差を加えた加速グリッド系にてイオンを高速に噴射することで推進力を得る電気推進機であり、少ない推進剤で効率よく加速できるという指標(比推力)が高いという特徴を有している。加速グリッド系からイオンビームを放出する際には、加速効率のよいグリッド系を構築する必要があるか、この加速系は多数の孔からなる薄い板で構成されており、実験によってグリッド孔径やグリッド間隔、印加電圧を変えてパラメトリックに評価することは現実的かつ効率的な方法ではない。そこでシミュレーションにより加速グリッド系の設計・評価等が行われてきた。本講演の前半部では、それらの例を示しながらシミュレーションの果たした役割について述べる。後半部では、イオンエンジンの加速グリッド系の寿命評価に焦点を当てる。イオンエンジンのグリッドは、高速なイオンの噴射の副産物である遅いイオンや大きな発散角を持ったイオン、また中性粒子の衝突を受け損耗を受ける。それら損耗を評価するためのシミュレーション法と適用例を示す。

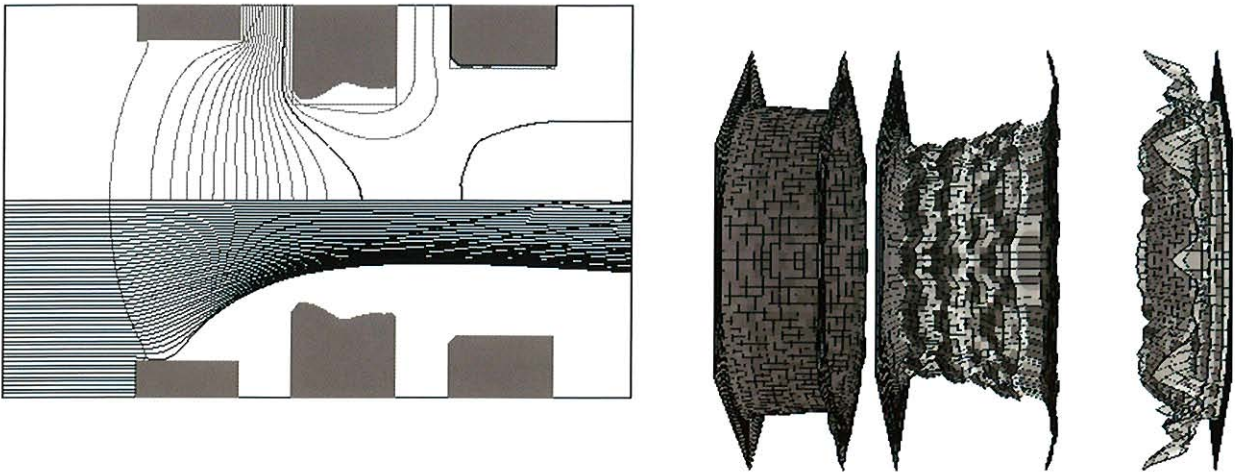


図 13 枚グリッドの損耗の様子 [(左)2次元軸対称モデル, (右)3次元モデル]

# Numerical Simulations of Ion Beam Optics and Grid Erosion for Ion Engine Systems

Masakatsu Nakano

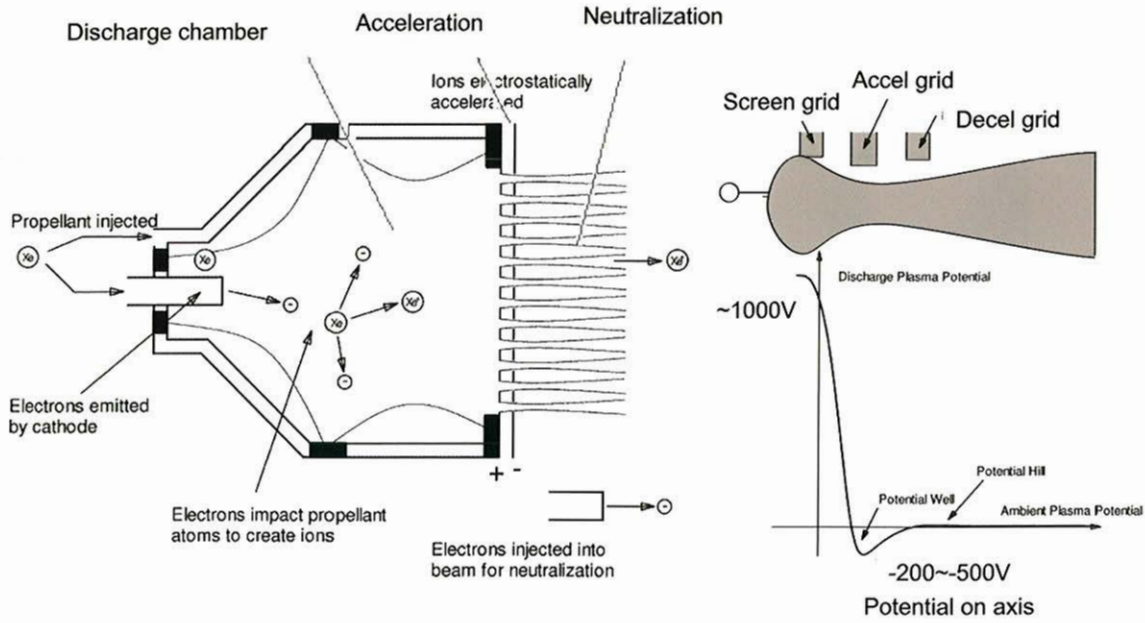
Tokyo Metropolitan College of Aeronautical Engineering

## Outline

- **Simulation needs**
  - Optics design
    - Achieve higher thrust performance
    - Avoid direct impingement, electron backstreaming
  - Lifetime evaluation
    - Grid erosion
- **New 3-D simulation code**
  - Ions from elastic collisions
  - Neutrals
  - Redeposition (sticking effect)



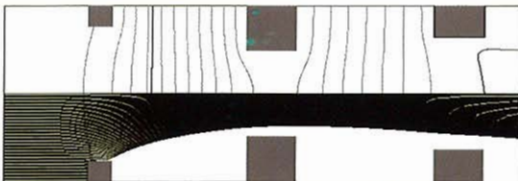
# Ion engine system



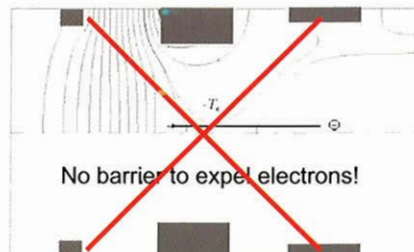
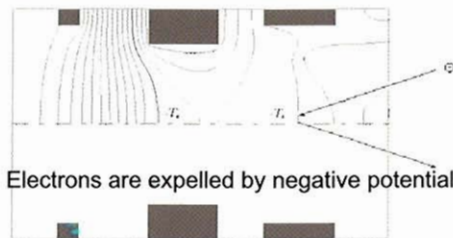
# Simulation needs

- Parametric study
  - Grid optics design
    - Achieve higher thrust performance
    - Avoid direct impingement and electron backstreaming

Screen grid    Accel grid    Decel grid



Direct impingement

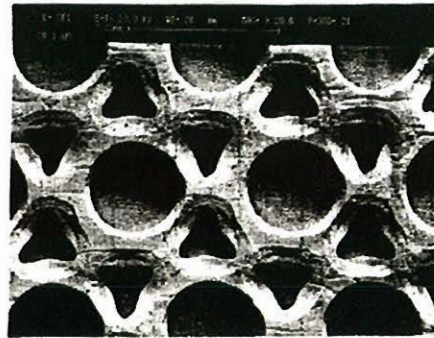
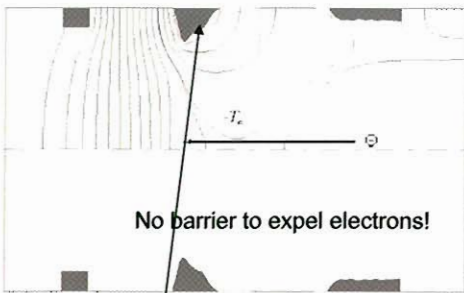
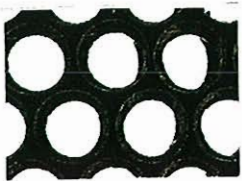
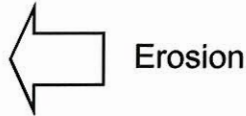


Negative accel voltage is not enough.

# Simulation needs

- Lifetime estimation of the grids

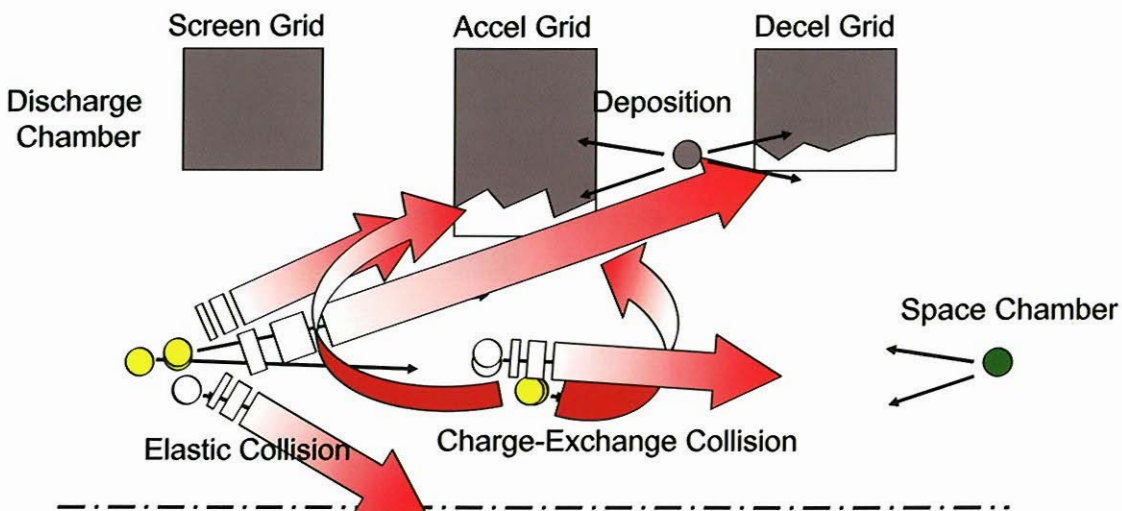
- Electron backstreaming
- Structural failure



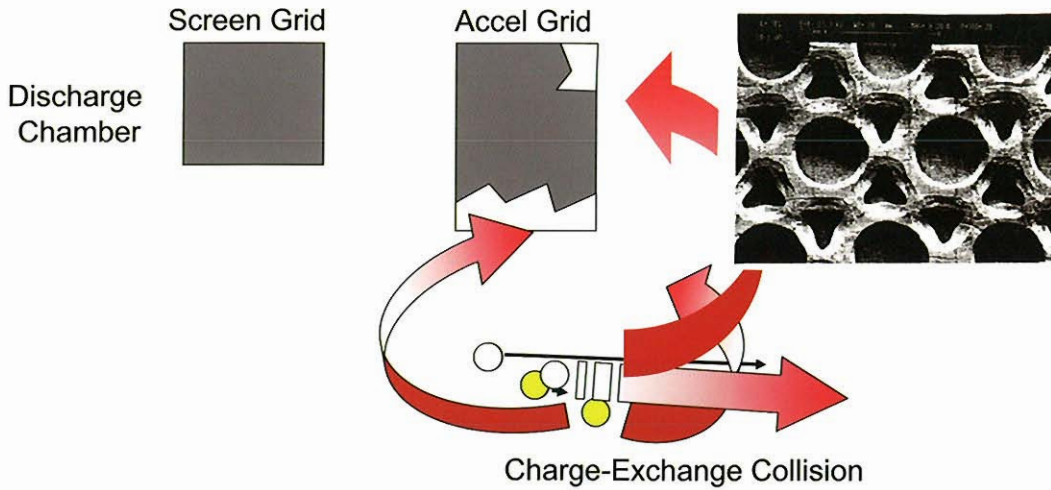
Downstream side of the accel grid

The accel grid is too eroded to apply negative voltage.

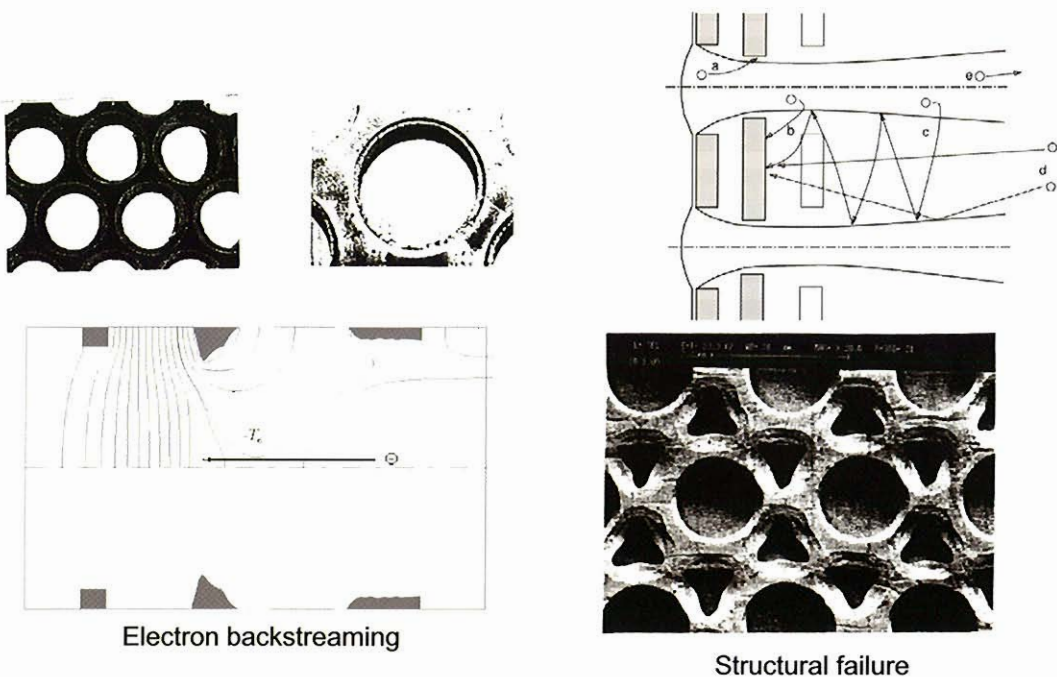
## Grid erosion (3-grid system)



# Grid erosion (2-grid system)



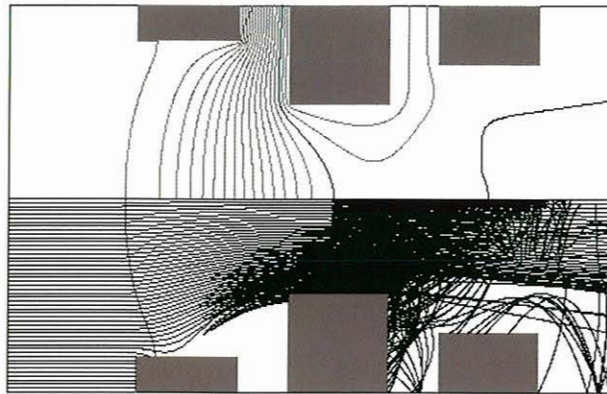
# Lifetime estimation of the grids



## Grid life simulation for 3-grid system

### Geometry change of the grid system

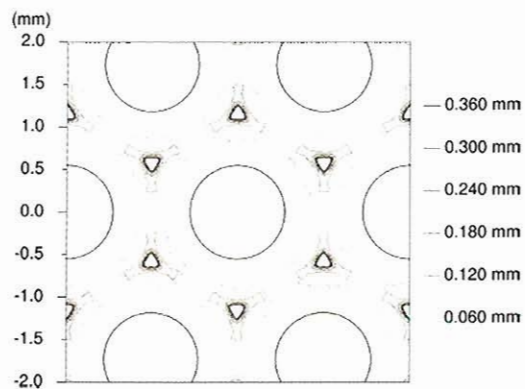
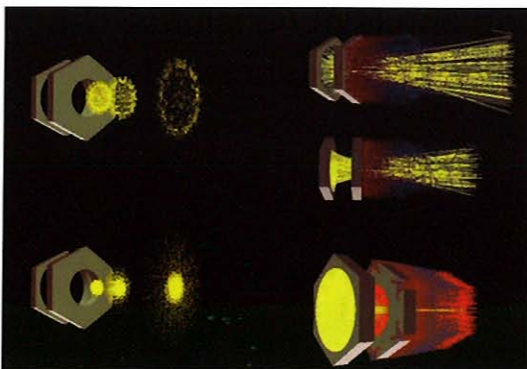
- 2-D asymmetric model (Nakano and Arakawa(1999))
- Erosion due to the sputtering of CE ions



## Grid life simulation for 2-grid system

### 3-D simulation (Nakano and Arakawa(1999))

- Erosion due to the sputtering of CE ions



# New optics code

- Motivation

- More correct and reliable lifetime estimation
  - Geometry change of the grid system by erosion and redeposition
  - More accurate model
    - Tracking following particles
      - » Mainstream ions
      - » Ions and neutrals from elastic collisions
      - » Charge exchange ions and neutrals
    - Sticking effect of sputtered atoms
- Design tool
  - Simple
    - Ions, neutrals and atoms are considered as beams
    - Electron density is calculated from Boltzmann relationship

## Model

- Potential and densities

- $\nabla\phi = -(\rho_i - \rho_e)/\epsilon$ 
  - $\rho_i = \sum J_k / v_{izk} / S$
  - $\rho_e = \rho_{e0} \exp(-e\phi / k_B T_e)$

- Beam trajectories

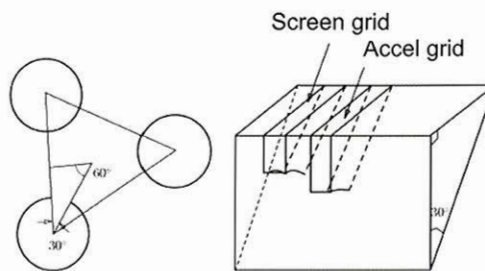
- $M\mathbf{v}\nabla\mathbf{v} = -q\nabla\phi$

- Collisions

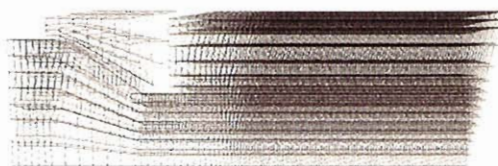
- $J_{ce} = \sum J_k |\mathbf{v}_{ik} - \mathbf{v}_n| n_n \sigma_{ce} \Delta t_k$
- $J_{els} = \sum J_k |\mathbf{v}_{ik} - \mathbf{v}_n| n_n \sigma_{els} \Delta t_k$

- Sputtering

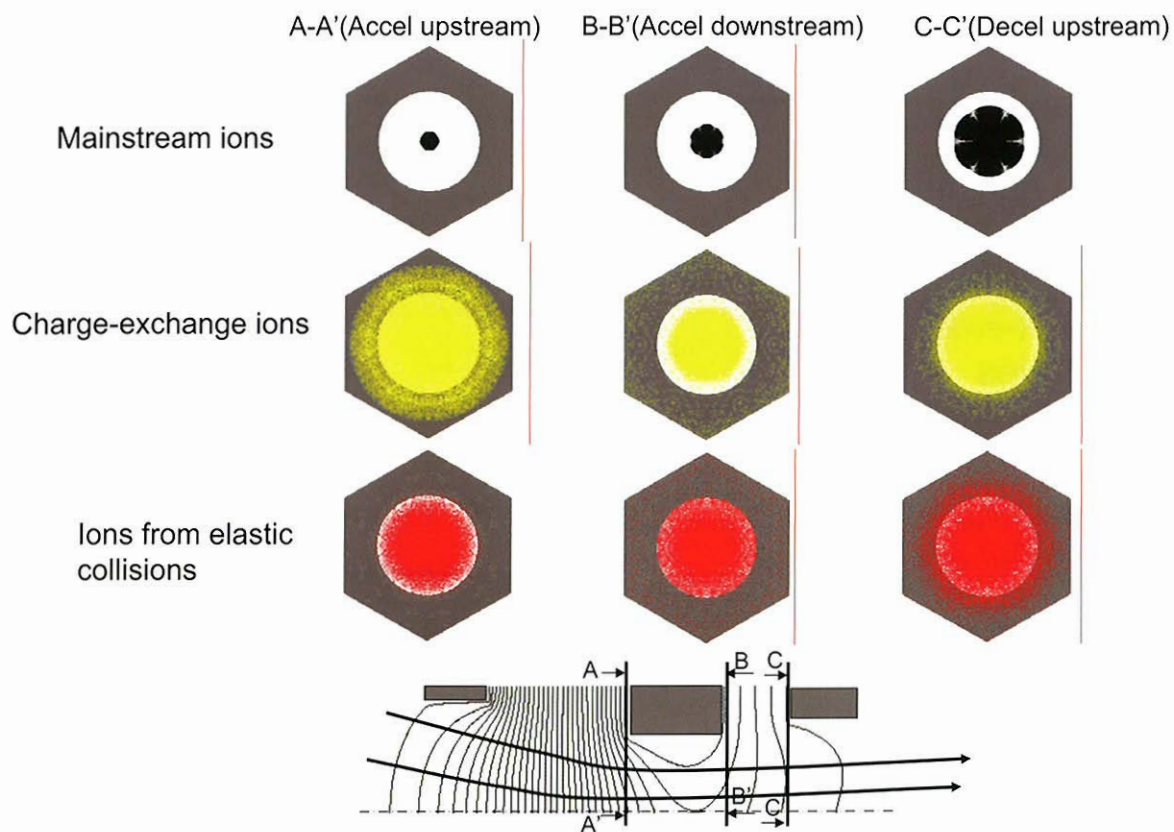
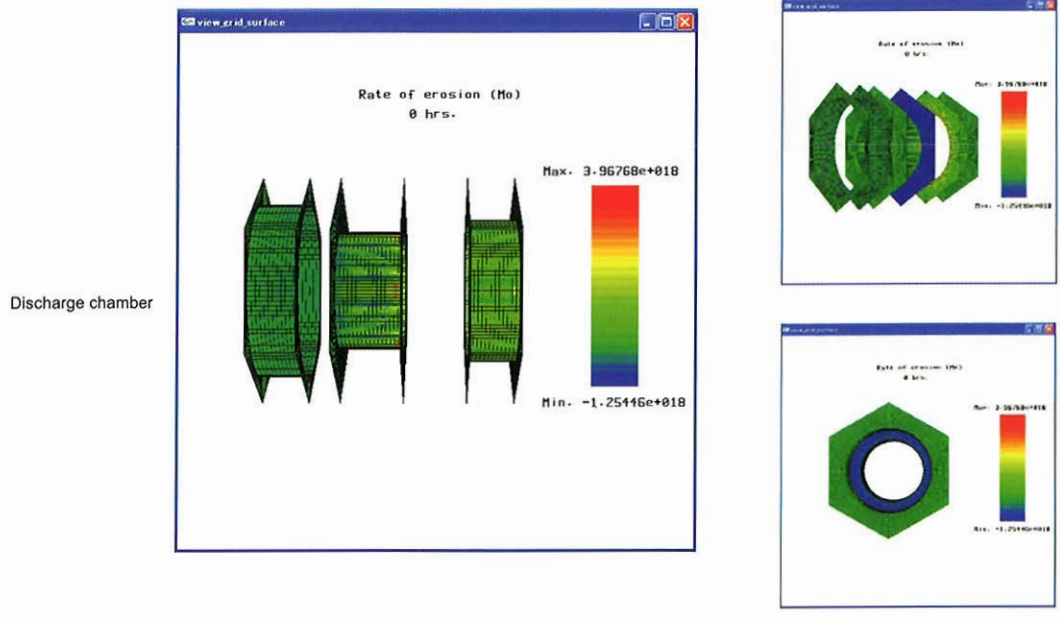
- $m_i = J/e \times Y(E, q)$



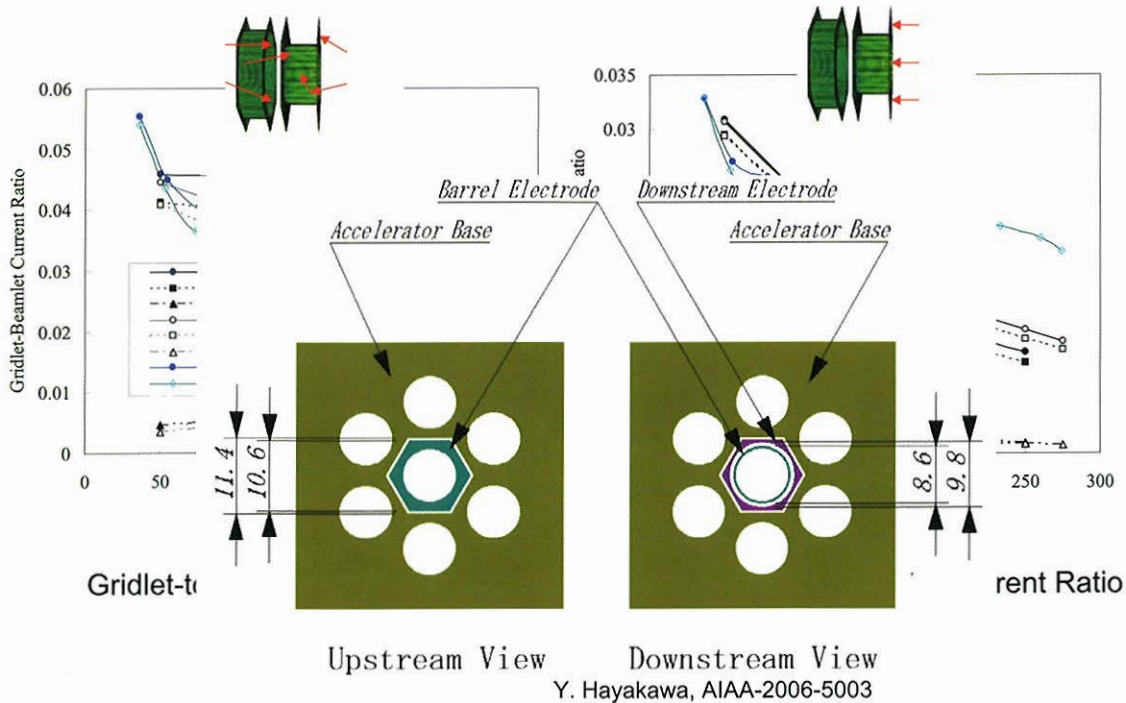
Simulation domain



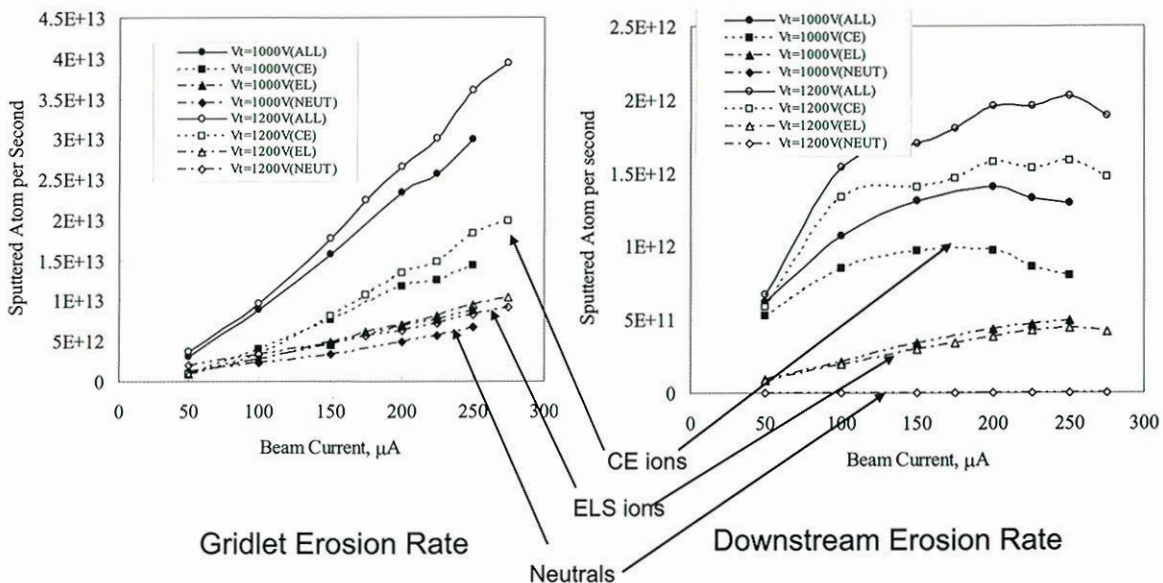
# Grid geometry change from BOL to 10000hrs



## Comparison of accel grid current

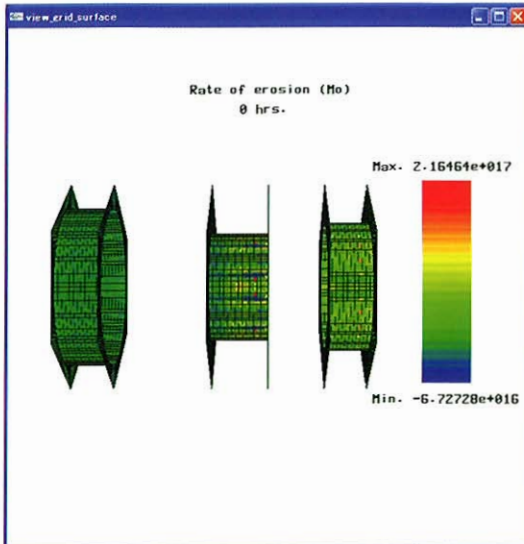


## Effect of elastic ions and neutrals on erosion

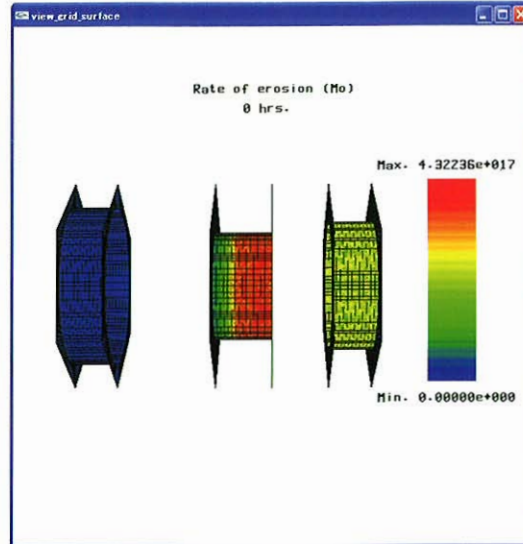


# Effect of redeposition

## NAL 3-grid system from BOL to 40,000hrs



With sticking effect



Without sticking effect

## Summary

- Simulation
  - Grid optics design
  - Lifetime estimation
- New simulation code
  - Elastic collision
  - Neutrals
  - Sticking effect
- Need more reliable database
  - Sputtering yield
  - Collision cross section
  - Sticking factor
  - Electron model
    - Electrons behave as  $\rho_e = \rho_{e0} \exp(-e\phi/k_B T_e)$  ?



## MUSCAT project and its application to plasma plume analysis

Takanobu MURANAKA, Shinji HATTA, Jeongho KIM, Mengu CHO  
(LaSEINE, Kyushu Institute of Technology)

Hiroko O. UEDA, Kiyokazu KOGA, Tateo GOKA (JAXA)

E-mail: [muranaka@ele.kyutech.ac.jp](mailto:muranaka@ele.kyutech.ac.jp)

Development of MUSCAT (Multi-Utility Spacecraft Charging Analysis Tool) had started in November 2004 as a quantitative spacecraft charging analysis tool in Japan. In the middle of development term, the beta version of MUSCAT has been released on March 2006 as the first version of integrated software. The integrated GUI tool of MUSCAT, called “Vineyard,” had been developed, which conducts the MUSCAT simulation on local Windows® PC. Functions of “Vineyard” have parameter input panels including 3D satellite model, data converter from parameters in the GUI format into those in the solver format. As the development of the physical functions, fundamental physical elements such as photoelectron emission, secondary electron emission, auroral electrons had been included. As a result, the solver enables fundamental charging analyses at GEO, LEO and PEO, which makes MUSCAT feasible for multi-utility use. Parallelization and tuning of the code have almost been achieved, and 8CPUs parallel computation can calculate absolute potential of a large-scale satellite model in a half size of maximum computation region of 256x64x128 in two days. Experiments for the code validation were made at LaSEINE in KIT. Spatial distribution of electric potential around the electrode of a Langmuir probe and IV characteristic curve were measured, and we had good agreement in experimental results and the numerical ones. These results show that the physical functions of MUSCAT simulate charging processes quite well.

For a function of plasma plume analysis of the MUSCAT solver, we consider a model of active emission of ions, which employs a fixed analytical beam ion profile and electrons of Boltzmann distribution. Distributions of CEX ions are obtained by PIC method, and electric field is obtained by solving non-linear Poisson equation. Backflow of CEX ions to spacecraft surface would contribute to fluctuations of the surface potential. The modeling and coding of that are now under development. Final version of MUSCAT will be released in March 2007 with this function.

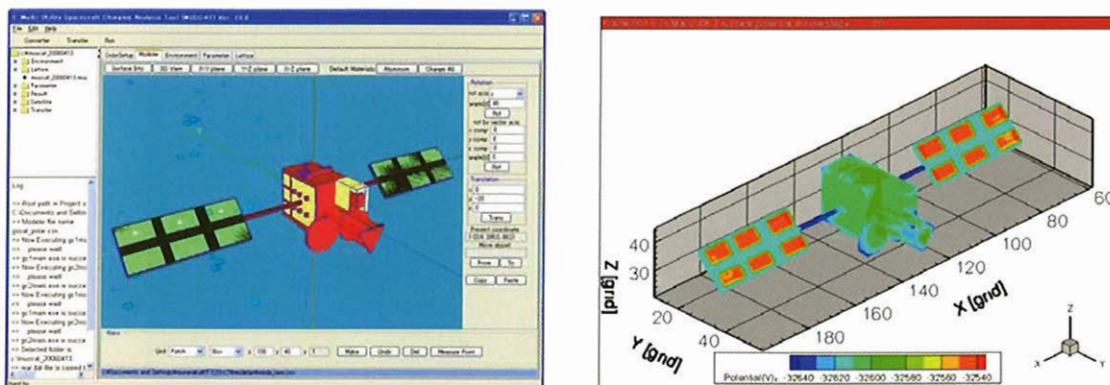


Fig. 1. A model of the WINDS satellite composed by the 3D satellite modeler of “Vineyard” (left), and the numerical result of satellite surface potential of the model (right).



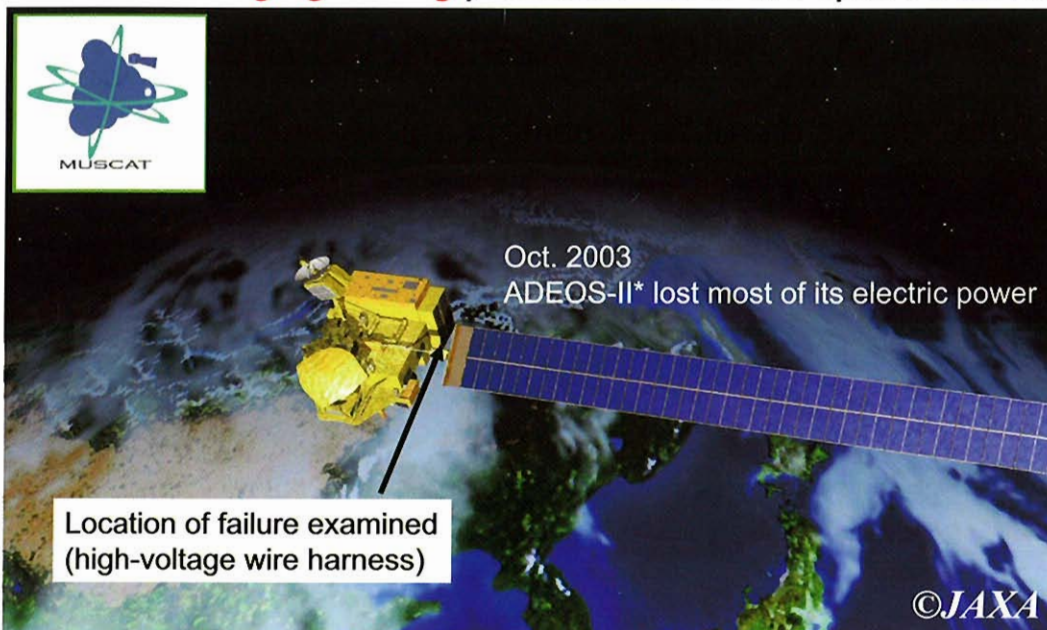
## MUSCAT project and its application to plasma plume analysis

OTakanobu Muranaka, Shinji Hatta, Jeongho Kim,  
Satoshi Hosoda, Mengu Cho  
(LaSEINE, Kyushu Institute of Technology)  
Hiroko O. Ueda, Kiyokazu Koga, Tateo Goka  
(JAXA)

JAXA/JEDI workshop  
2-3 October 2006, Tokyo, JAPAN

## Quantitative Analysis Tool is Required

Spacecraft **Charging-Arcing** problem lead to the spacecraft failure



\*ADEOS-II: Polar Orbit Satellite: paddle size 3 x 24 (m) (JAPAN)

1

# MUSCAT: Multi-Utility Spacecraft Charging Analysis Tool

## multi-purpose satellite charging analysis tool

- Schedule
  - Nov. 2004 (started)--Mar. 2006 (β ver.) --Mar. 2007 (final ver.)
- Modeling of interaction between spacecraft and space environment
  - Calculation of satellite charging at LEO, GEO, PEO
- High-speed computation
  - Parallelization and tuning of algorithm
  - Calculation completed in half a day with workstation (final)
  - Simple calculation method in the final version (final)
- Graphical User Interface (GUI)
  - 3D satellite modeling with JAVA3D
  - Input of initial parameters (material, environment, numerical)
  - Output of numerical results

2

## Framework of the development

General overview		JAXA
Code development	Solver Speeding up GUI	KIT
Offering space environmental parameters		JAXA
		NICT
Validation experiment		KIT
		ISAS/JAXA
Validation by large scale calculation		GES(Kyoto Univ., NIPR)

3

## Functions of the Beta Version

- GUI
  - Integrated GUI tool, “Vineyard”
- Solver
  - Includes fundamental physical element functions at LEO, GEO, and PEO
- Speeding-up
  - Users can perform a large scale computation (full scale:256x128x128)
- Experiment (explain if it has enough time)
  - Fundamental validation of the solver
- Plasma plume analysis (topic of near future work)

4

## Development of GUI

# “Vineyard” conducts computation

## “Vineyard”-Integrated GUI Tool

### Input parameters

Windows PC

- 3D satellite modeling
- Input parameters of materials etc.

### GUI-Solver converter

- To converter GUI model to rectangular grid model

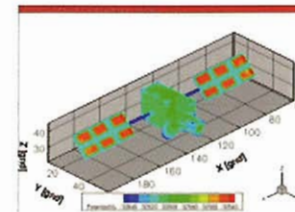
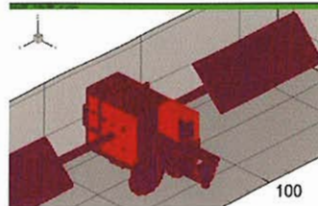
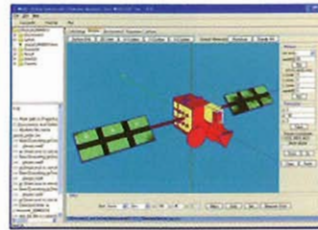
### Solver

Workstation

- Speeding up by parallelization

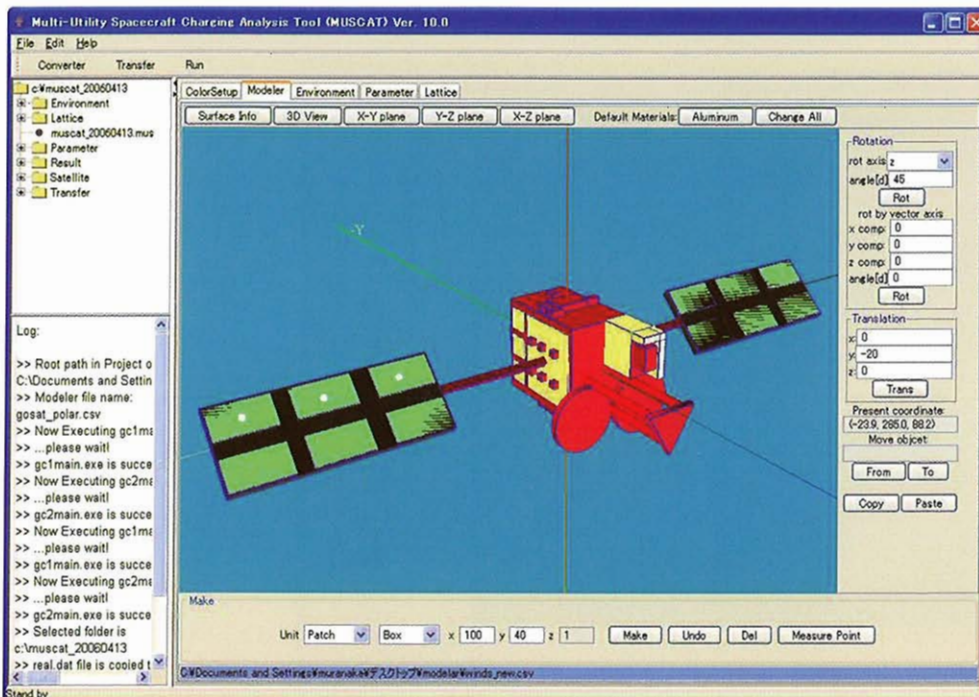
### Output of the results

Windows PC



6

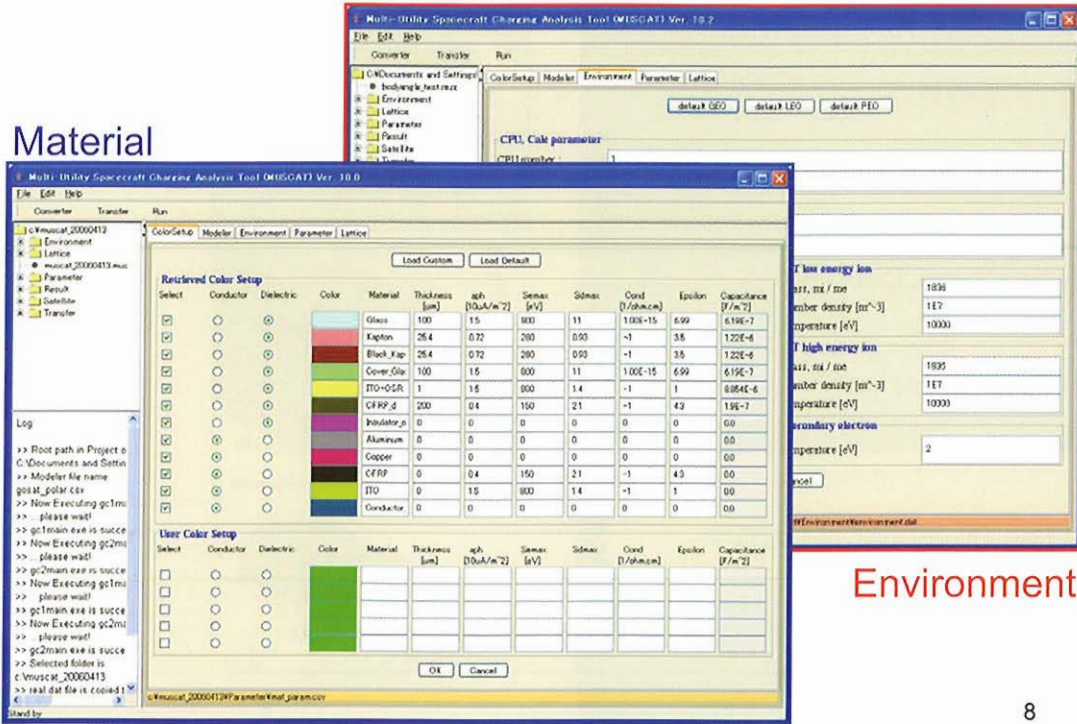
## 3D Satellite Modeler of “Vineyard”



7

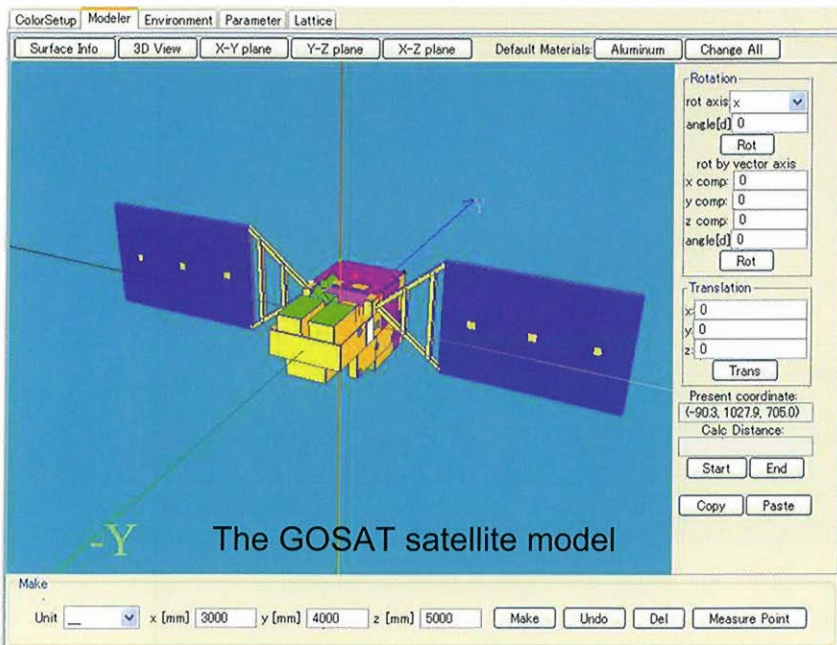
# Parameter Setup Panels of "Vineyard"

## Material



Environment

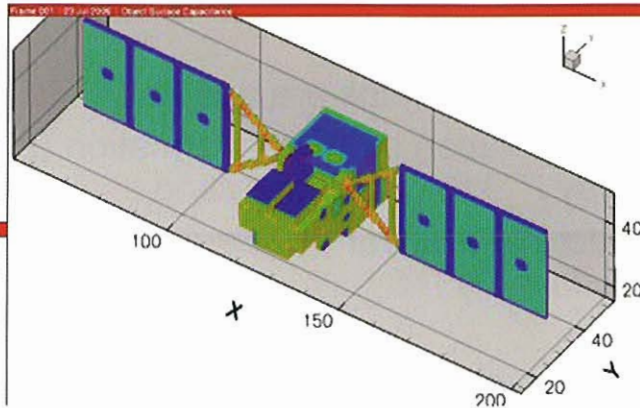
# Example of Large Scale Satellite modeling



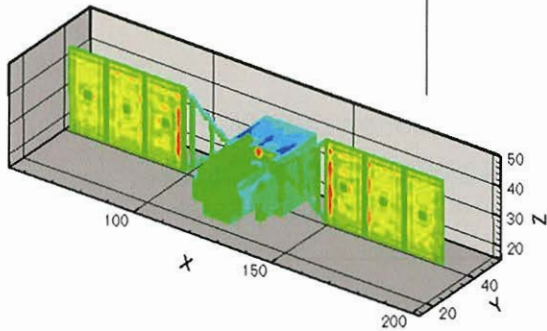
## Converter and numerical result

The GOSAT satellite model

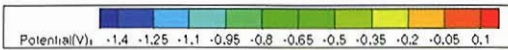
Surface Potential  
(Numerical Result)



Grid Satellite Object by "Converter"



Scale: 256x64x128  
Object element: about 10,000



10

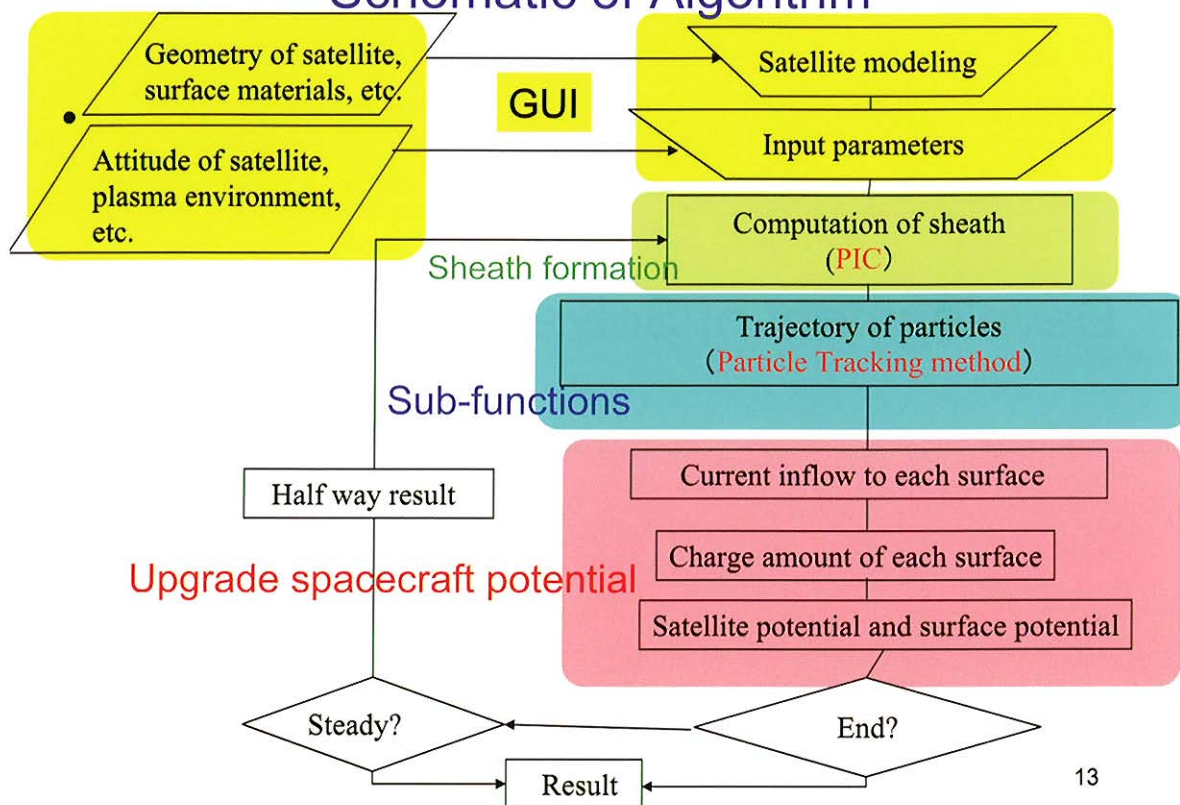
## Development of Solver

## Features of MUSCAT Solver

- Electrostatic(ES) particle code
- Rectangular numerical grids are adopted
- Independent calculation of sheath formation (by PIC) and particle flow (by PT) to reduce iteration time
- Update spacecraft potential by calculating net charge on the spacecraft surface by PT
  
- Included physical elements in PT part at present
  - Ambient electrons and ions (double Maxwellian distribution option)
  - Photoelectron emission(PEE) & Secondary electron emission(SEE)
  - Bulk conductive current
  - Auroral electrons
- These fundamental physical elements enables users to simulate spacecraft charging at GEO, LEO and PEO

12

### Schematic of Algorithm



13



## Examples of PEE and SEE Computations

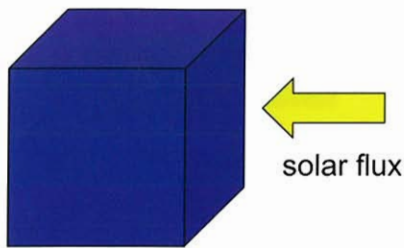
### Numerical parameters

Domain (grid)	32x32x32
Object size (grid)	4x4x4
Spatial width (m)	0.2
Temporal width (s)	10 <sup>-5</sup> ~10 <sup>-3</sup>

### Material parameters

PE current density (A/m <sup>2</sup> )	4.2x10 <sup>-5</sup>
PE temperature (eV)	1.5
SE E <sub>max</sub> (eV)	300
SE δ <sub>E<sub>max</sub></sub>	2.0
SE temperature (eV)	2.0

Conductive cube

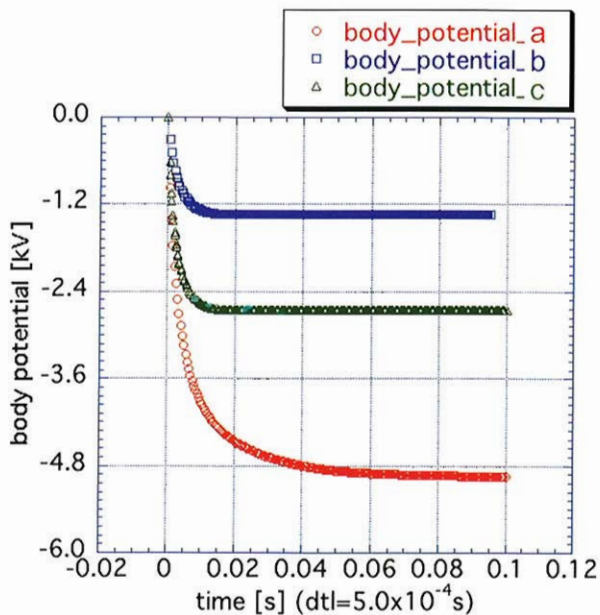


Floating potential

PE: Photoelectron  
SE: Secondary electron

14

## Examples of PEE and SEE Computations



Ambient Ions and Electrons

$n=2 \times 10^7$  [m<sup>-3</sup>],  $T=1.0$  [keV]

$\lambda_D = 52.5$  (m)

	photo	second
a	x	x
b	○	○
c	○	x

Absolute potential

$\phi_b > \phi_c > \phi_a$

15

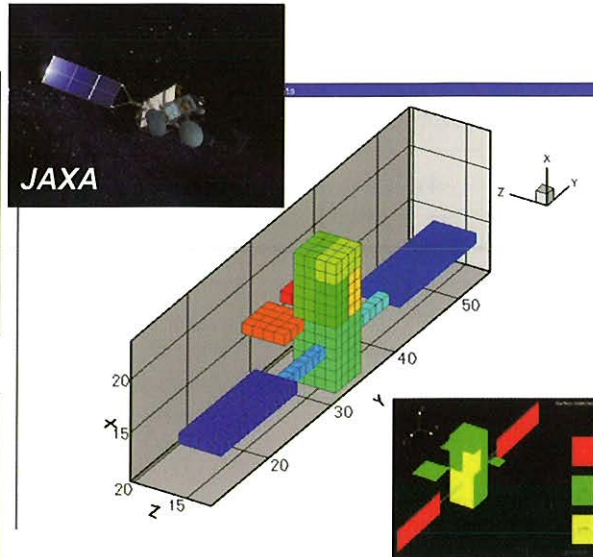
# Example of Integrated Solver Test

## Numerical parameters

Domain (grids)	32x64x32
Number of grids (object)	610
Spatial width (m)	0.625
Temporal width (x10 <sup>-2</sup> s)	1.0-1.7

## Environment parameters

Electron density (cm <sup>-3</sup> )	1.25
Electron temperature (keV)	7.5
Ion density (cm <sup>-3</sup> )	0.25
Ion temperature (keV)	10



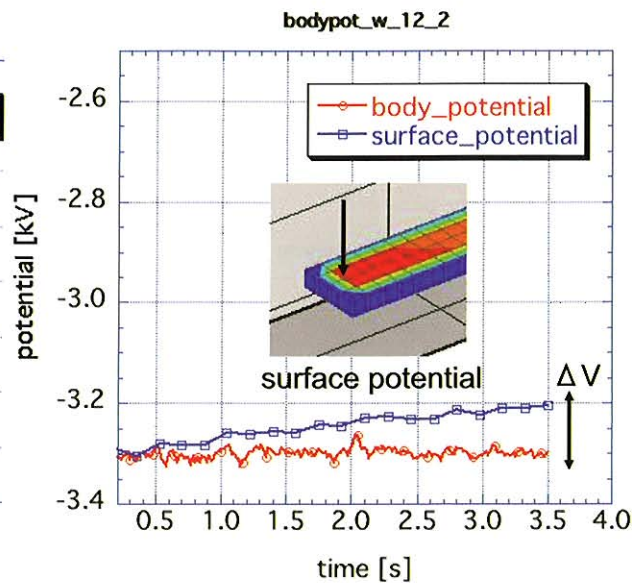
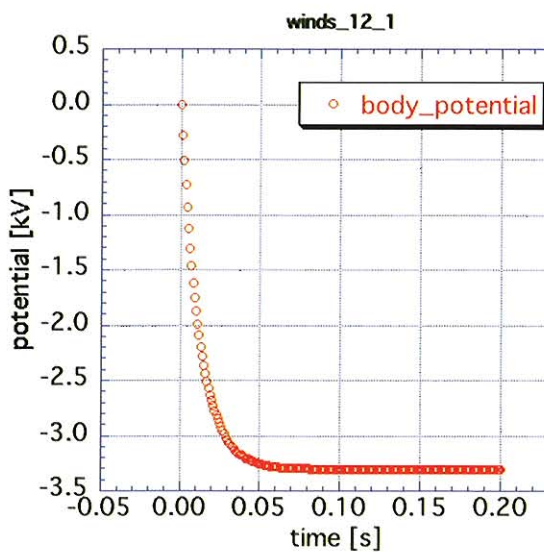
the WINDS satellite model adopted to MUSCAT calculation

with ambient plasmas, PEE, SEE, conductive current

16

# Numerical Result of Absolute Potential

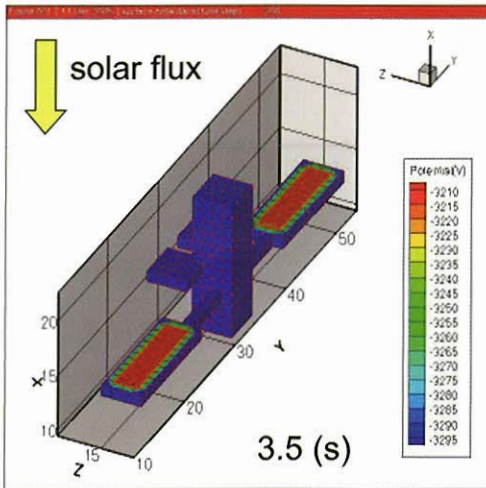
LT=0:00,  $\Delta V=90$  (V) @3.5 (s)



17

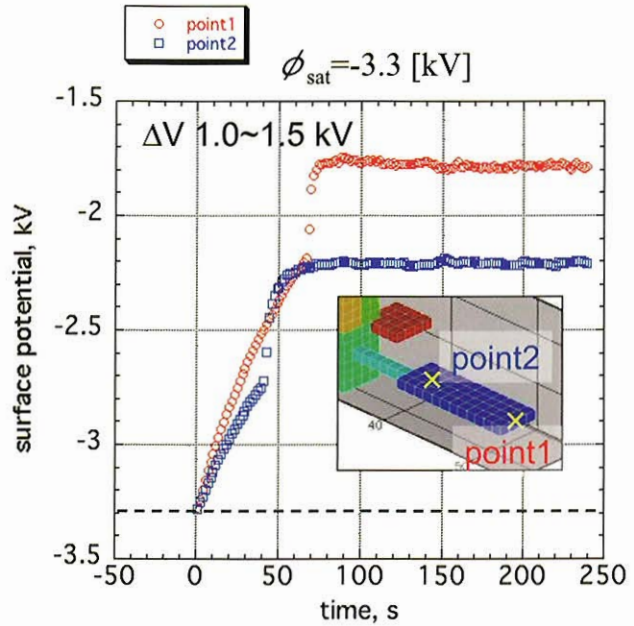
# Numerical Results of Differential Voltage

## 3D-image



$$\phi_{CG} >$$

$\phi_{sat}$   
for PEE and SEE effects



Absolute potential is fixed at -3.3 kV  
to reduce iteration time

18

## Speeding up (Tuning and Parallelization)

## Development Platform

- Shared memory parallel (SMP) workstation
  - Server of 2nodes,
  - 4CPUs for each, 8CPUs in total
- CPU       Itanium II 1.3GHz
- Memory   16GB
- HD        660GB
- OS
  - SuSE Linux Enterprise Server
- Compiler
  - Intel Fortran for Linux ver.8.1
  - Intel C++ for Linux ver.8.1



20

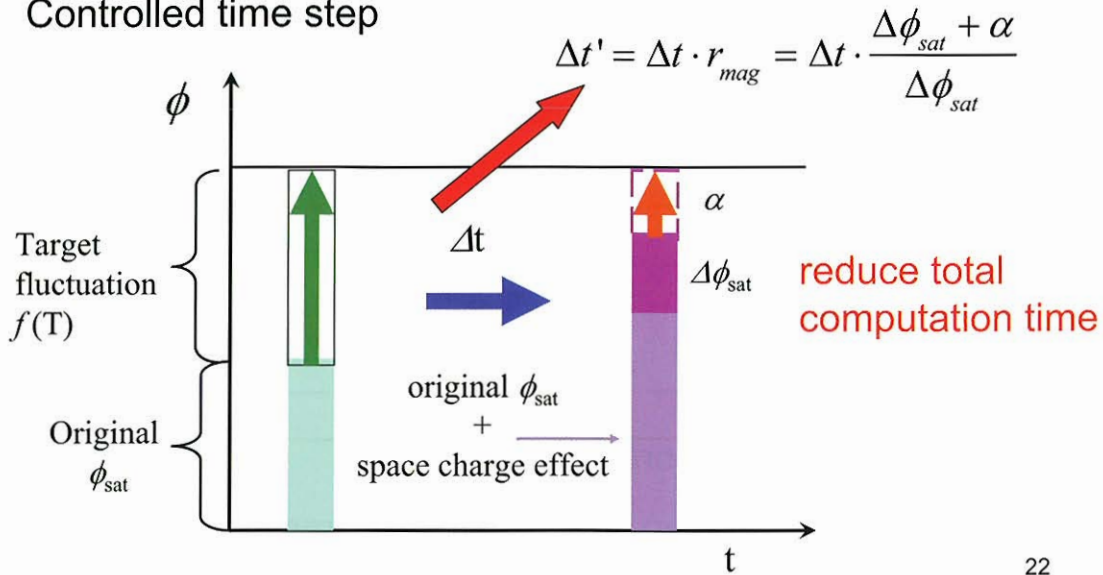
## Speeding up of Computation

- Goal of calculation speed (final version)
  - Using **workstation on the market**,
  - The calculation of **PEO satellite** is (severe condition to numerical resources ),
  - Completed in about **half a day**
- Status at present
  - Hardware
    - **Parallelization** with Open-MP to PIC and PT parts
    - Modify particle arrangement to **reduce memory access time**
  - Algorithm
    - **Time step control method (to reduce iteration time)**
    - Modification of PT algorithm  
(to reduce the number of computation for particles)

## Modification of Time Step Control

Considering the fluctuation of satellite potential

Controlled time step



22

## Example of Numerical Result

Frame 001 | 26 Mar 2006 | surface potential at time step = 20

WINDS(256\*64\*64)

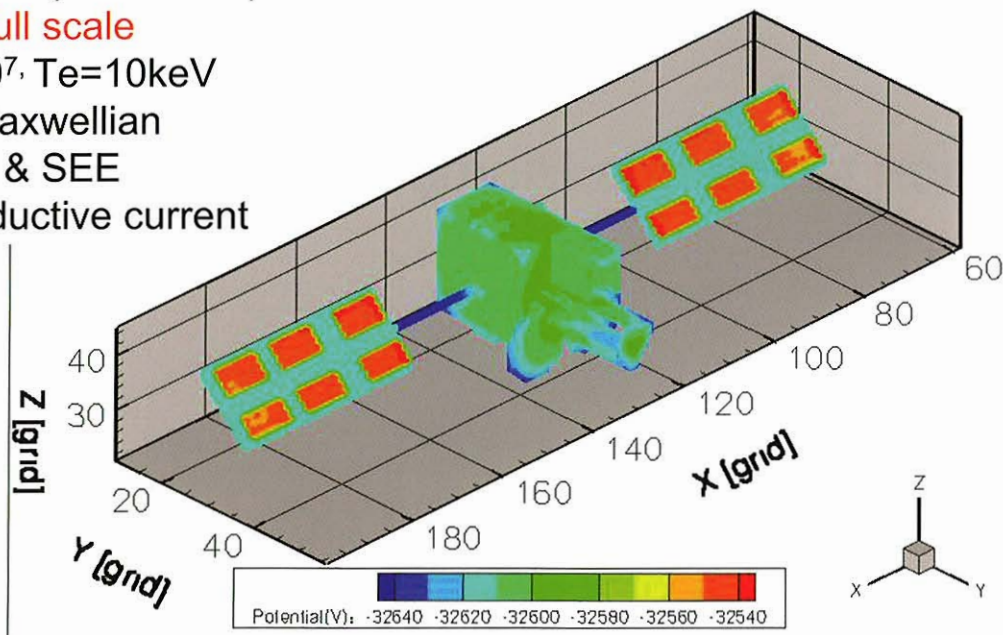
1/4 full scale

$n=10^7$ ,  $T_e=10\text{keV}$

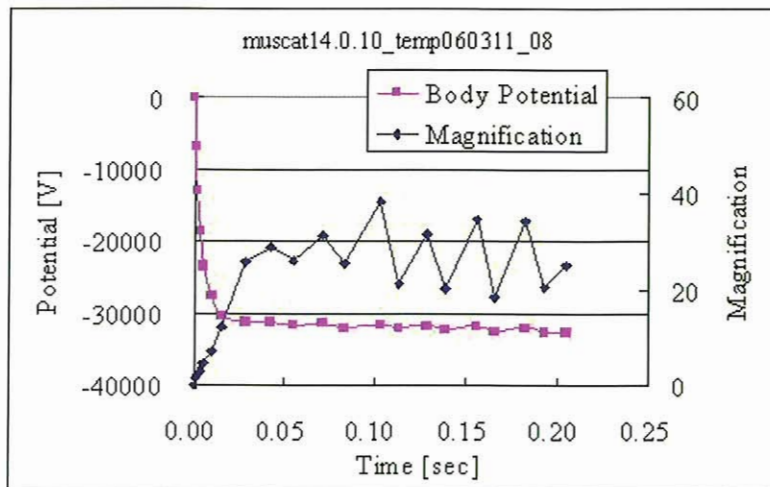
D. Maxwellian

PEE & SEE

Conductive current



## Example of Numerical Result



Total 20step **total computation time is almost 1/10 !**  
 (200 steps more w/o time step control)

Computation time: about 2.5h/step with 8 CPUs at present  
 (almost 2 days in total)

24

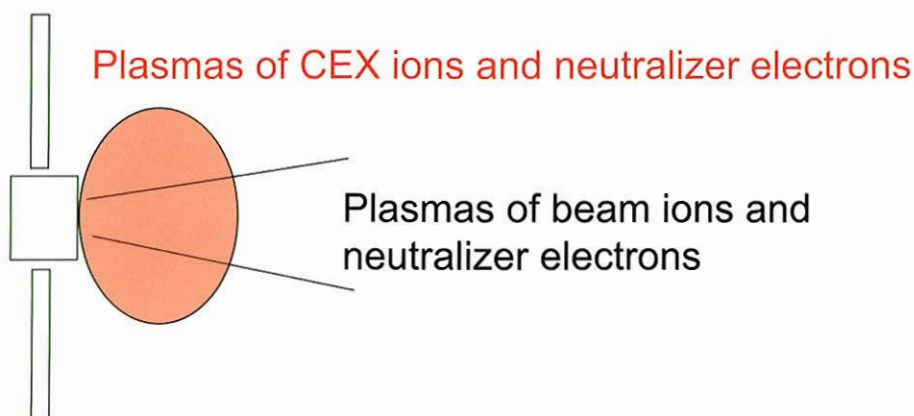
## Application to Plasma Plume Analysis

## Application to Plasma Plume Analysis

- Plasma plume analysis for electric propulsion
  1. Contamination of spacecraft by CEX ions
    - Ion flux to spacecraft surface
  2. Power loss due to dense plasmas near solar array paddle
    - Electron density near spacecraft surface
  3. Relaxation of local spacecraft charging
    - Ion flux to the spacecraft surface
  4. Fluctuation of spacecraft potential in the case of neutralization failure
    - Dynamic interaction between neutralizer and plume plasmas
- For the MUSCAT solver, 1 and 2 are considered

26

## Basic Scheme of Plasma Plume Analysis



- CEX ions generated in beam plasma diffuse from positive electric potential in the beam plasma
- Ambipolar diffusion of CEX ions and neutralizer electrons
- Parameters of  $n_{bi}$ ,  $n_e$ ,  $n_{ce}$ ,  $\Phi$ , and  $T_e$  are important

27

## Basic Scheme of Plasma Plume Analysis

- Plasma plume modeling from 1995

			nbi	ne	ncex	Te	Electric Potential	Maximum Electric Potential in the Beam	Satellite Potential	B.C.
Roy	1996	generic ion thruster	Analytical	Boltzmann	particle	variable	Poisson equation	?	fixed or floating?	Neuman
Oh	1999	SPT100	particle	=nbi+ncex	particle	fixed	$\frac{e\phi}{kT_e} = \ln\left(\frac{n_e}{n_o}\right)$	NA	fixed? array=-92V	NA
Wang	2001	DS1	Analytical	Boltzmann	particle	fixed	Poisson equation	Maximum $\Phi_p$ at thruster exhaust	fixed at 0	Neuman
Van Gilder	2000	generic ion thruster	particle	=nbi+ncex	particle	fixed	$\frac{e\phi}{kT_e} = \ln\left(\frac{n_e}{n_o}\right)$	0	fixed	NA
Tajmar	2001	SMART1	particle	=nbi+ncex	particle	fixed	$\frac{e\phi}{kT_e} = \ln\left(\frac{n_e}{n_o}\right)$	Maximum $\Phi_p$ at thruster exhaust	fixed at 0	NA
Boyd	2005	SPT100	particle	fluid equation	particle	fluid equation	Poisson equation		dielectric surface	Dirichlet

28

## Basic Scheme of Plasma Plume Analysis

- Ion beam profile
  - Fixed, obtained analytically [Ref. ex. Roy, 1996]
  - Modeling by “Vineyard” (GUI tool of MUSCAT)
- CEX ions and Electric Potential
  - Obtain time evolution of  $n_{cex}$  profile by PIC
  - Solve following non-linear Poisson equation

$$-\varepsilon_o \nabla^2 \phi = e \left( n_{bi}(x) + n_{cex}(x) - n_o \exp\left(\frac{e\phi}{kT_e}\right) \right)$$

$n_o$ : maximum density at plume exhaust point

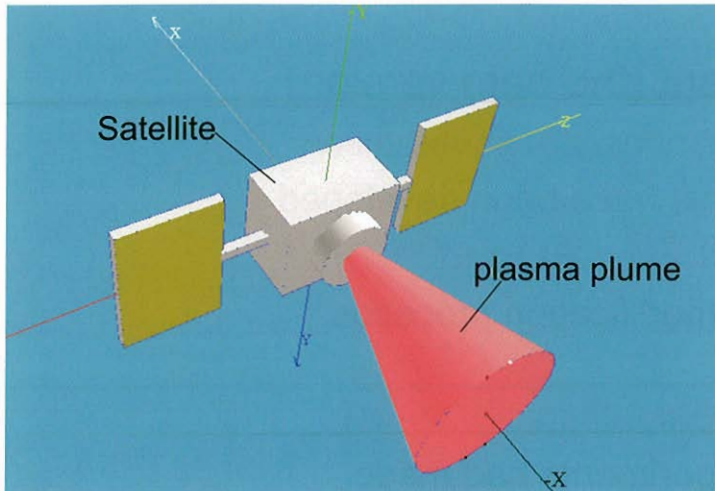
adopt Newton-Raphson + SOR method

29



## Image of the Plume Modeling by the Final Version of MUSCAT

- Determine Ion engine parameters by GUI

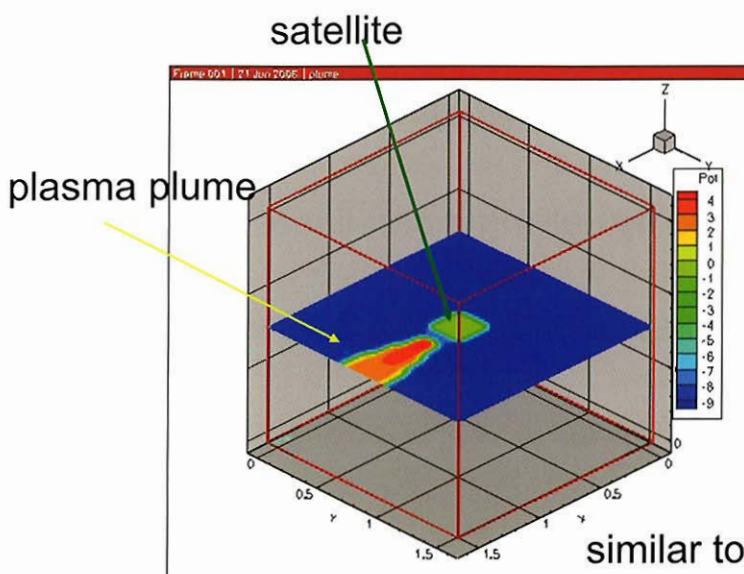


### Ion Engine Parameters

- ion(gas) species
- beam ion density
- neutral particle density
- electron temperature
- beam expansion angle

30

## Preliminary numerical result



similar to Dr. Wang's method

- Ion engine parameter: ETS-8

31

## Summary

- The beta version of MUSCAT had been released
  - The first version of **integrated software**
- Current status of development (the beta version)
  - Integrated GUI tool “**Vineyard**” **conducts computation**
  - Fundamental physical elements have been developed (able to calculate charging at **LEO, GEO and PEO**)
  - Parallelization and algorithm modification proceeds speeding-up (able to **perform large scale computation in 2days**)
  - Validation by fundamental experiments had made

32

## Summary

- Plasma plume analysis
  - Basic scheme of the analysis has been determined
  - Follow CEX ions by PIC
  - Electric potential is obtained by solving a non-linear Poisson equation
  - Initial parameters are installed by MUSCAT modeler

33

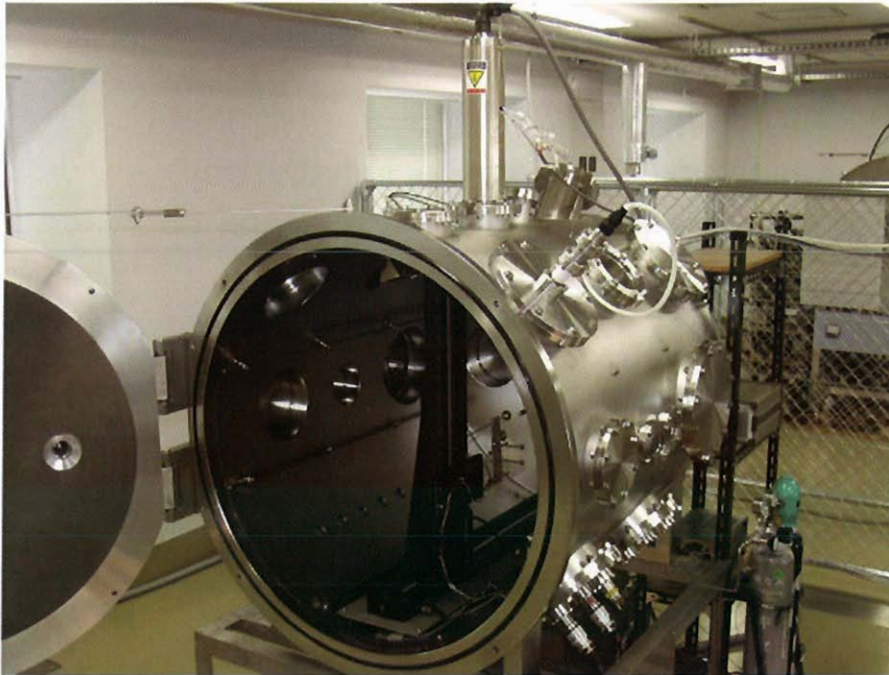
## Future Schedule

- **Final version of MUSCAT (April, 2007)**
  - Data transfer function by “Vineyard”
  - Tuning and speeding-up (PEO satellite, in half a day)
  - Additional physical elements (internal charging etc.)
  - Further validation by experiments and large scale simulation
  - Feedback from users

34

## Experiments for Code Validation

## Validation Experiment Facility



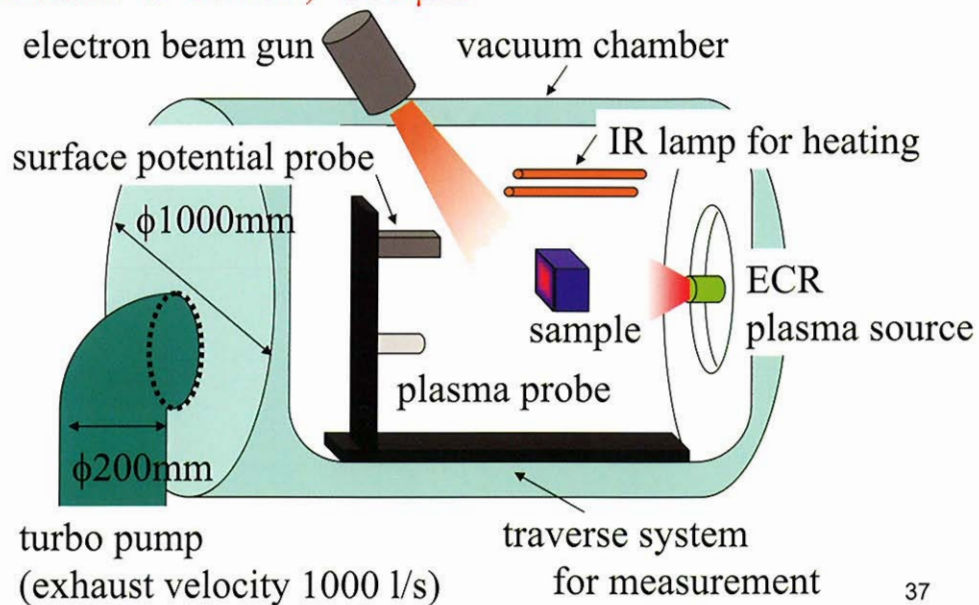
Chamber to simulate Polar Earth Orbit Environment 36

## Schematic of the Chamber

Simulate LEO, GEO and PEO environment

Ambient plasma: density  $10^{11} \sim 10^{12} \text{m}^{-3}$ , temperature 2~3 eV

Electron beam : ~30 keV, ~300  $\mu\text{A}$

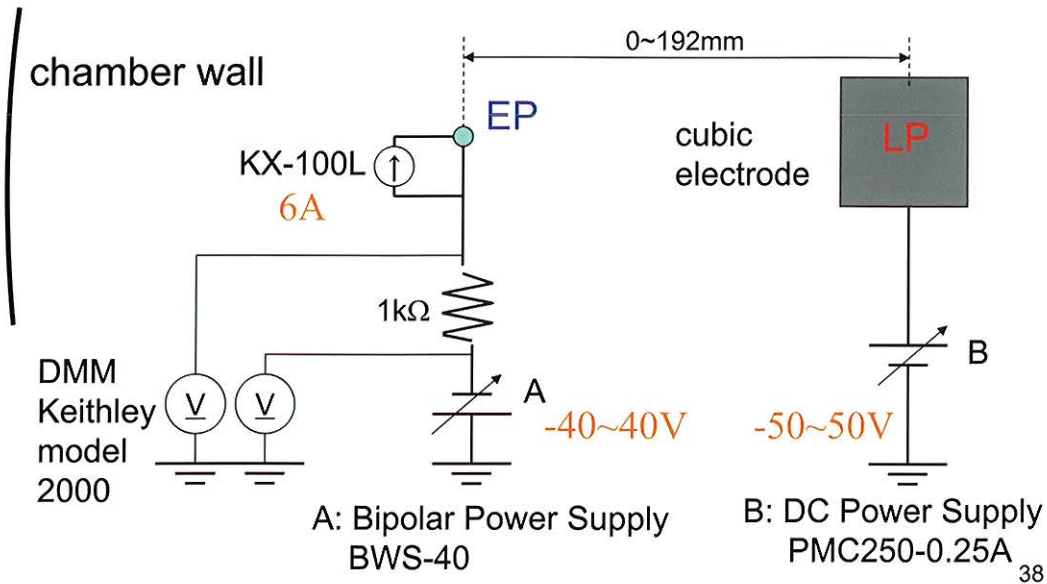


37

## Schematic of Probe Circuit

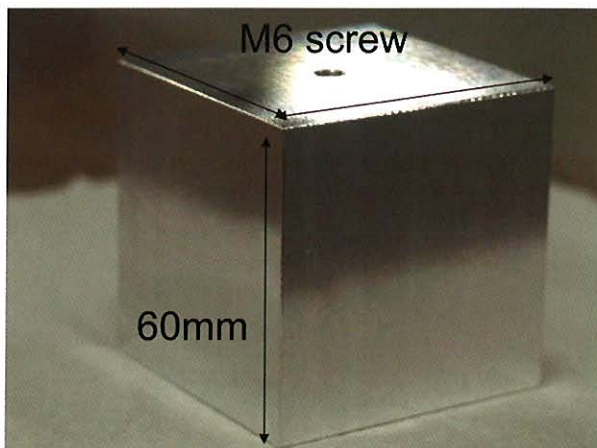
Emissive probe (EP): for electric potential

Langmuir probe (LP): for IV characteristic curve



## Cubic Electrode of Langmuir Probe

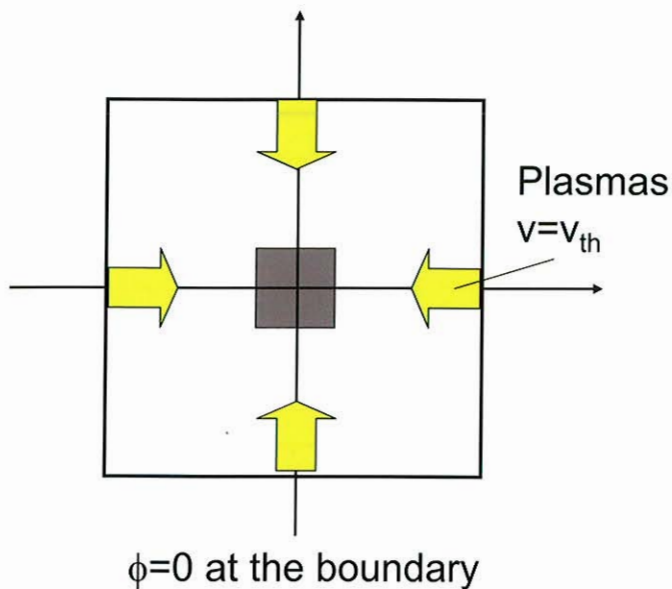
Adjust the shape to **rectangular grid** system of MUSCAT



Aluminum cube  
size=(60mm)<sup>3</sup>~(10λ<sub>D</sub>)<sup>3</sup>  
( T=2 eV, n=3x10<sup>12</sup> m<sup>-3</sup> )

# Simulation Geometry

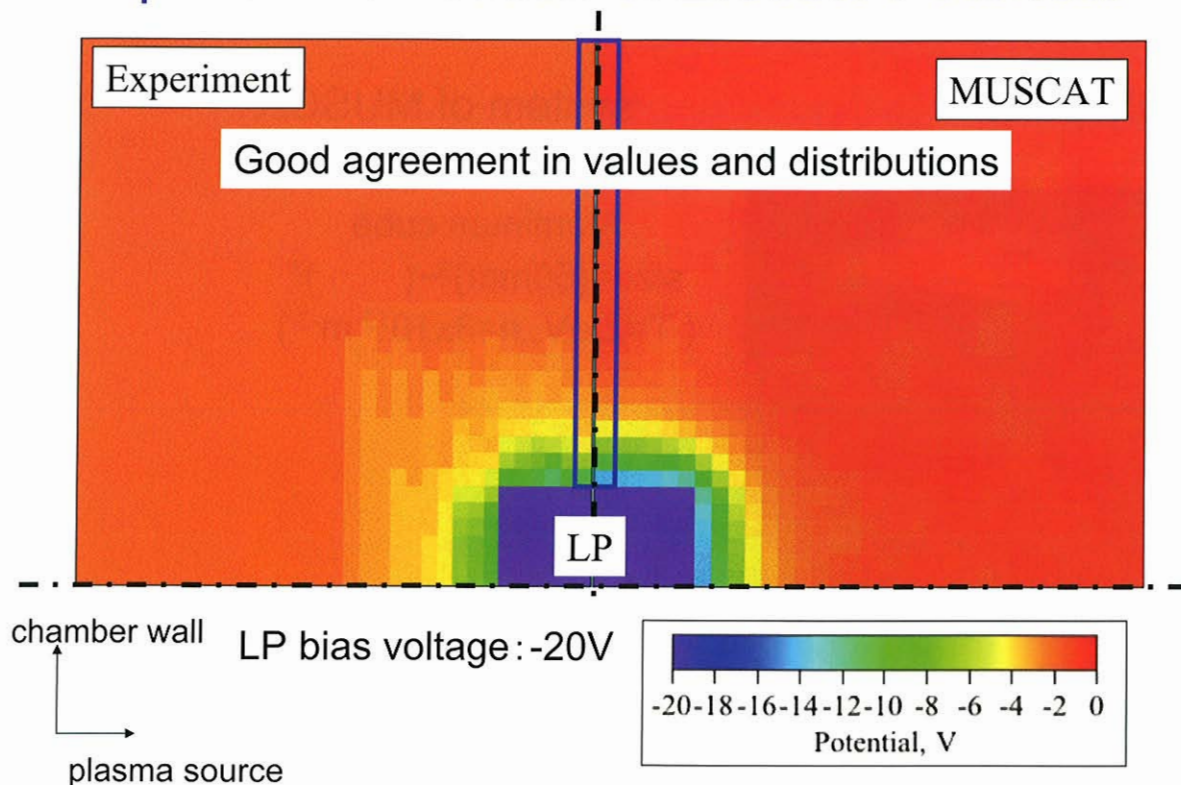
MUSCAT employs Rectangular grid system



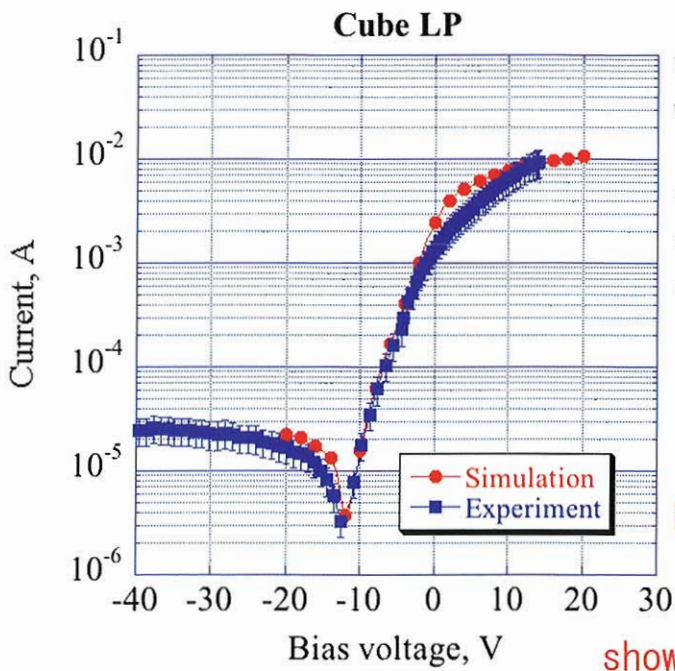
size(grid)  
domain: 64x64x64  
object : 10x10x10  
 $\Delta x : 6\text{mm}(1.0\lambda_D)$   
(  $T=2\text{ eV}$ ,  $n=3 \times 10^{12}\text{ m}^{-3}$  )

40

# Spatial Distribution of Electric Potential



## I-V Characteristic Curves



V is revised by subtracting  $V_s$  from  $V_p$

$$V = V_p - V_s$$

$V_p$ : probe potential

$V_s$ : space potential(plasma)

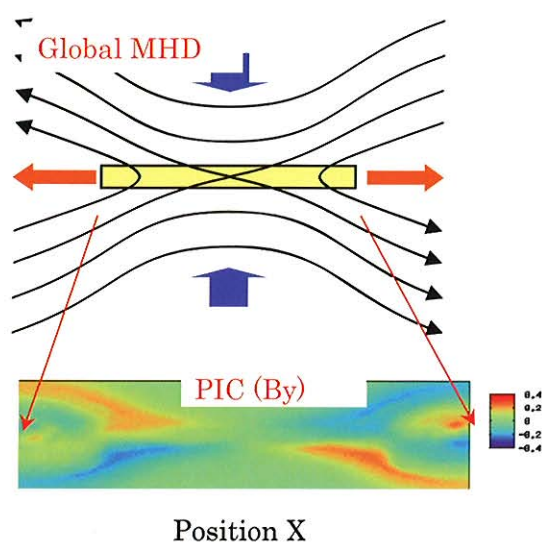
Both are in good agreement

shows accuracy of the solver

## Development of Macro-Micro Interlocked Simulation Algorithm

Tooru Sugiyama, Kanya Kusano  
 The Earth Simulator Center / JAMSTEC  
 E-mail: tsugi@jamstec.go.jp

A fluid description of plasmas is useful to investigate the global structure in space plasma, such as the magnetosphere and heliosphere. It can reproduce the time evolution of macroscopic variations of density, bulk velocity and so on. On the other hand, the microscopic dynamics of plasmas should be described by spatial and velocity distribution in the phase space. Wave-particle interaction process is the typical example for the application of the microscopic description. For these micro- and macroscopic description, different kinds of numerical approach may work well, respectively, e.g. MHD simulation for the macroscopic phenomena and PIC simulation for microscopic process. However, it is widely accepted that the cross-scale interaction between micro and macro processes plays a crucial role, for instance, in the diffusion region in the magnetic reconnection process. Therefore, a new model which can treat MHD-scale dynamics including particle kinetic effects is necessary. We have developed the new simulation method called “Interlocked simulation”, in which MHD and PIC simulations are simultaneously performed. Here, we show its algorithm and some examples.



interlocked simulation. MHD simulation is performed to solve the global structure of the system, and PIC simulation is performed to investigate the kinetic effects in the diffusion region. Bottom: Results from the PIC simulation in X-Z 2D plane. Plotted is Y component of the magnetic field. By embedding the results from PIC simulation into MHD simulation, we can perform global fluid simulations including particle kinetic effects.

Top: A schematic illustration of the



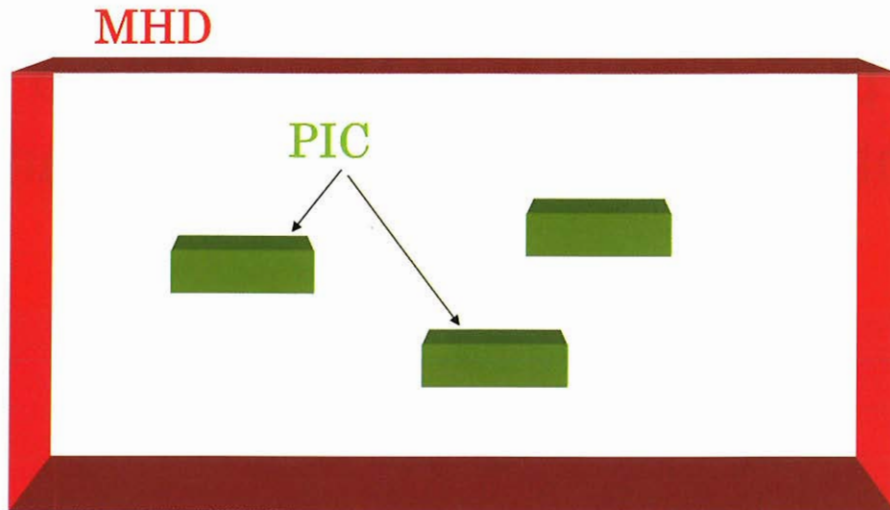
# Development of Macro-Micro Interlocked Simulation Algorithm

Tooru Sugiyama, Kanya Kusano  
The Earth Simulator Center

## Simulations in plasma physics

- Fluid dynamics
  - MHD model
    - large scale
- Particle dynamics
  - PIC (Particle in Cell) model
    - kinetics
- Multi-physics This study
  - Interlocked model
    - large scale fluid simulations including kinetic effects are able to be performed.

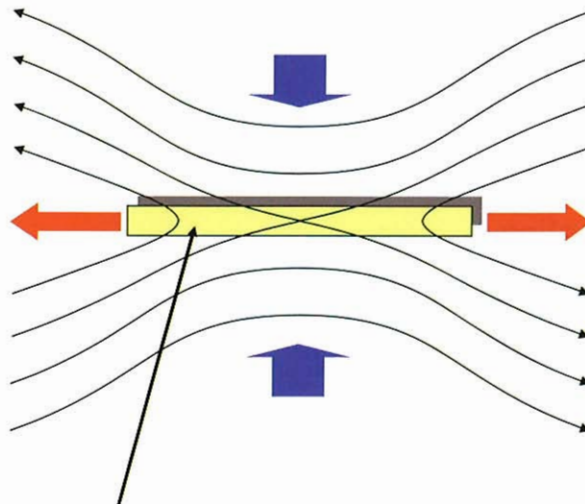
# Concept of the Interlocked simulation



PIC simulations embedded in MHD simulation

## Application of the Interlocked simulations: Magnetic Reconnection

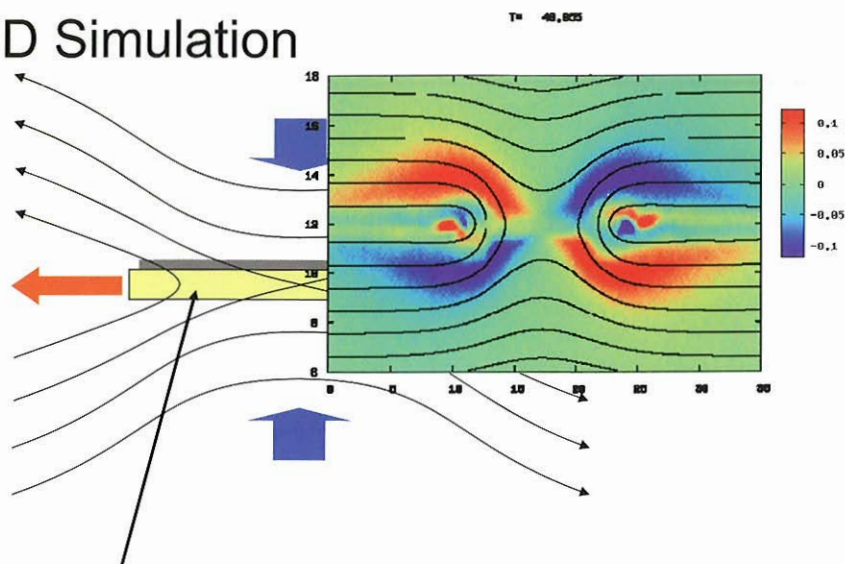
### Global MHD Simulation



PIC Simulation in the diffusion region

## Application of the Interlocked simulations: Magnetic Reconnection

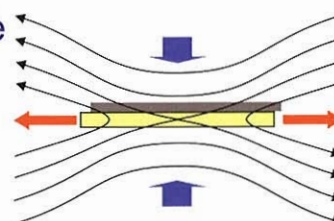
### Global MHD Simulation



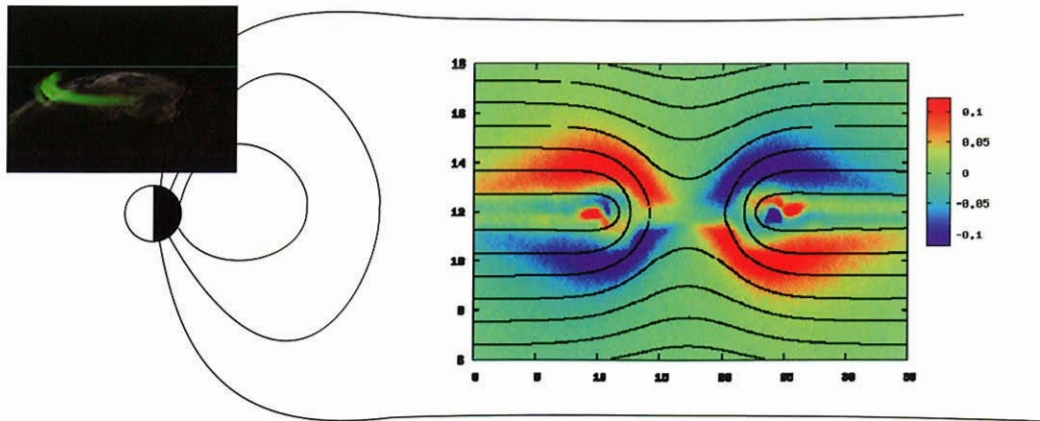
### PIC Simulation in the diffusion region

## Useful Points of the Interlocked simulation

- For MACRO part (MHD)
  - Diffusion process is precisely included.
- For MICRO part (PIC)
  - Realistic boundary conditions are imposed.
    - Non uniform conditions in space
    - Non stationary conditions in time

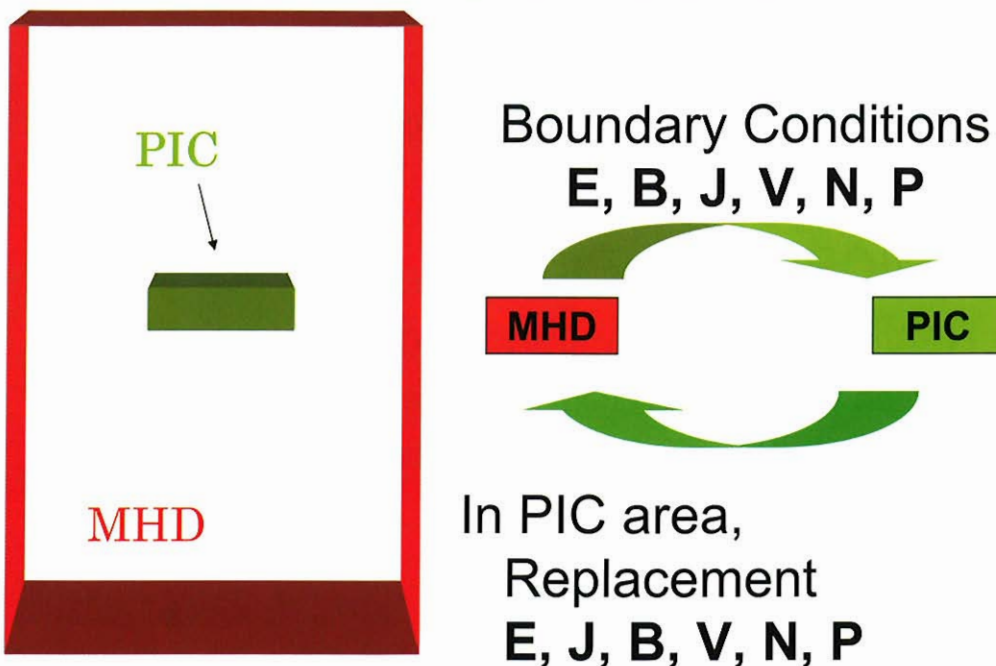


# M-I Coupling and Magnetic Reconnection



Magnetic Field Profile  
 color contour : out of plane component  
 curves: on the plane

## PIC simulations in MHD simulation



## Electric-Field Current-Density (MHD)

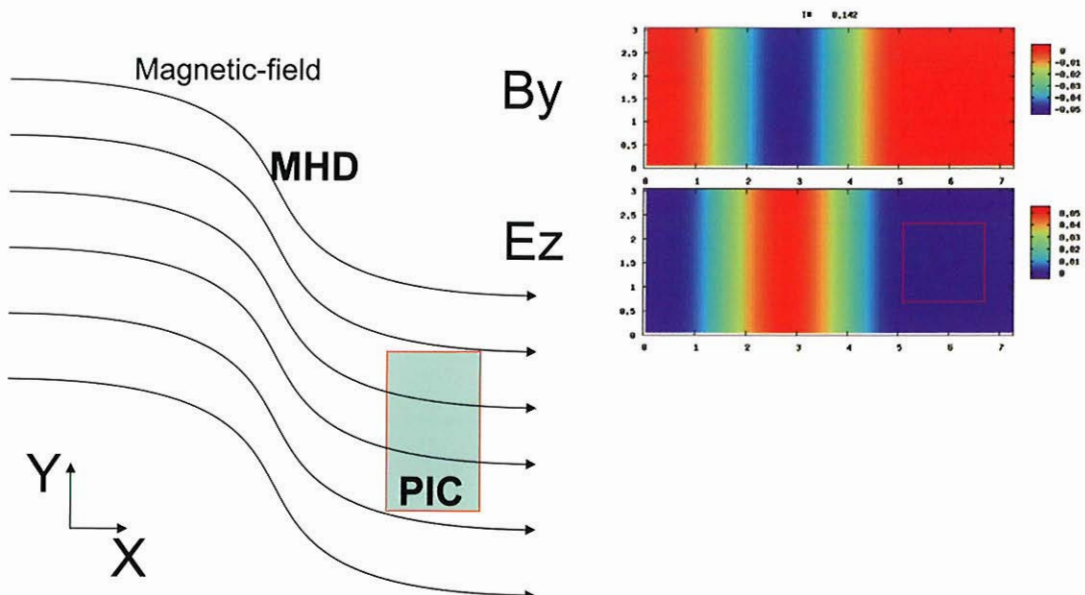
$$\mathbf{E} + \mathbf{V} \times \mathbf{B} = \eta \mathbf{J} + \frac{1}{ne} \mathbf{J} \times \mathbf{B} - \frac{1}{ne} \nabla \cdot \mathbf{P}_e + \frac{m_e}{ne^2} \frac{\partial \mathbf{J}}{\partial t}$$

$$\mathbf{J} = \nabla \times \mathbf{B}$$

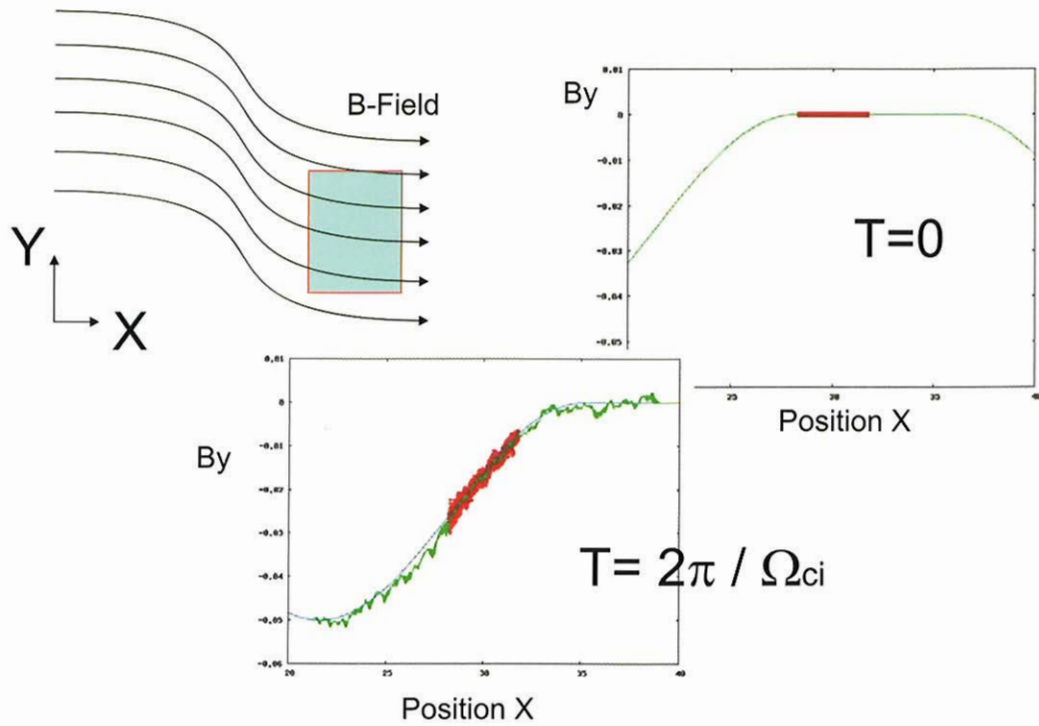
are not advanced in time.

**Data from PIC simulations are used.**

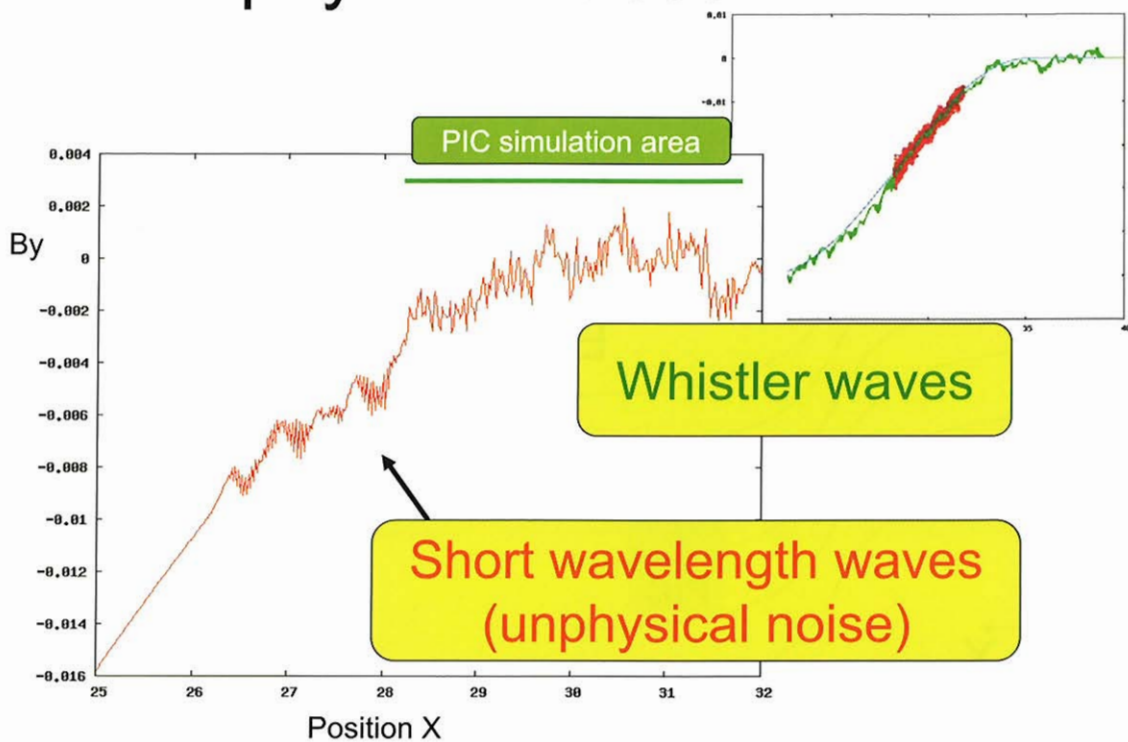
## Test on Alfvén Wave propagation



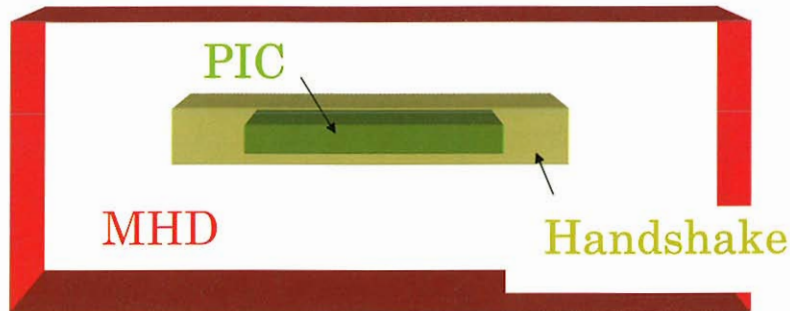
# Detailed waveform



# Unphysical noises in MHD



## PIC simulations in MHD simulation

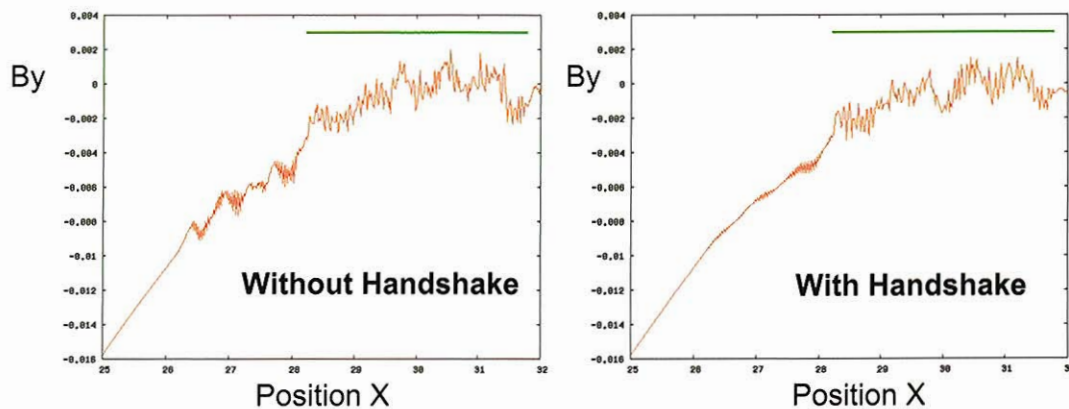


Handshake region is necessary to absorb

- High frequency waves (Whistler etc.) in PIC.
- Abrupt change of boundary condition from MHD to PIC.

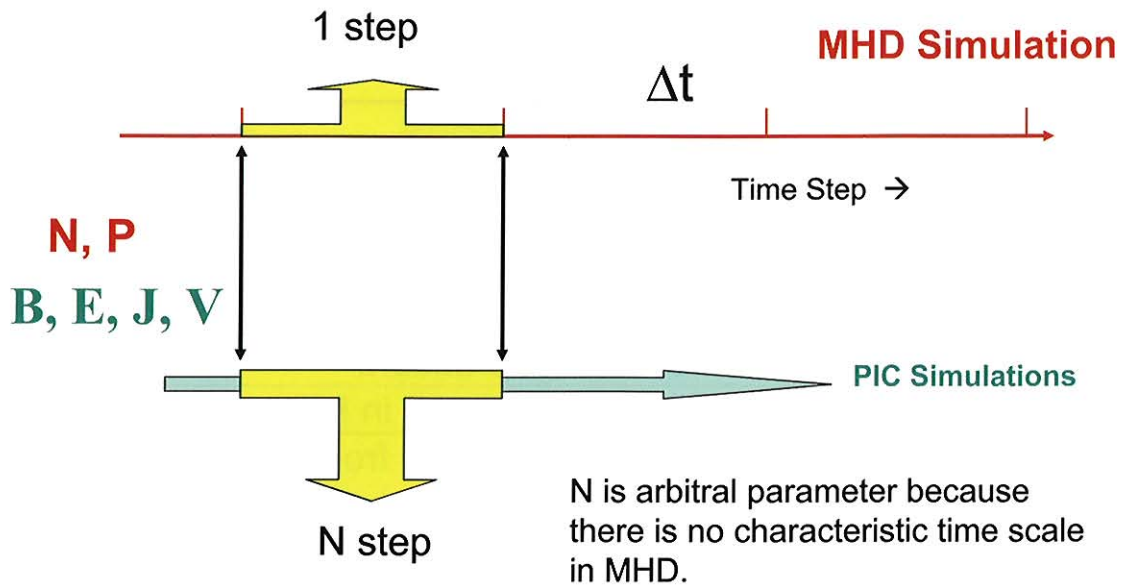
$$\mathbf{E}_{HS} = \alpha \mathbf{E}_{PIC} + (1 - \alpha) \mathbf{E}_{MHD} \quad (0 \leq \alpha \leq 1)$$

## Noise reduction using the handshake area

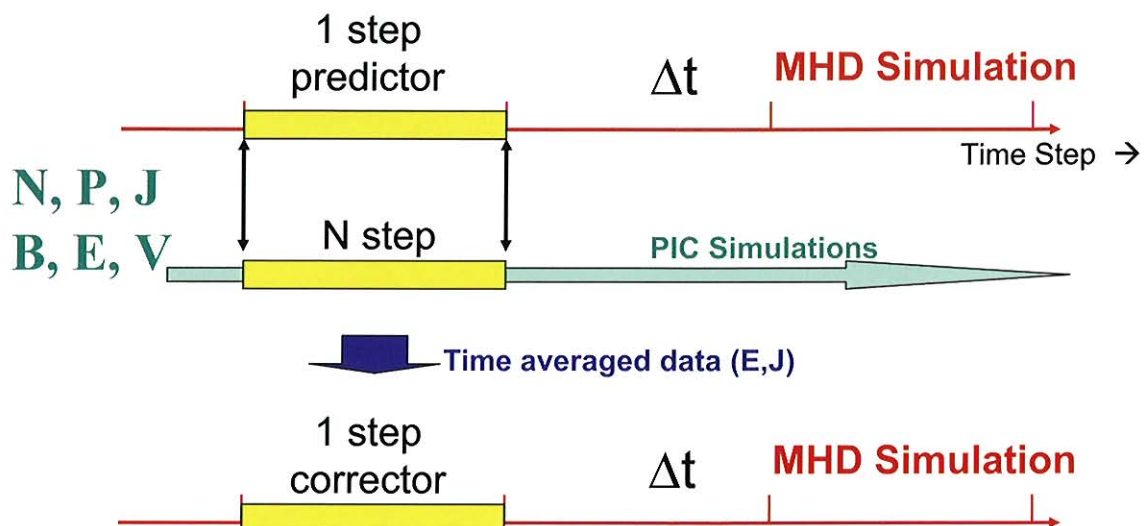


[more](#)

### Time sequence of the interlocked simulation

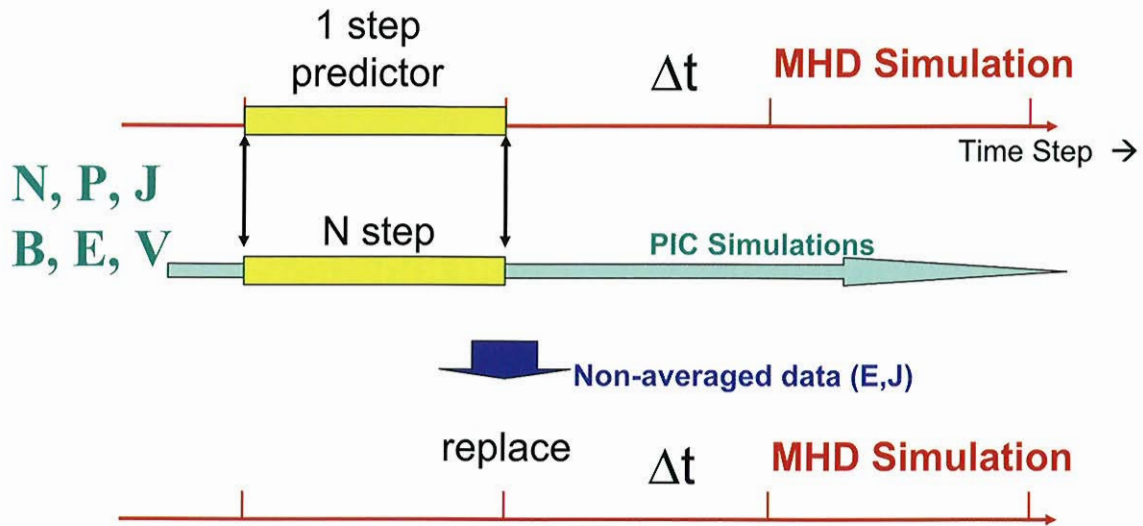


### Time sequence of the interlocked simulation (Predictor-Corrector algorithm)





## Time sequence of the interlocked simulation (Predictor-Replace algorithm)



## Program

```

if(rank==Macro) then
  do iT = 1, Nstep_Macro
    call Macro_work1
    ...
    call MPI_SEND
    call MPI_RECV
    ...
    call Macro_work2
  enddo
endif
    
```

```

if (rank==Micro) then
  do iT = 1, Nstep_Micro
    call Micro_work1
    ...
    call MPI_RECV
    call MPI_SEND
    ...
    call Micro_work2
  enddo
endif
    
```

## Summary

- **Macro-Micro Interlocked simulation is an effective way to investigate**
  - **Multi – Scale Simulation**
  - **Multi – Physics Simulation**
- **MHD-PIC interlocked model enables the global simulation including kinetic effects.**
- **Other combinations**
  - **PIC + HYBRID**
  - **HYBRID + MHD**
  - **PIC + HYBRID + MHD**

## 多体問題専用計算機”GRAPE-6”を用いた 微小スケールのプラズマの計算機実験

Micro-scale Plasma Simulation Using Numerical Calculation Accelerator “GRAPE-6”

藤野 将生<sup>1</sup> 大谷 洋<sup>1</sup> 篠原 育<sup>2</sup> 臼井 英之<sup>3</sup>

<sup>1</sup> 有限会社 リヴィールラボラトリ

<sup>2</sup> 宇宙航空研究開発機構 宇宙科学研究本部

<sup>3</sup> 京都大学 生存圏研究所E-mail: [masao@reveal-lab.com](mailto:masao@reveal-lab.com)

現在のプラズマの主要な計算機実験法である PIC 法では、デバイ長よりも小さいスケールでの実験はその原理上困難となっています。私達は、今までの手法では計算機実験を行うことのできなかつた微小スケールでのプラズマの計算機実験の手法を確立し、プラズマのデバイ長が宇宙機と比べて大きくなる深宇宙においての宇宙機の性能評価法を確立することを目指して研究・開発を行っています。具体的には、天文の分野で使われている多体問題専用計算機”GRAPE-6”を用いて、プラズマ内の粒子にかかるクーロン力を直接計算することにより、プラズマ内の粒子の動きを直接追う純粋な粒子法の確立を目指しています。プラズマ内の粒子の動きを直接に追う場合、プラズマに含まれる粒子の数が膨大であるため、計算時間も膨大になってしまいます。そこで、”GRAPE-6”の粒子間の相互作用を高速に計算する能力に注目し、現実的な時間内での粒子法によるプラズマの計算機実験を行いたいと考えております。現在、その第1段階として、”GRAPE-6”を用いた粒子法のラングミュアプロードモデルによる検証を行っています。

この研究は JAXA オープンラボによる支援を受けて行われています。

# Grape6 BL4

*The most suitable for a Cluster system*

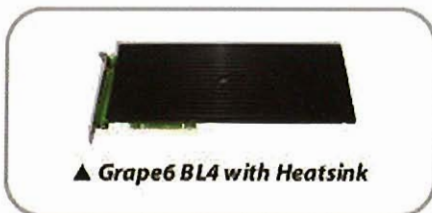
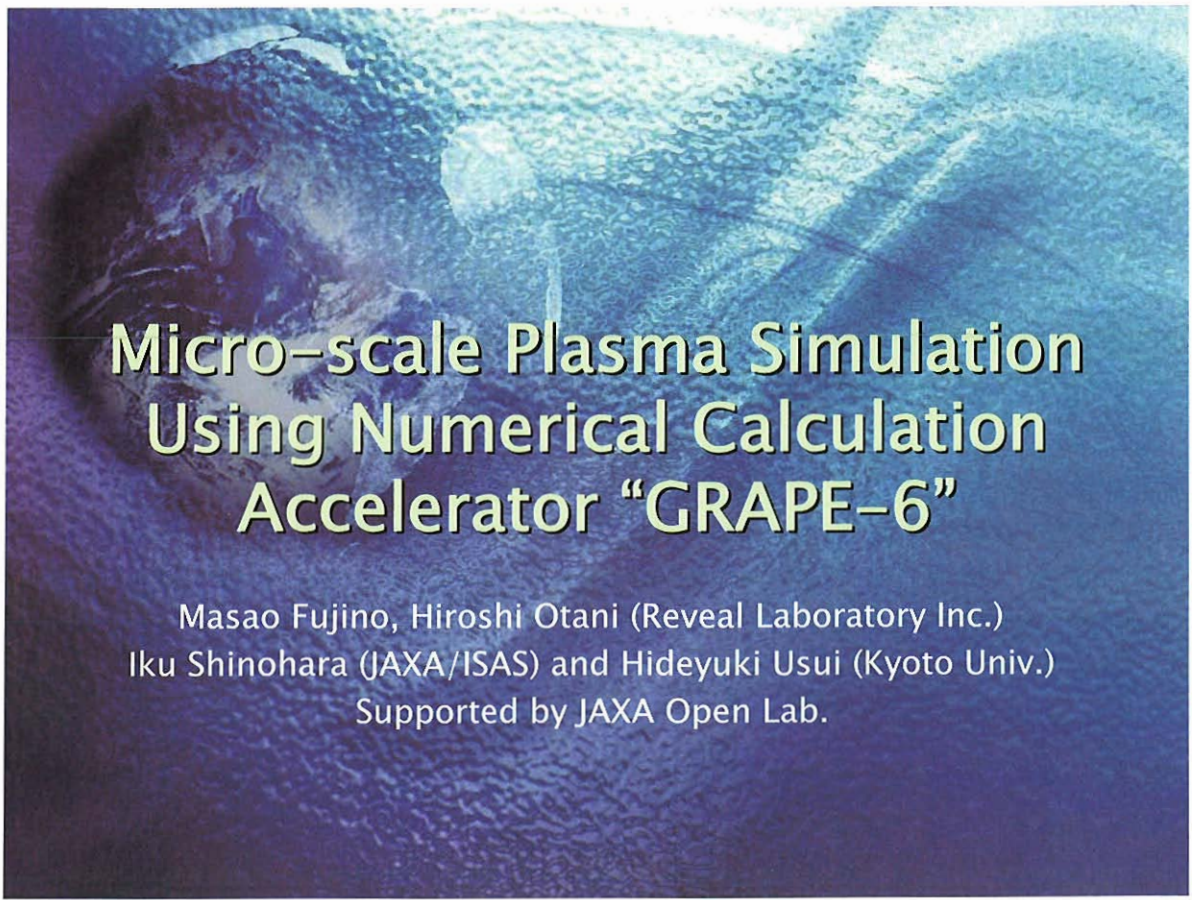
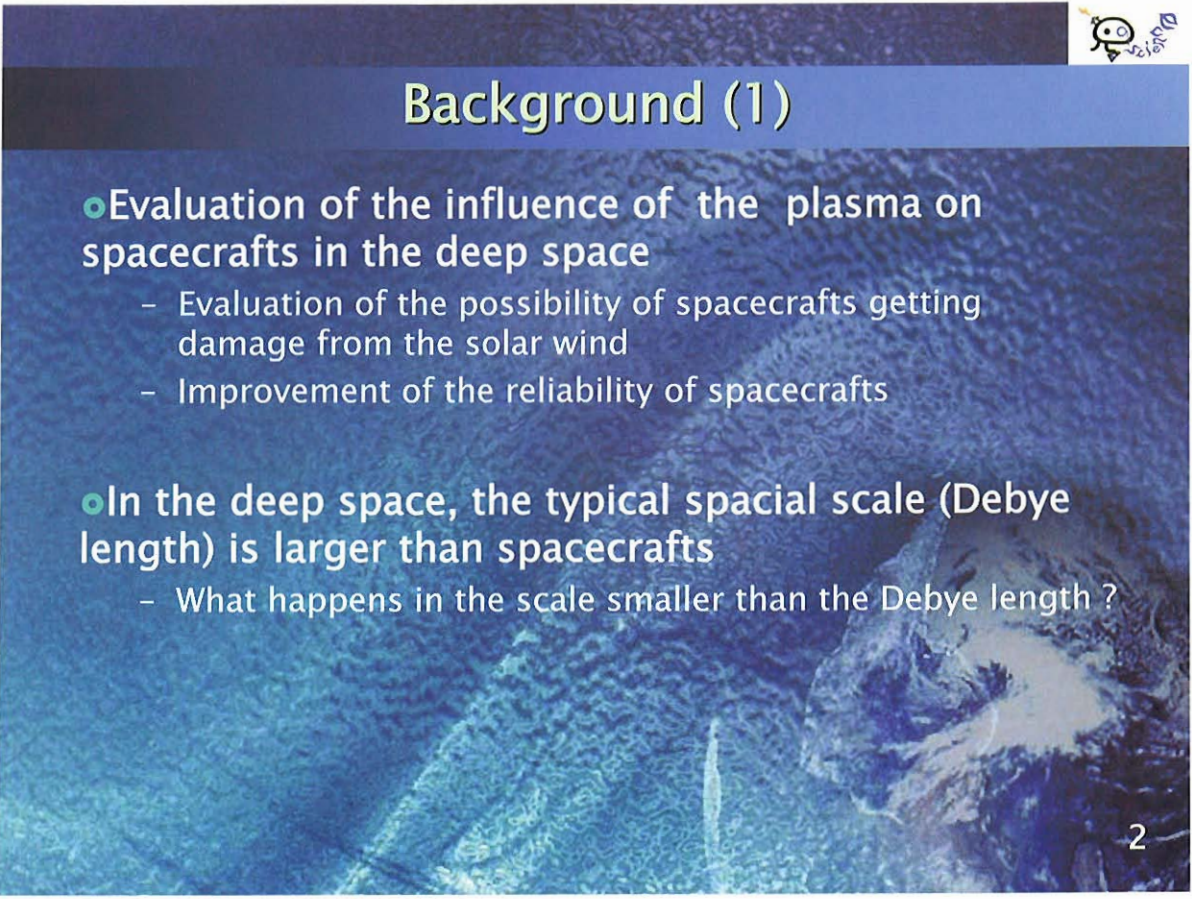


図1 多体問題専用計算機 ”GRAPE-6”

A visualization of a micro-scale plasma simulation, showing a complex, turbulent structure with a central bright region and surrounding darker, textured areas. The colors range from deep blue to light blue and white.

# Micro-scale Plasma Simulation Using Numerical Calculation Accelerator “GRAPE-6”

Masao Fujino, Hiroshi Otani (Reveal Laboratory Inc.)  
Iku Shinohara (JAXA/ISAS) and Hideyuki Usui (Kyoto Univ.)  
Supported by JAXA Open Lab.

A slide titled 'Background (1)' with a blue background and a small cartoon character in the top right corner. The slide contains two main bullet points with sub-points. The background features a faint, large-scale visualization of plasma simulation.

## Background (1)

- Evaluation of the influence of the plasma on spacecrafts in the deep space
  - Evaluation of the possibility of spacecrafts getting damage from the solar wind
  - Improvement of the reliability of spacecrafts
- In the deep space, the typical spacial scale (Debye length) is larger than spacecrafts
  - What happens in the scale smaller than the Debye length ?



## Background (2)

- PIC (Particle In Cell) method (Traditional)
  - Assumption of the scale larger than the Debye length
  
- Particle method (This work)
  - It can be used for the simulation whose scale is equal to or smaller than the Debye length
  - It is needed to calculate the Coulomb force on every particles from every other particles
  - The calculation time will be longer
  - Shorten the calculation time by using “GRAPE-6”

3



## GRAPE-6 –Functionality

- Calculation of potential, acceleration and jerk
  - In the case of the same time step interval
  - Input parameters are masses, positions and velocities of the particles
  - They are most dominant in N-body simulations. Typically, their calculation costs are O(N^2)

$$\phi_i = \sum_{j \neq i} -Gm_j \frac{1}{(r_{ij}^2 + \epsilon^2)^{1/2}}$$

$$\mathbf{a}_i = \nabla \phi_i = \sum_{j \neq i} Gm_j \frac{\mathbf{r}_{ij}}{(r_{ij}^2 + \epsilon^2)^{3/2}}$$

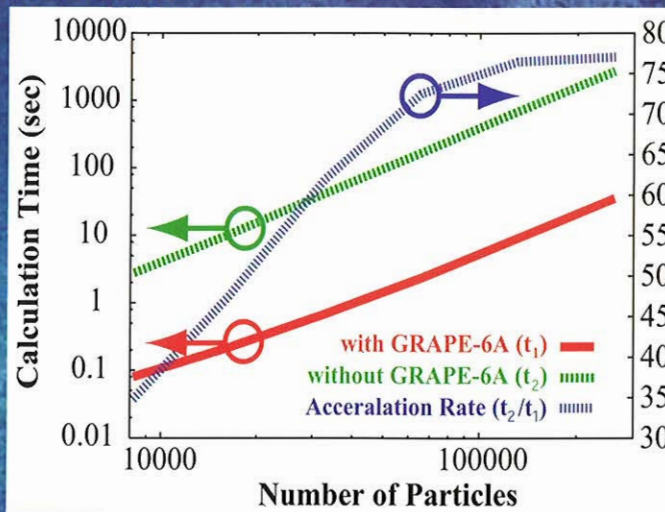
$$\mathbf{j}_i = \sum_{j \neq i} Gm_j \left[ \frac{\mathbf{v}_{ij}}{(r_{ij}^2 + \epsilon^2)^{3/2}} - 3(\mathbf{v}_{ij} \cdot \mathbf{r}_{ij}) \frac{\mathbf{r}_{ij}}{(r_{ij}^2 + \epsilon^2)^{5/2}} \right]$$

4



## GRAPE-6 –Performance

- A few ten times faster than the Intel Pentium 4 3.0GHz
  - In the case it calculates all interactions without any approximation



5

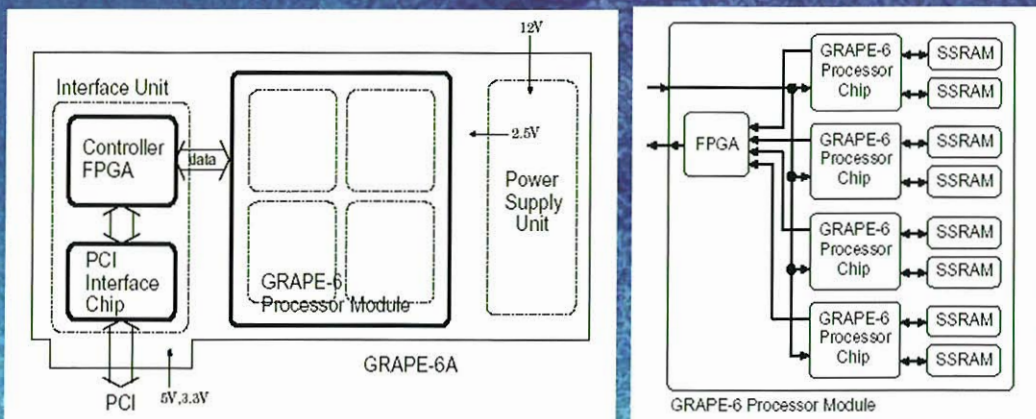
## GRAPE-6 –Architecture (1)

- Pipelines dedicated for the gravity calculation
  - A kind of Digital Signal Processor (DSP)
  - Specialized in potential, acceleration and jerk calculation
  - Additionally, neighboring particle detection calculation
- Effective memory transfer
  - Minimized instruction transfer to the GRAPE-6 processor
  - 1 real pipeline acts as 8 virtual pipelines by time division
- Accelerator board works by calling the C/Fortran Functions (API)
  - After sending data to the GRAPE-6 board, receiving data of calculation result from it

6

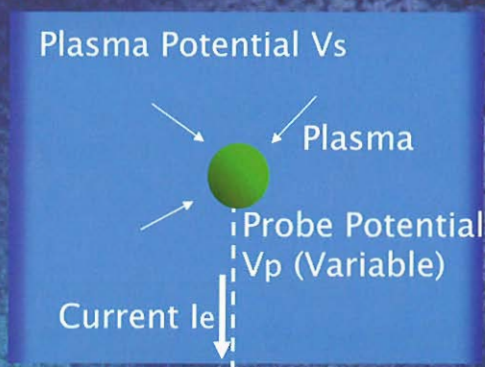
## GRAPE-6 –Architecture (2)

- GRAPE-6 processor
  - 0.25um process, 100MHz clock frequency
- SRAM
  - Stores 271,444 particles at the maximum (16MB x 2)
- FPGA
  - One is for the controller, the other is for reduction operation



7

## Simulation Target –Langmuir Probe



- Change the probe potential  $V_p$  and measure the current  $I_e$
- From the relationship between  $V_p$  and  $I_e$ , estimate the electron temperature  $T_e$  and density  $N_e$
- Compare the estimated  $T_e$  and  $N_e$  to the value of those initially assumed

8

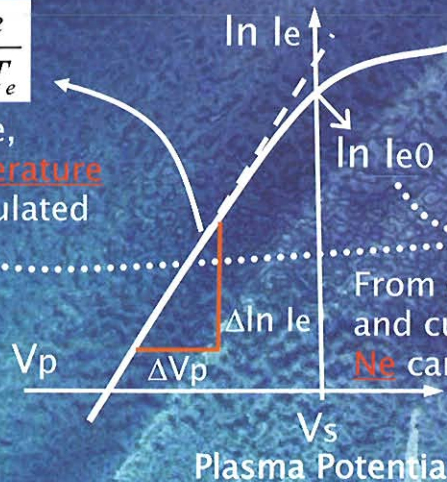


## Electron Temperature and Density –Langmuir Probe

Voltage–current characteristic  
of Langmuir probe

$$\frac{d \ln I_e(V)}{dV} = \frac{e}{kT_e}$$

From the slope,  
**electron temperature**  
 $T_e$  can be calculated



$$N_e = \frac{I_{e0}}{eS} \sqrt{\frac{2\pi m_e}{k_B T_e}}$$

From electron temperature  $T_e$   
and current  $I_{e0}$ , **electron density**  
 $N_e$  can be calculated

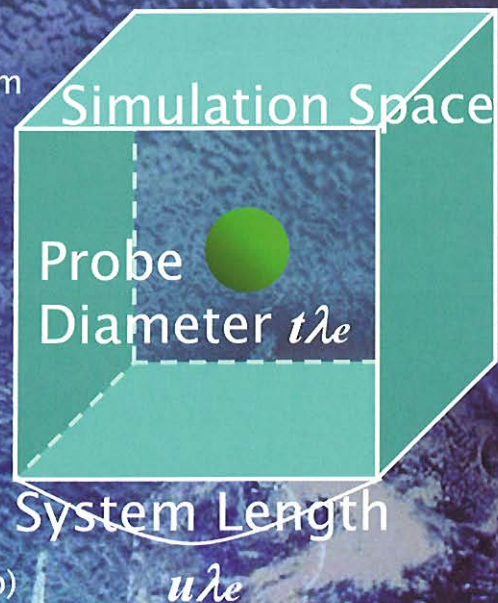
$I_e$ : electron current,  $I_{e0}$ : electron current when  $V_p = V_s$ ,  $e$ : electron charge,  $k_B$ : Boltzmann constant,  $m_e$ : electron mass,  $S$ : surface area of the probe

9

## Simulation Conditions



- **Initial condition**
  - Positions are uniformly random
  - Velocities are subject to Boltzmann distribution
- **Inter boundary condition**
  - Constant potential at probe surface (Imaginary charge method)
- **Outer boundary condition**
  1. Perfect elastic reflection
  2. Periodic
  3. Non-constant inward flux (Inward flux is the same as outward flux at each time step)
  4. Constant inward flux



10





## Time Evolution

- Coulomb force is calculated by GRAPE-6

$$\phi_i = \frac{1}{4\pi\epsilon_0} \sum_{j \neq i} \frac{q_j}{(r_{ij}^2 + \epsilon^2)^{1/2}}$$

$$\mathbf{a}_i = \frac{q_i}{m_i} \nabla \phi_i = \frac{1}{4\pi\epsilon_0} \frac{q_i}{m_i} \sum_{j \neq i} \frac{q_j}{(r_{ij}^2 + \epsilon^2)^{3/2}} \mathbf{r}_{ij}$$

- Time integration is calculated by host MPU (Leapfrog method)

$$\mathbf{r}(t + \Delta t) = \mathbf{r}(t) + \mathbf{v}(t)\Delta t + \frac{1}{2} \mathbf{a}(t)\Delta t^2$$

$$\mathbf{v}(t + \Delta t) = \mathbf{v}(t) + \frac{1}{2} [\mathbf{a}(t) + \mathbf{a}(t + \Delta t)]\Delta t$$

11



## Time Interval Limitation

- Limitation by thermal velocity

$$\sqrt{\langle v_{ex}^2 \rangle} \Delta t = s \lambda_e \quad (0 < s < 1) \Rightarrow \Delta t = s \left( \frac{\epsilon_0 m_e}{e^2 N_e} \right)^{1/2}$$

- In this work, s is chosen as

$$s = \frac{1}{128}$$

※The same result also comes from the limitation by plasma frequency

$$\omega_e \Delta t = s \quad (0 < s < 1) \Rightarrow \Delta t = s \left( \frac{\epsilon_0 m_e}{e^2 N_e} \right)^{1/2}$$

12



## Particle Number Limitation (1)

- Limitation by memory cost

- Position, velocity or acceleration costs each 24 bytes
- Maximum memory is about 1GB on a single workstation

$$N \leq 10^7$$

- Limitation by calculation cost

- This is most dominant factor in a particle method
- A few hundred time step can be calculated in a day on a single workstation hosting GRAPE-6 board
- One time step is about 30 sec when  $N=262,144$  and using  $O(N^2)$  direct scheme with GRAPE-6 board

$$N \leq 10^6$$

13



## Particle Number Limitation (2)

- Limitation by electron current resolution

- Current induced by a single electron is much smaller than the theoretical current in Langmuir probe whose potential is zero

$$i_e = \frac{e}{\Delta t} = \frac{e}{s\lambda_e} \sqrt{\langle v_{ex}^2 \rangle} = \frac{e}{s\lambda_e} \left( \frac{k_B T_e}{m_e} \right)^{1/2}$$

$$I_{e0} = \frac{1}{4} e N_e S \langle v_e \rangle = \frac{1}{4} e N_e \pi (t\lambda_e)^2 \left( \frac{8k_B T_e}{\pi m_e} \right)^{1/2}$$

$$\frac{i_e}{I_{e0}} = \sqrt{\frac{2}{\pi}} \cdot \frac{1}{st^2 \lambda_e^3 N_e} = \sqrt{\frac{2}{\pi}} \cdot \frac{1}{st^2 N_{eD}} \quad (N_{eD} = \lambda_e^3 N_e)$$

$$\frac{i_e}{I_{e0}} < \frac{1}{10}, s = \frac{1}{128}, t = \frac{1}{4} \Rightarrow N_{eD} > 1.63 \times 10^4$$

14

## Simulation Parameters

$$\begin{cases} N = 2 \cdot (u\lambda_e)^3 N_e = 16N_{eD} \cong 262,144 (u = 2) \\ \lambda_e = 0.32 \text{ m} \end{cases}$$

$$\Rightarrow \begin{cases} N_e = \frac{N_{eD}}{\lambda_e^3} = 5.00 \times 10^5 \text{ m}^{-3} \\ T_e = \frac{\lambda_e^2 e^2}{\epsilon_0 k_B} N_e = 10.7 \text{ K} \end{cases}$$

$$\Rightarrow \begin{cases} \sqrt{\langle v_{ex}^2 \rangle} = 1.27 \times 10^4 \text{ m} \cdot \text{s}^{-1} \\ \Delta t = 1.96 \times 10^{-7} \text{ s} \end{cases}$$

Simulation Space

Constant Flux

Probe Diameter  $\lambda_e/4$

System Length  $2\lambda_e$

15

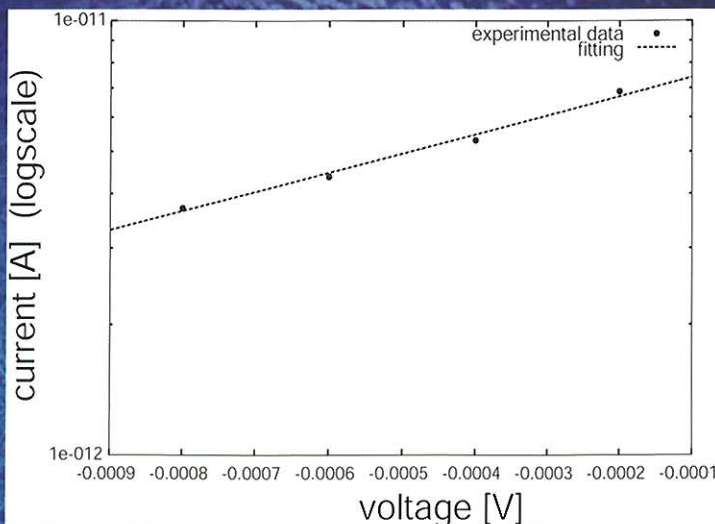
## Simulation Result (1)

- Electron current fluctuates because the number of electrons came in a probe in a time step is discrete
- Estimated current is defined by the average current after a few hundred time steps

16

## Simulation Result (2)

- Estimated Ne and Te from Langmuir probe I-V characteristic (right figure)



	Simulation	Theory	Error
Ne	4.99e5	5.00e5	0.24 %
Te	11.4	10.7	6.5 %

## Conclusion

- Micro-scale plasma simulation with  $O(N^2)$  direct scheme is performed on a single workstation with GRAPE-6
  - Calculation time with GRAPE-6 is 14 hours (400 time steps) while without GRAPE-6 it is about 1 month
- Assumed and estimated value of Ne and Te is very close in the negative low voltage limit
  - It is probable error is enlarged in the negative high voltage limit because  $i_e/i_e0$  becomes large
  - $i_e/i_e0=1/10$  is not enough small



## Future Work

- **Increase the number of real particles**
  - To reduce the error in negative high voltage range
  - With Barnes-Hut tree algorithm
- **Remove the inter boundary geometry restriction**
  - With charge simulation technique or boundary element method (BEM) instead of imaginary charge technique
- **Introduce super-particle**
  - To scale the electron temperature and density

## Research of Magnetoplasma Sail (MPS): A Quick Review

Ikkoh Funaki, Hiroshi Yamakawa, and MPS Research Group

Japan Aerospace Exploration Agency  
Sagamihara, Kanagawa, 229-8510 Japan.  
TEL/FAX:042-759-8570  
E-mail:funaki@isas.jaxa.jp

A quick review of plasma sail propulsion is provided to close up the technical and physical issues of plasma sail. A spacecraft propulsion system utilizing the energy of the solar wind was firstly proposed by Prof. Winglee in 2000. Although Winglee proposed an M2P2 (mini-magnetospheric plasma-propulsion) design with a small (20-cm-diameter) coil and a small helicon plasma source, it was criticized by Dr. Khazanov in 2003. He insisted that: 1) MHD is not an appropriate approximation to describe M2P2 design by Winglee, and with ion kinetic simulation, it was shown that the M2P2 design could provide only negligible thrust; 2) considerably larger sails (than that Winglee proposed) would be required to tap the energy of the solar wind. We started our study in 2003, and it is shown that moderately sized magnetic sails can produce sub-Newton-class thrust in the ion inertial scale ( $\sim 70$  km). We continue our efforts to make a feasibly sized plasma sail (Magnetoplasma sail) by optimizing the magnetic field inflation process Winglee proposed. However, several physical issues (action and reaction force of the MPS, finite Larmor radius effect in the far region of the MPS, and so on) were shown to remain to be solved before we proceed to a system design of a spacecraft propelled by MPS.

JAXA/JEDI Workshop on Plasma Simulation (2006.10.2-3)

# **Research of Magnetoplasma Sail (MPS): A Quick Review**

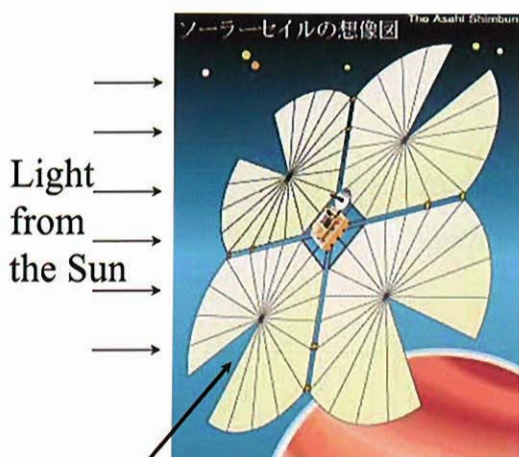
**Ikkoh Funaki, Hiroshi Yamakawa  
and  
MPS Research Group**

## **Outline**

1. Background
  - Principles of MagSail and MPS (Magnetoplasma Sail)
  - Status of M2P2 (Mini-Magnetospheric Plasma-Propulsion by Winglee)
2. Goal of our MPS Research
3. Status of MPS Research in Japan
  - Numerical Simulations
  - Experiment in Vacuum Chamber
4. Summary

# 1. Background

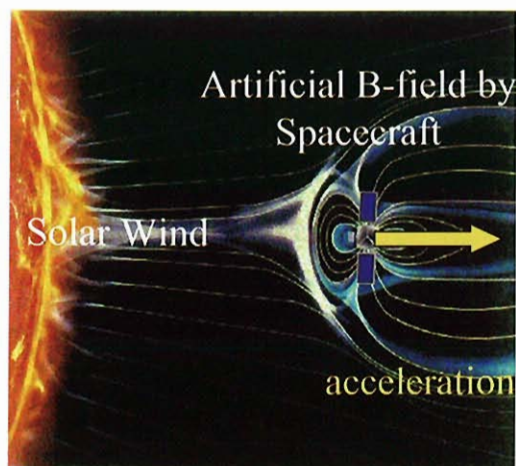
## Spacecraft Propulsion Using Solar Energy



Mirror

### Solar Sail

- Thrust production by light pressure
- low acceleration



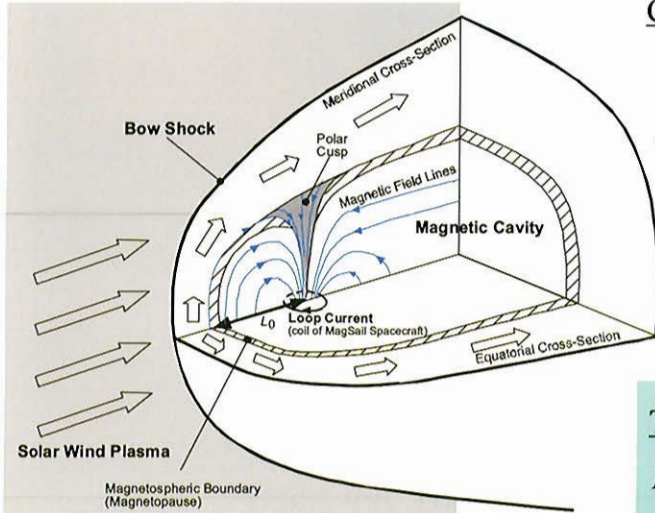
### Magnetic Sail (MagSail)

- Thrust production by the solar wind
- high acceleration for M2P2?

inflation B-field with plasma jet



# Plasma Flow of Pure MagSail and its Thrust



Plasma Flow and B-field of MagSail

Characteristic Length of MagSail  
(Stand-off distance,  $L_0$ )

$$L_0 = \sqrt[6]{\frac{\mu_0 M^2}{8\pi^2 n m_i u^2}}$$

$M$ : dipole moment  
 $n m_i u^2$ : solar wind dynamic pressure

$L_0$  is derived from pressure balance:

$$n m_i u^2 = \frac{(2B_{mp})^2}{2\mu_0} \quad \text{and} \quad B_{mp} = \frac{\mu_0 M}{4\pi L_0^3}$$

Thrust of Magsail (Drag Force)

$$F = C_d \frac{1}{2} \rho u_{sw}^2 S$$

$$= C_d \frac{1}{2} \rho u_{sw}^2 (\pi L_0^2)$$

┌ ── solar wind dynamic pressure  
└ ── non-dim. Thrust coefficient  
    (a function of  $L_0, \rho, u_{sw}$ )

# MagSail with Plasma Jet (M2P2/MPS)

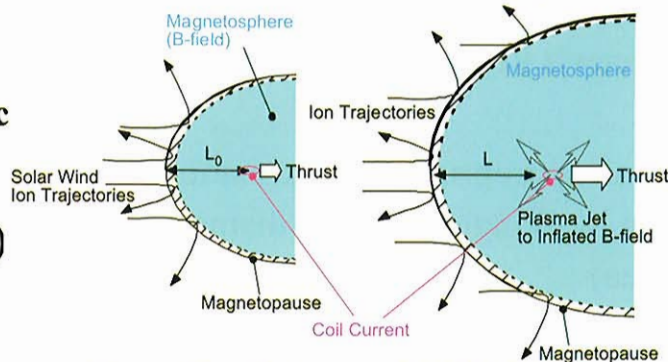
Mini-Magnetospheric Plasma Propulsion

MagnetoPlasma Sail

**Schematics of Magnetic Field Inflation:**

$$\text{Large } F = C_d \frac{1}{2} \rho u_{sw}^2 (\pi L^2)$$

by enlarging  $L$

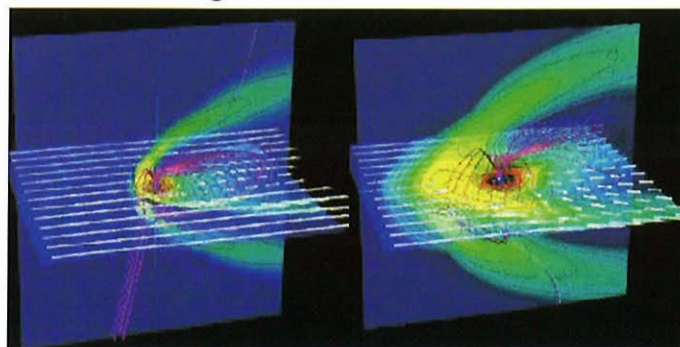


Pure MagSail

M2P2/MPS

**MHD Simulation**

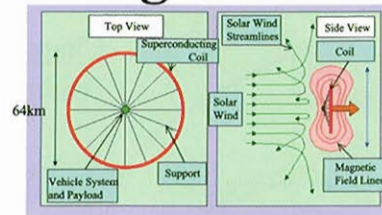
by Winglee (SATIF2000)



## Research History of Magnetic Sails

### Zubrin(JSR1990)

First proposal of Magnetic Sail (MagSail)  
20-N pure MagSail using 64-km-diameter coil

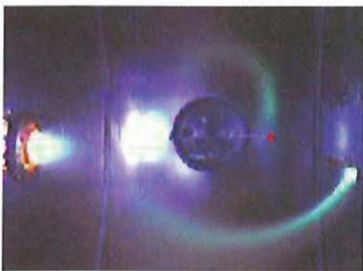


### Winglee(JGR 2000)

Mini-Magnetospheric Plasma Propulsion (MagSail with Plasma Jet)  
using 20-cm-diameter coil and high-density plasma source

### Winglee(AIAA Conf. 2001, 2003)

Ground experiment on M2P2 prototype



### Khazanov(AIAA Conf.2003, JPP 2005)

From numerical simulations (MHD+Hybrid)  
M2P2 (Winglee's design) was denied because of  
its negligible thrust production.

### Slough(AIAA Conf., 2005)

New concept: Plasma Magnet

## Controversy of Winglee's M2P2 Concept

Khazanov's Report (J. Propul. Power, 2005)

- MHD is not an appropriate approximation to describe M2P2 design by Winglee (10-cm-diameter coil with plasma source)
- With ion kinetic simulation, it was shown that the M2P2 design could provide only negligible thrust.
- $L$  (stand-off distance of magnetic cavity)  $\gg$  ion inertial scale (70 km), hence, considerably larger sails (than that Winglee proposed) would be required to tap the energy of the solar wind.

## 2. Goal of Our MPS Research

Design a sub-Newton-class MPS for 1000-kg-class deep space spacecraft that is suitable for a H-IIA launch by:

1. finding  $L$  (stand-off distance of magnetosphere) for  $F=0.1\sim 1\text{N}$
2. clarifying thrust production mechanism of MPS
3. optimizing the magnetic field inflation process

## 3. Status of MPS Research

# Status of MagSail/MPS Research

○=Finished, △= Going on, ×= Not started yet

Cases	Input and Output for Simulation	Numerical Simulation		Experiment
		MHD	Hybrid (ion particle, electron fluid)	Scale-model Experiment
Pure MagSail	$F$ for various $L_0$ ( $C_d$ for various $r_{Li}/L$ )	○	○	△
MPS	$F$ and $L$ for various plasma jet and $L_0$ ( $C_d$ and $r_{Li}/L$ for various $r_{Li}/L_0$ and $\beta_0$ )	△	×	△

$$F = C_d \frac{1}{2} \rho u_{sw}^2 (\pi L_0^2) \text{ for pure MagSail}$$

$$F = C_d \frac{1}{2} \rho u_{sw}^2 (\pi L^2) \text{ for MPS with } L=L(L_0, \beta_0), \beta_0 = \frac{1}{2} \rho_0 u_0^2 \Big/ \frac{B_0^2}{2\mu_0}$$

## Why MHD and Ion Hybrid Simulation?

Because the solar wind and the B-field interaction is in transitional regime

Characteristic length:

1) Cavity (magnetopause) size:  $L_0$

2) Skin depth of magnetopause:

$$\delta = c/\omega_p$$

3) Ion Larmor radius

$$\text{at magnetopause: } r_{Li} = \frac{m_i u_{sw}}{e \cdot 2B_{mp}} \sim 70 \text{ km}$$

**Non-dimensional parameters and conditions for  $L_0=10\sim 70\text{km}$ :**

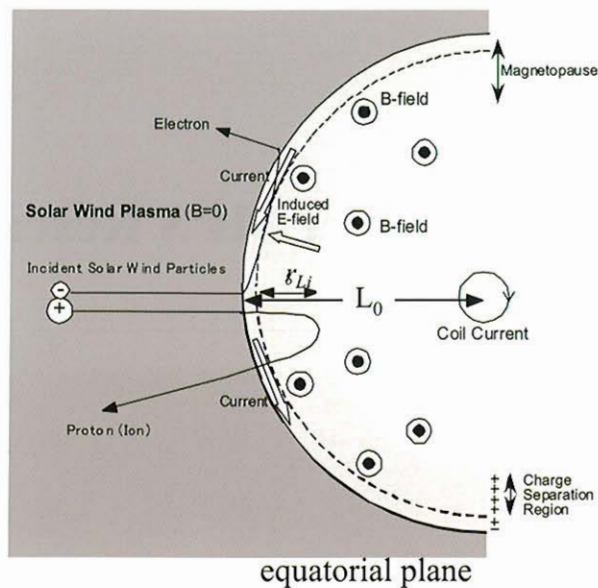
1)  $\delta/L_0 < 0.1$

2)  $1 < r_{Li}/L_0 < 7$

3) Mag. Reynolds No.

$$Rm = \sigma \mu_0 u_{sw} L_0 \gg 1$$

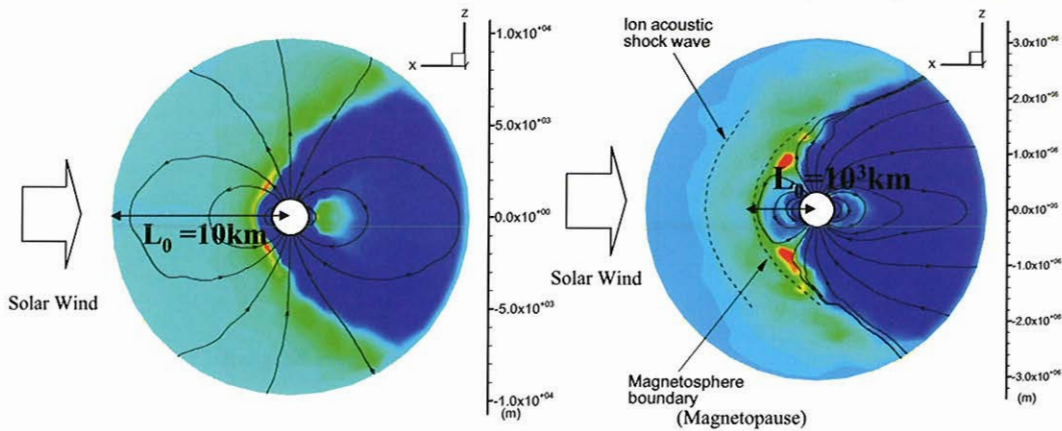
4) Mach No.  $M_i = \frac{u_{sw}}{\sqrt{\gamma RT_{sw}}} \sim 8$



**Flow around MagSail (coil current)**  
charged particle behavior near magnetopause

# Plasma Flow around Pure MagSail

Hybrid plasma simulation: ion particle/electron fluid (by K.Fujita, JAXA)



$m=4 \times 10^4 \text{ Tm}^3, L_0=10 \text{ km}, r_L/L_0=10$  (at  $L_0$ )     $m=4 \times 10^{10} \text{ Tm}^3, L_0=10^3 \text{ km}, r_L/L_0=0.1$  (at  $L_0$ )  
 $r_L$ : ion Larmor radius

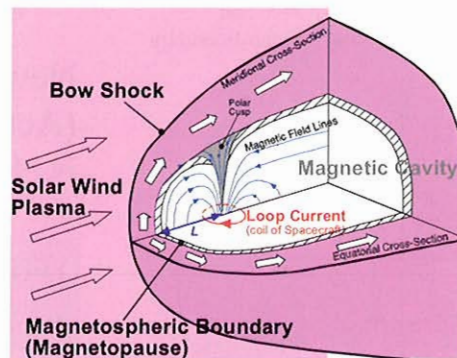
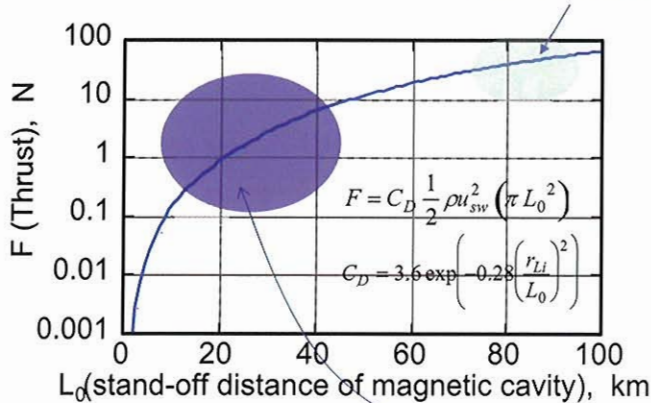
## Distribution of Ion Number Density and Magnetic Field Lines

- ion trajectory deformation by  $\mathbf{u} \times \mathbf{B}$
- small interacting area  $\ll L_0^2$
- $C_d \sim 0.5$
- MHD-like interaction with a shock
- interacting area  $\sim L_0^2$
- $C_d \sim 3.6$

# Thrust Characteristics of Magsail

Effect of Stand-off Distance ( $L_0$ ) on Thrust ( $F$ )

20-N-class (Zubrin)



Definition of  $L_0$

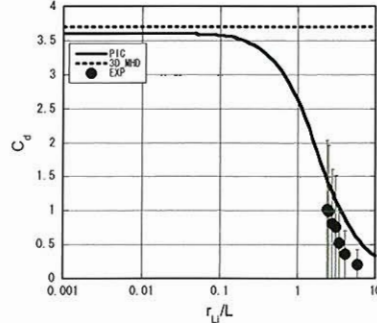
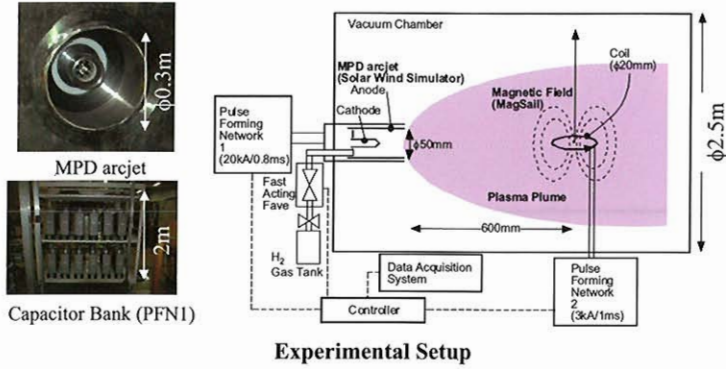
Target: 1-N-class MagSail (for 1,000-kg-spacecraft)

## Empirical relation between $L_0$ and thrust of MagSail ( $F$ )

$C_D$  formulation by Fujita, J. Space Science and Technol., 2004

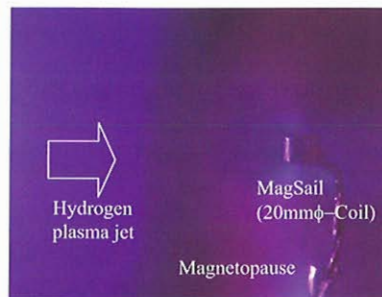
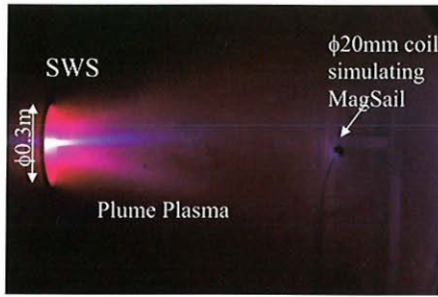
# Magnetic Sail Experimental Simulator

- scale-model experiment of 0.1-N-class pure MagSail in a vacuum chamber
- whole MPS system may be demonstrated in the future



Experimental Setup

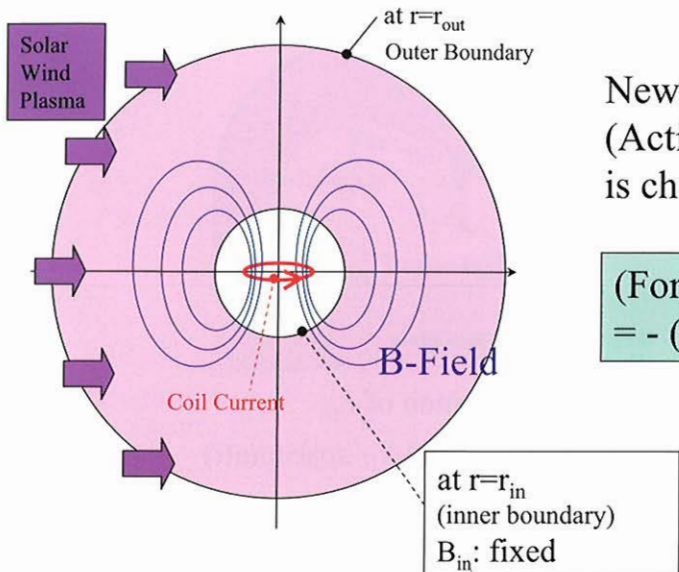
$C_d$  for 0.1-1N class pure MagSail



Operation of Solar Wind Simulator and MagSail Close-up view of a Plasma Flow around Coil

H<sub>2</sub> 0.4g/s, PFN1:4.0kV, 1.9T at the coil center (plasma duration:0.8ms, density: 10<sup>18</sup>/m<sup>3</sup>, velocity: 50 km/sec)

## Calculation Region, Boundary Conditions, and Thrust Evaluation for Pure MagSail



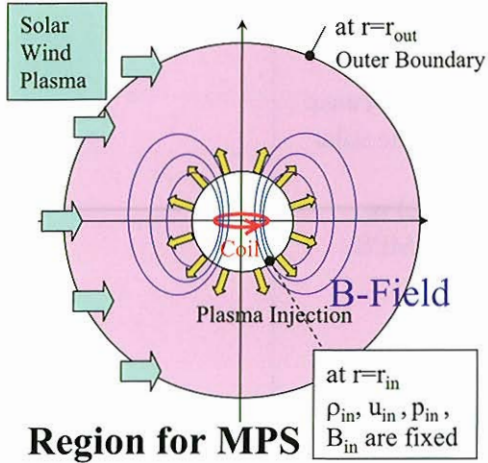
Newton's 3rd Law (Action and Reaction Force) is checked:

$$\text{(Force exerting on Coil)} = - \text{(Force on solar wind plasma)}$$

Lorentz force  
Drag force

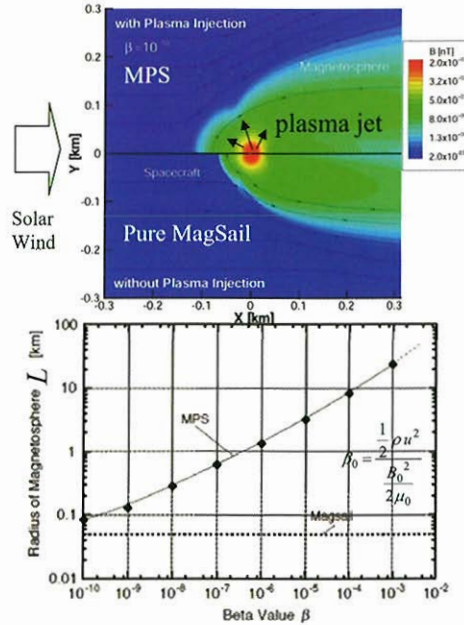
Region for Pure MagSail

# Calculation Region, Boundary Conditions, and Thrust Evaluation for MPS



(Force exerting on Coil)  
 $\neq$  - (Force on solar wind plasma)

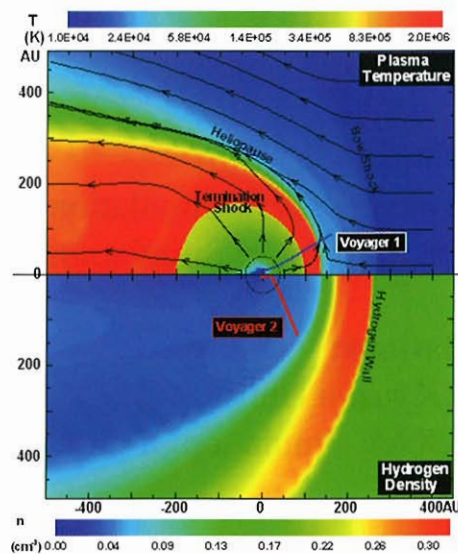
- Newton's 3rd Law (Action and Reaction Force) is violated??
- boundary condition problem?
  - $\text{div}B > 0$  trouble?



Simulation Results of MPS and Pure MagSail (by Otsu, Shizuoka Univ.)

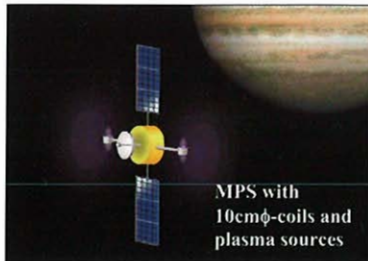
## Remaining Issues of MPS Simulation

1. In our current MHD simulation, force of MPS is evaluated by the momentum change of the solar wind. "How thrust exerts on the coil current" should be answered (by precisely analyzing the magnetic field near the coil).
2. Far from the coil, an MHD-scale flow will transit to an ion kinetic scale. Hybrid simulation is required at least at this region far ( $> 1$  km) from the coil.
3. Efficient and low cost way to inflate the magnetic field are under survey.



The structure of Heliosphere: MPS field may be analogous to Heliosphere except its small pause size ( $L \sim 10$  km).

## 4. Summary

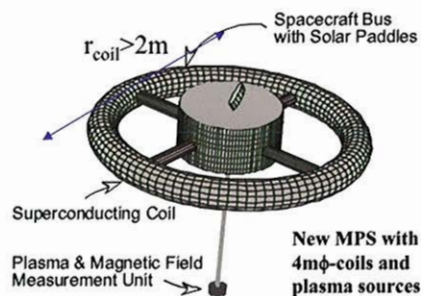


### MPS (2003) started with small coil:

- produces only 1-mN-class thrust because of very weak coupling between the solar wind and the B-field.
- ~10-km-radius magnetopause ( $L$ ) is necessary for 0.1- to 1-N-class MPS.

### New MPS design (2005) with 4m-diameter coil:

- will produce  $> 0.5$  N for 10kW
- efficient and low-cost B-field inflation strategy is surveyed.
- two important physical issues: Newton's 3rd Law, effect of ion inertial scale physics on thrust production



## Today's Presenters

### MHD simulations:

Mr. Nishida (Tokyo Univ.): Simulation of pure MagSail

Dr. Otsu (Shizuoka Univ.): Simulation status of MPS

### Hybrid Simulations:

Dr. Kajimura (Kyushu Univ.):

(Dr. Fujita (JAXA): simulation of pure MagSail (when requested))



## MHD Study on Pure Magnetic Sail

Hiroyuki Nishida

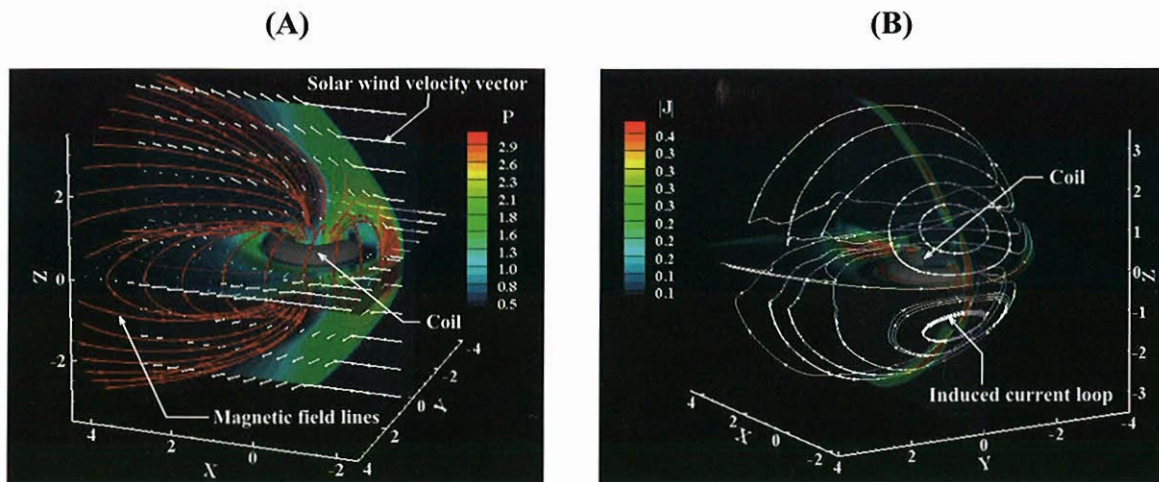
University of Tokyo

E-mail: [nishida@isas.jaxa.jp](mailto:nishida@isas.jaxa.jp)

Hiroyuki Ogawa, Ikkoh Funaki, Hiroshi Yamakawa and Yoshifumi Inatani  
Japan Aerospace Exploration Agency

Magnetic Sail is a deep space propulsion system which captures the momentum of the solar wind by a large artificial magnetic field produced around a spacecraft. To verify the momentum transfer process from the solar wind to the spacecraft, we simulated the interaction between the solar wind and the artificial magnetic field of Magnetic Sail using magnetohydrodynamic model. The result showed the same plasma flow and magnetic field structure as those of the Earth. The change of the solar wind momentum results in a pressure distribution on the magnetopause. The pressure on the magnetopause is then transferred to the spacecraft through the Lorentz force between the induced current along the magnetopause and the current along the coil of the spacecraft. The simulation successfully demonstrated that the solar wind momentum is transferred to the spacecraft via the Lorentz force. The drag coefficient (thrust coefficient) of the Magnetic Sail was estimated to be 5.0.

Figure 1: Flow field and magnetic field around Magnetic Sail (A), and induced currents around Magnetic Sail (B).



JAXA/JEDI workshop on numerical plasma simulation for spacecraft environment

## MHD Study on Pure Magnetic Sail

H.Nishida

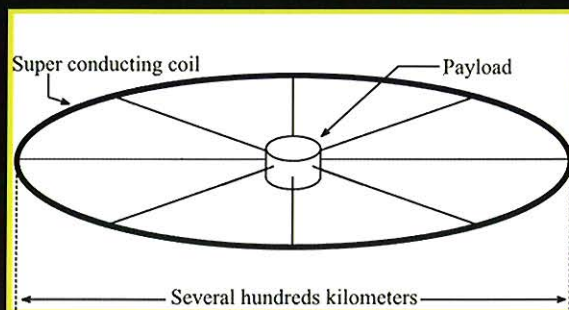
*University of Tokyo*

H.Ogawa, I.Funaki, H.Yamakawa and Y.Inatani

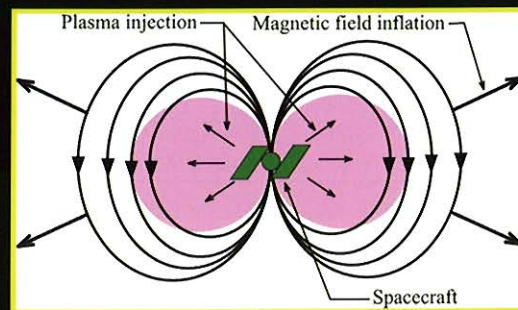
*Japan Aerospace Exploration Agency*

## Magnetic Sail and Magneto Plasma Sail (MPS)

➤ Propulsion systems generating thrust through the interaction between the solar wind and the magnetic field produced around the spacecraft.



Magnetic Sail



Magneto Plasma Sail (MPS)  
(M2P2)

- Magneto Plasma Sail is a more realistic propulsion system.

## Previous researches

Some numerical researches about thrust generation mechanism and performance of those propulsion systems by kinetic model of ion

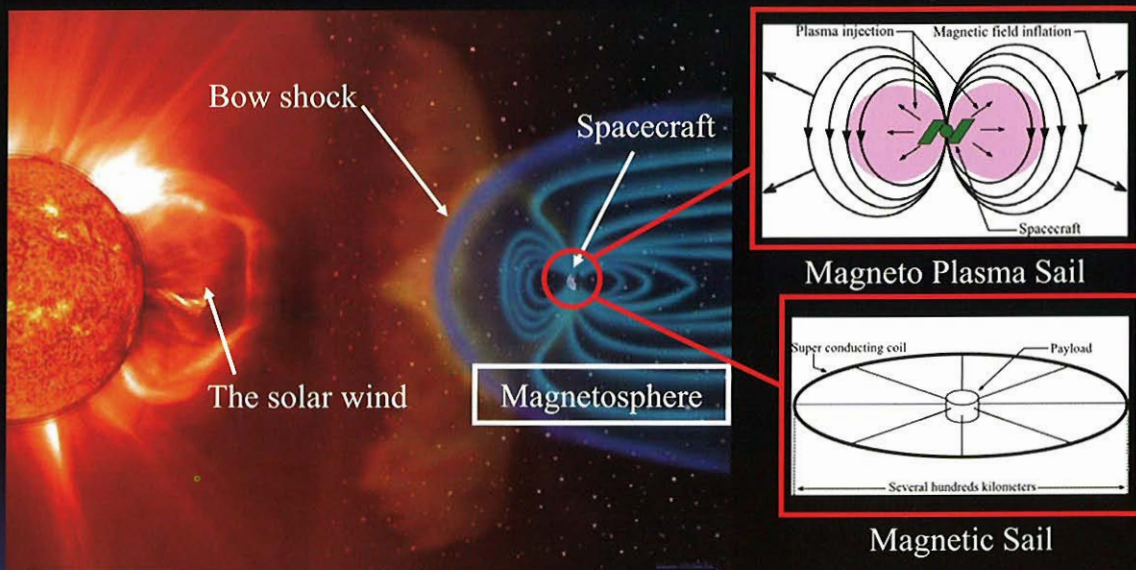
- Hybrid code; Khazanov, Omidi, Saha, et al ....
- Particle-in-Cell code; Fujita, et al ....

Research based on magnetohydrodynamics (MHD) is needed, too.

Because ...

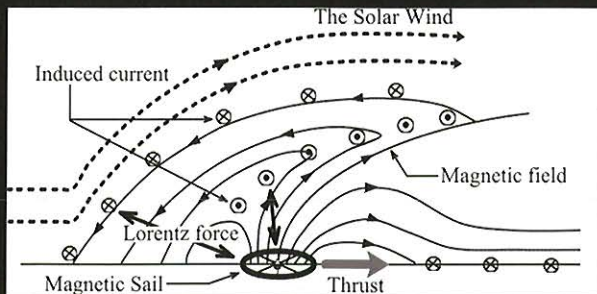
- The small interaction in kinetic scale of ions generating only small thrust
- Kinetic simulation needs high numerical cost.
- Researches based on MHD; Winglee, Zubrin, ....

## Principle of propulsion

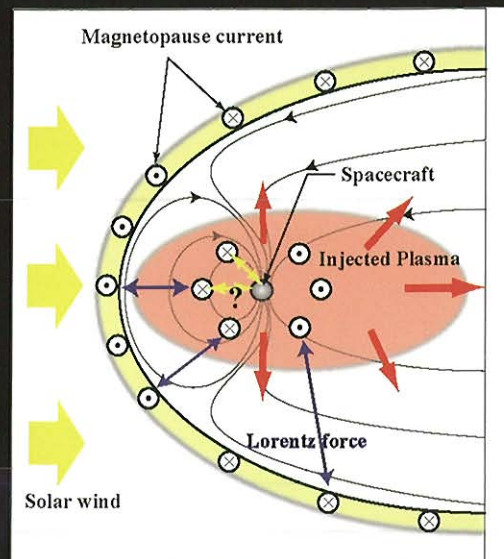


Interaction between the solar wind and the magnetic field around the spacecraft

## Principle of propulsion



Magnetosphere around Magnetic Sail



Magnetosphere around Magneto Plasma Sail

- Momentum of the solar wind is transferred to the spacecraft through electromagnetic interaction

## Objectives

In this study, the interaction between the solar wind and the magnetic field of Magnetic Sail is simulated based on magnetohydrodynamics.

- By two-dimensional MHD simulation,
  - identifying action and reaction forces and their balance in order to verify the momentum transfer process.
- By three-dimensional MHD simulation,
  - estimating the thrust vector and the torque on the Magnetic Sail.

## Governing Equations and Numerical Methods

- Normalized ideal magnetohydrodynamic equations

$$\frac{\partial \rho}{\partial t} + \nabla \cdot (\rho \mathbf{v}) = 0$$

$$\frac{\partial \rho \mathbf{v}}{\partial t} + \nabla \cdot (\rho \mathbf{v} \mathbf{v} + p \mathbf{I}) = \mathbf{J} \times \mathbf{B}$$

$$\frac{\partial \mathbf{B}}{\partial t} - \nabla \times (\mathbf{v} \times \mathbf{B}) = 0$$

$$\frac{\partial E}{\partial t} + \nabla \cdot \left[ \left( E + p + \frac{B^2}{2} \right) \mathbf{v} - \mathbf{B}(\mathbf{B} \cdot \mathbf{v}) \right] = 0$$

$$\mathbf{J} = \nabla \times \mathbf{B}$$

- Numerical method:

- Flux-Corrected Transport (FCT) scheme
- TVD Lax-Friedrich scheme with 8-wave formulation

$t$  : time

$\rho$  : density,

$p$  : pressure,

$\mathbf{v}$  : velocity vector,

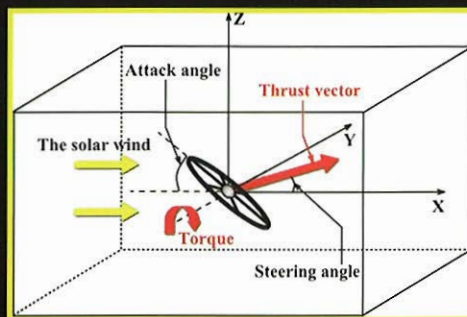
$\mathbf{B}$  : magnetic flux vector,

$\mathbf{I}$  : unit matrix,

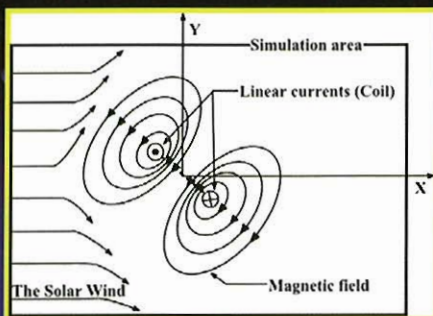
$\mathbf{J}$  : current vector,

$E$  : energy density.

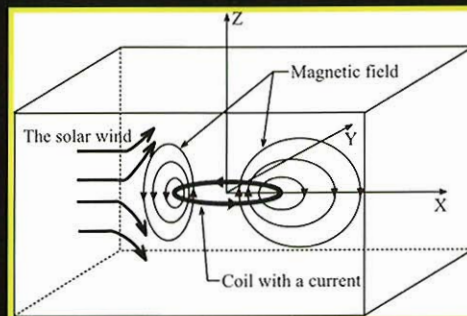
## Computational Models



The definition of the coordinate system.



Simulation box of two-dimensional simulation.



Simulation box of three-dimensional simulation.

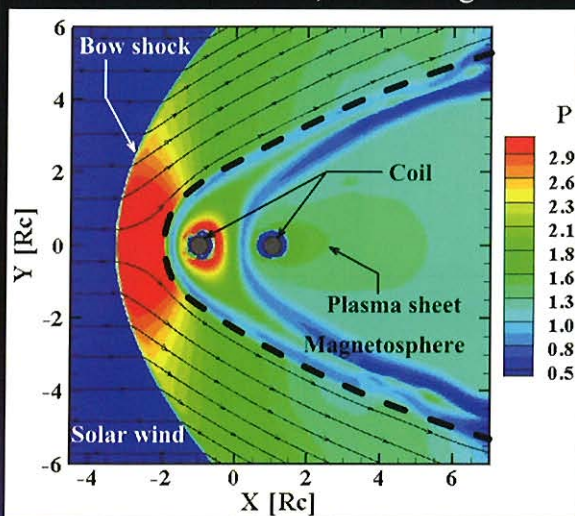
## Computational Parameters

Solar wind velocity	0.917 (400km/sec)	
Solar wind pressure	$8.68 \times 10^{-2}$ (20 eV)	
Solar wind density	$5.0 (5m_i \times 10^6 \text{ kg/m}^3)$	
IMF	0 T	
Coil currents	$1.2 \times 10^{12}$ In 2D simulation	$9.6 \times 10^{12}$ In 3D simulation
Attack angle	0 ~ 90 deg	
Simulation area	$-5 < X < 7, -6 < Y < 6$ In 2D simulation	$-2.5 < X < 4.5, -4 < Y < 4, -3.5 < Z < 3.5$ In 3D simulation

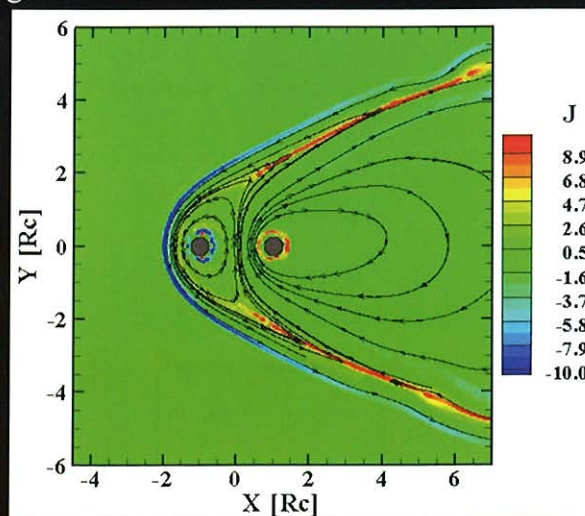
(In normalized value)

## Two-dimensional Simulation – Flow Field

Rc = radius of the coil, attack angle = 0 degrees



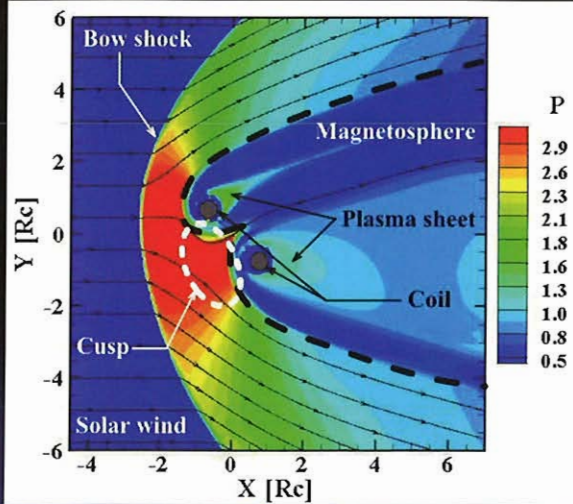
Pressure contours and streamlines



Induced current contours and magnetic field lines

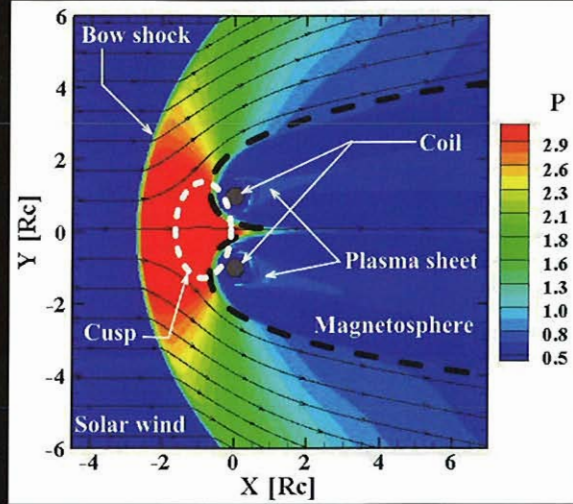
## Two-dimensional Simulation – Flow Field (2)

Attack angle = 45 degrees



Pressure contours and streamlines

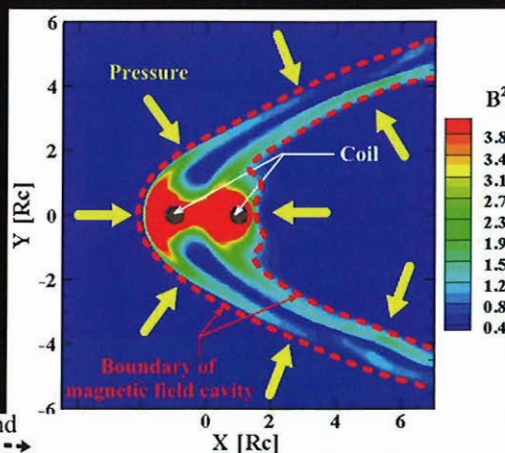
Attack angle = 90 degrees



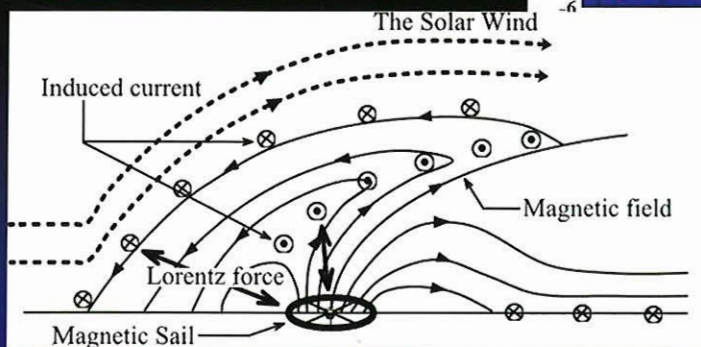
Pressure contours and streamlines

## Identifying action and reaction forces

- F1: Momentum change of the solar wind.
- F2: Force acting on the magnetosphere by the solar wind pressure.
- F3: Lorentz force between the induced current and the coil's current.

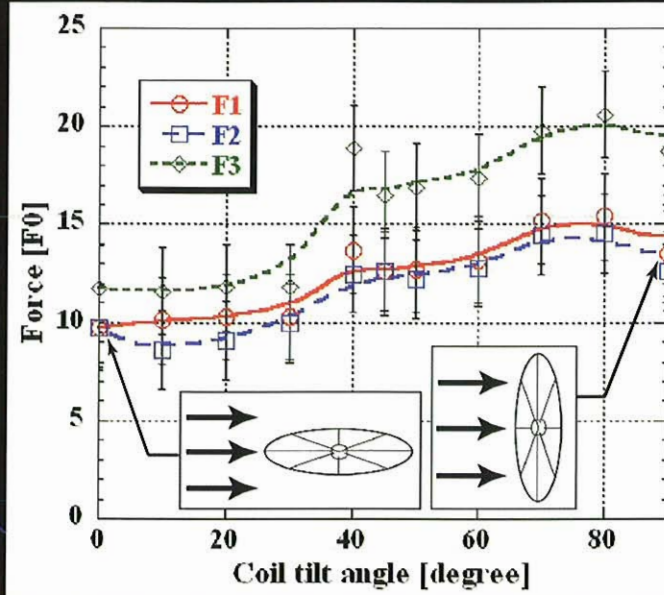


The magnetic field intensity contours and the magnetic field cavity pressed by the solar wind pressure



Lorentz force between the induced current and the coil's current (F3)

## Evaluation of forces

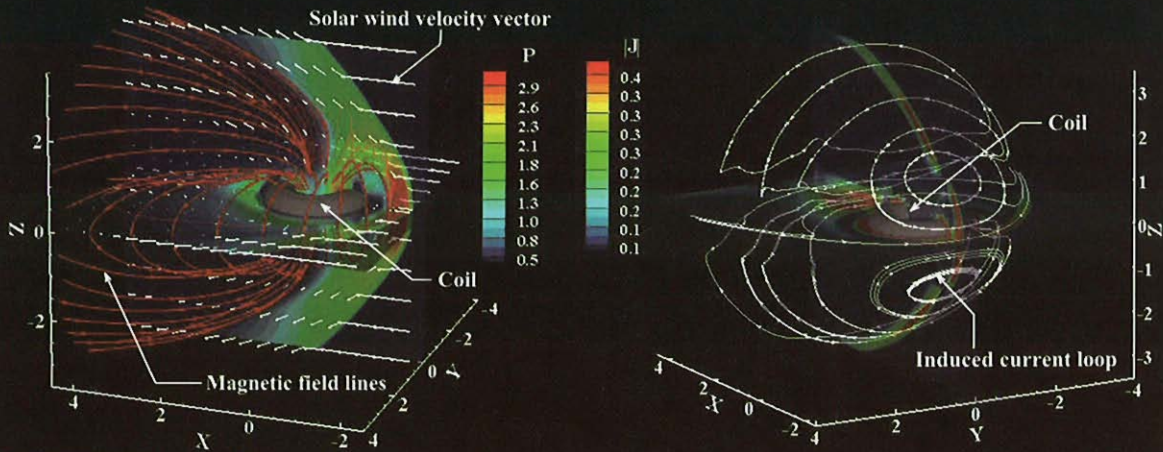


The relation between the attack angle and forces in normalized value

- Each force is of the same order and in same trend. These three forces are the same.

## Three-dimensional Simulation – Flow Field

attack angle = 0degrees



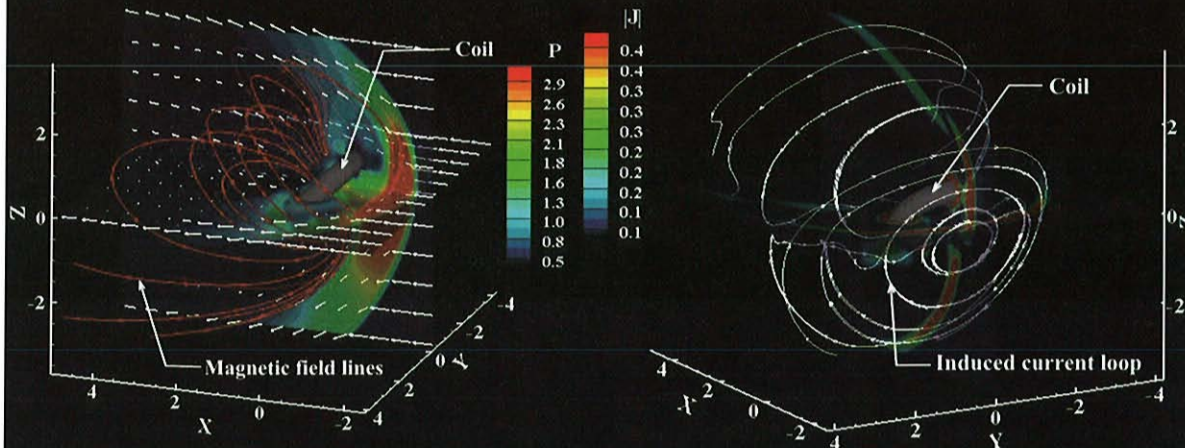
Magnetic field lines, flow velocity vectors and pressure contours.

Induced current contours and induced current lines.



### Three-dimensional Simulation – Flow Field (2)

attack angle = 45degrees

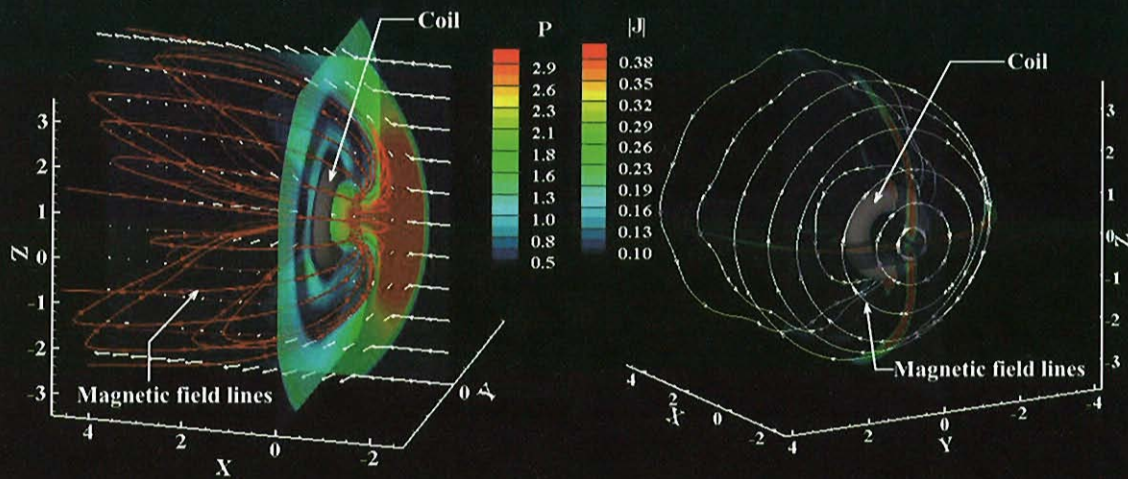


Magnetic field lines, flow velocity vectors and pressure contours.

Induced current contours and induced current lines.

### Three-dimensional Simulation – Flow Field (3)

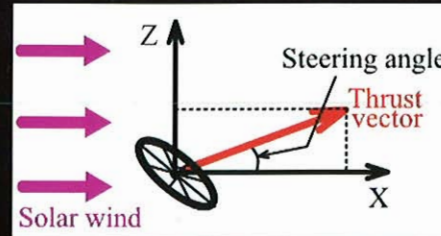
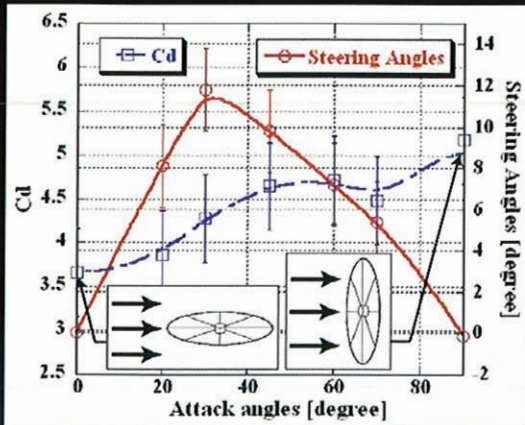
attack angle = 90degrees



Magnetic field lines, flow velocity vectors and pressure contours.

Induced current contours and induced current lines.

# Thrust vectors

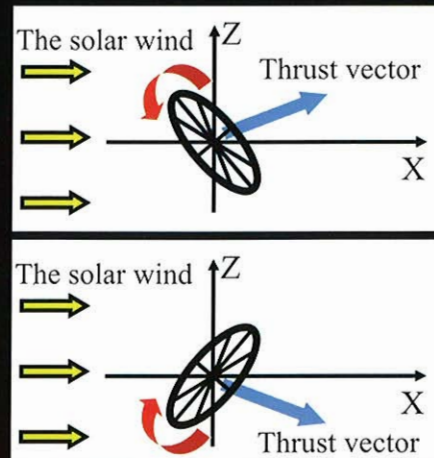
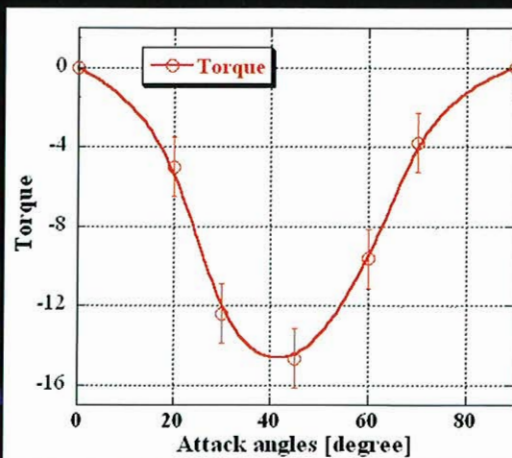


Drag coefficient  $C_d = D / \left( \frac{1}{2} \rho v^2 S_c \right) : S_c = \pi r_r^2$   
 $r_r =$  shock stand off distance from the center of the coil.

The relation between attack angle and the thrust vector.

- Highest thrust in 90 degrees.

# Torque



The relation between attack angle and the torque.

- Magnetic Sail has static stability around 0 degrees in attack angles.

## The validity of MHD assumption

The scale of Magnetic Sail

Radius of the coil [km]	Current in the coil [kA]	Thrust [N]	Max Torque [N.m]	rLi/rr	MHD validity
10	4	2.25	4.5k	1.25	×
20	8	9	36k	0.625	△
40	16	36	284k	0.315	△
100	40	225	4500k	0.125	○
200	80	900	18000k	0.0625	○

- When  $rLi/rr \ll 1$ , MHD validity satisfied.
- In this simulation, when radius of the coil > 100km, MHD assumption is valid.

## Summary

The Magnetic Sail was simulated based on magnetohydrodynamicis to verify the momentum transfer process, and to estimate the thrust vector and the torque.

- The simulation successfully demonstrated that the change of the momentum of the solar wind is transferred to the spacecraft via the Lorentz force.
- The maximum drag coefficient (thrust coefficient) is estimated to be 5.0 when the attack angle is 90 degrees.
- Maximum steering angle is estimated to be 12 degrees when the attack angle is 30 degrees.
- Magnetic Sail can control the thrust vector by changing the attack angle, but cannot maintain a constant attack angle without dynamic attitude control due to the static stability.

## **MPS まわりの流れ場の MHD 解析の現状について**

Current Status of MHD Simulation for Magneto Plasma Sail

大津 広敬

静岡大学工学部機械工学科

E-mail: thootu@ipc.shizuoka.ac.jp

磁気プラズマセイル (Magneto Plasma Sail; MPS) とは、探査機まわりに磁気圏を形成し、高速のプラズマ流である太陽風を「磁場の帆」で受け止め、太陽風の動圧を推力として利用する推進システムである。本推進システムにおける推力は「帆」に相当する磁気圏の大きさに比例するため、磁気圏を拡大するために、探査機周りに形成された磁場にプラズマを噴射することにより、効率よく磁気圏を広げる方法が検討されている。本報告では、探査機周りの流れ場がどのように形成されるかを調べるために、電磁流体方程式による数値シミュレーションを行い、噴射プラズマによる磁気圏の変化や太陽風と磁場の干渉の様子を調べた。その解析結果について報告する。

JAXA/JEDI Workshop (2006/10/3)

# Current Status of MHD Simulation for Magneto Plasma Sail

Hiroataka Otsu (Shizuoka University)

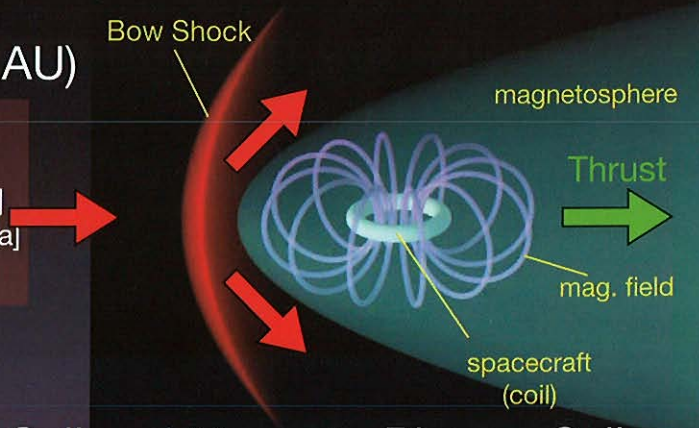
## Contents

- What is Magneto Plasma Sail (MPS) ?
- Numerical Method
- CFD analysis for Mag Sail
- CFD analysis for MPS
  - Inflation of magnetic field
  - Thrust estimation
- Summary

## Propulsion system utilizing the solar wind

- Solar wind(@1AU)

Gas : H<sup>+</sup>, e<sup>-</sup>  
 Density : 5.0 [cm<sup>-3</sup>]  
 Velocity : 300~500[km/s]  
 Dynamic Pressure : 1[nPa]



- Thrust of Mag Sail and Magneto Plasma Sail

- Thrust is the drag force to the magnetosphere
- Thrust is transfered to spacecraft via electromagnetic effect
- Thrust = (dynamic pressure) x (size of magnetic field)

3

## Inflation of Magnetic Field

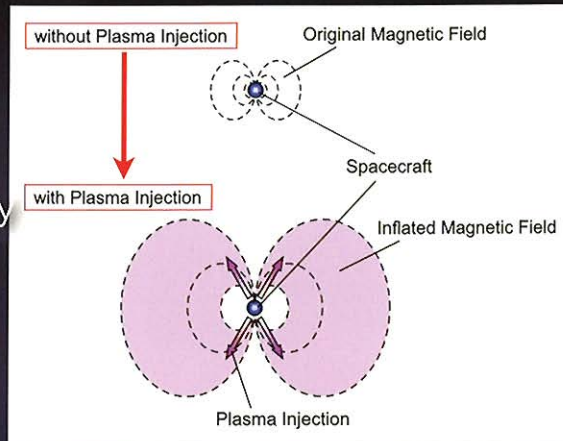
- Mag Sail

- Magnetic Field by Coil only
- Very large coil is necessary



- Magneto Plasma Sail

- Magnetic Field is inflated by injected plasma
- Large coil is not necessary



4

## Previous Works

### MHD Simulation

- Interaction between solar wind and magnetic field for Mag Sail
- Inflation of magnetic field without solar wind

No results for interaction between the solar wind and the **inflated** magnetic field

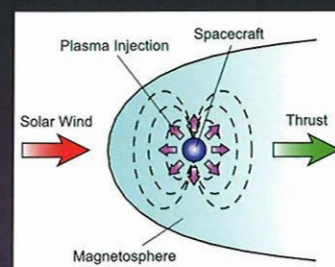
5

## Objective

- 3-dimensional MHD simulation for MPS  
Interaction + Inflation



- Effect of Injected Plasma
  - Dimension of magnetosphere
  - Thrust estimation



6

## Governing Equation

- Ideal MHD equation
- Magnetic field is separated into two parts
  - Initial magnetic field  $\mathbf{B}_0$
  - Induced magnetic field  $\mathbf{B}'$
  - Total magnetic field  $\mathbf{B} = \mathbf{B}_0 + \mathbf{B}'$

$$\frac{\partial}{\partial t} \begin{bmatrix} \rho \\ \rho \mathbf{u} \\ \mathbf{B}' \\ E'_t \end{bmatrix} + \nabla \cdot \begin{bmatrix} \rho \mathbf{u} \mathbf{u} + (p + \frac{\mathbf{B}' \cdot \mathbf{B}'}{2}) \mathbf{I} - \mathbf{B}' \mathbf{B}' \\ \mathbf{u} \mathbf{B}' - \mathbf{B}' \mathbf{u} \\ (E'_t + p + \frac{\mathbf{B}' \cdot \mathbf{B}'}{2}) \mathbf{u} - (\mathbf{u} \cdot \mathbf{B}') \mathbf{B}' \end{bmatrix} + \nabla \cdot \begin{bmatrix} 0 \\ (\mathbf{B}_0 \cdot \mathbf{B}') \mathbf{I} - (\mathbf{B}_0 \mathbf{B}' + \mathbf{B}' \mathbf{B}_0) \\ \mathbf{u} \mathbf{B}_0 - \mathbf{B}_0 \mathbf{u} \\ (\mathbf{B}_0 \cdot \mathbf{B}') \mathbf{u} - (\mathbf{u} \cdot \mathbf{B}') \mathbf{B}_0 \end{bmatrix} = -\nabla \cdot \mathbf{B}' \begin{bmatrix} 0 \\ \mathbf{B} \\ \mathbf{u} \\ \mathbf{u} \cdot \mathbf{B}' \end{bmatrix}$$

Density :  $\rho$    Velocity :  $\mathbf{u}$    Pressure :  $p$    Heat Ratio :  $\gamma$

time :  $t$    Energy :  $E'_t = \frac{p}{\gamma - 1} + \frac{1}{2} \rho \mathbf{u} \cdot \mathbf{u} + \frac{\mathbf{B}' \cdot \mathbf{B}'}{2}$

7

## Numerical Method

- Numerical Flux
  - Lax-Friedrich Scheme
  - MUSCL (Cubic Limiter)
- Time Integration
  - Euler Explicit Method
  - Local Time Step
- $\nabla \cdot \mathbf{B} = 0$  constraint
  - 8-wave Formulation
- Specific Heat Ratio  $\gamma = 5/3$

8

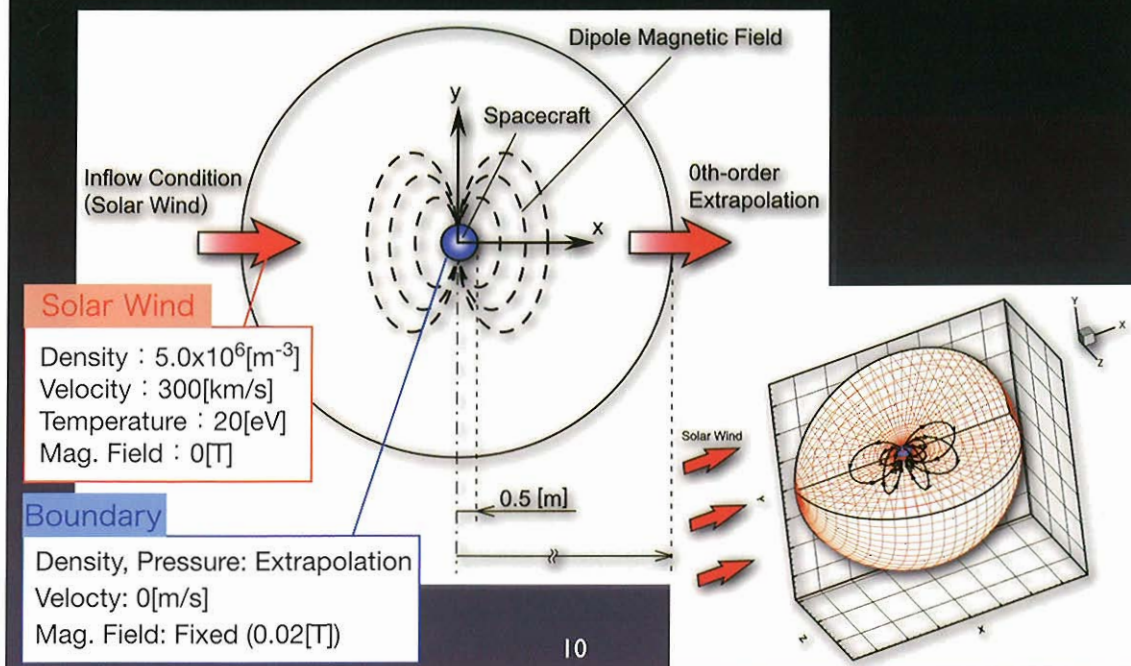


# without Plasma Injection

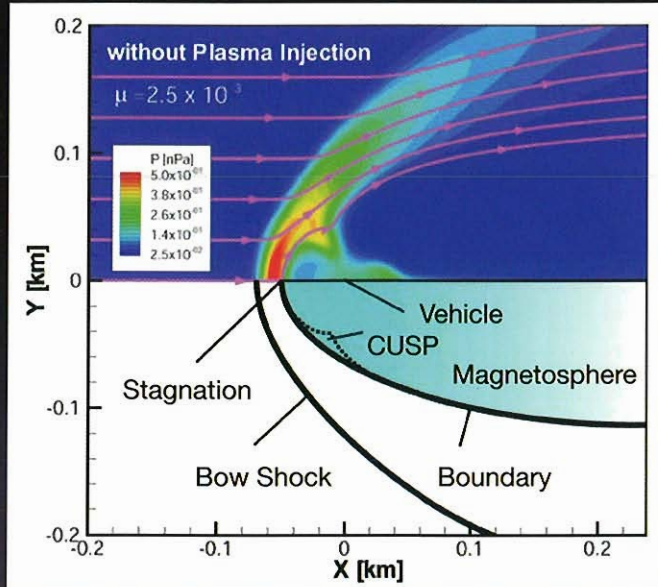
## Flow field around Mag Sail ( Assessment of Numerical Method )

9

### Calculation condition



## Flow field around Mag Sail



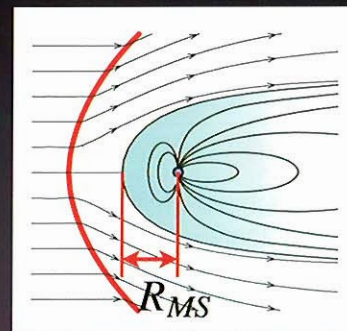
Flow field which is similar to the interaction between the Earth and the solar wind can be reproduced qualitatively.

11

## Quantitative Assessment

- Radius of Magnetosphere

	RMS [km]
CFD	0.0499
Theory	0.0486



Good agreement between CFD and theory!

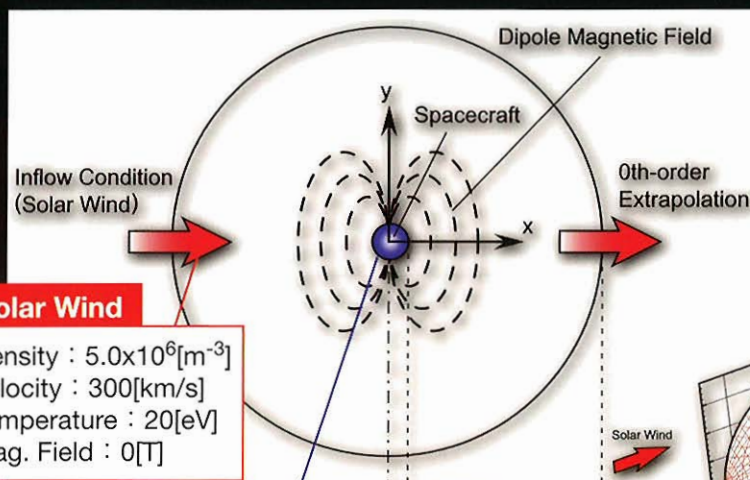
12

# with Plasma Injection

## Flow field around Magneto Plasma Sail

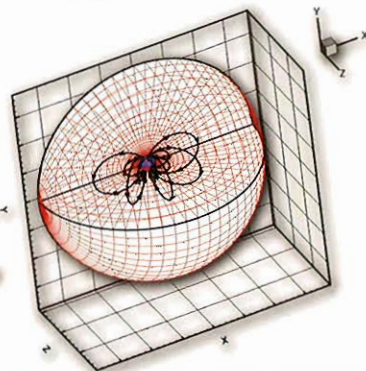
13

### Calculation condition



**Solar Wind**  
 Density :  $5.0 \times 10^6 [\text{m}^{-3}]$   
 Velocity : 300 [km/s]  
 Temperature : 20 [eV]  
 Mag. Field : 0 [T]

**Boundary**  
 Density, Pressure, Velocity: Fixed  
 Mag. Field: Fixed (0.02 [T])



14

## Injected Plasma

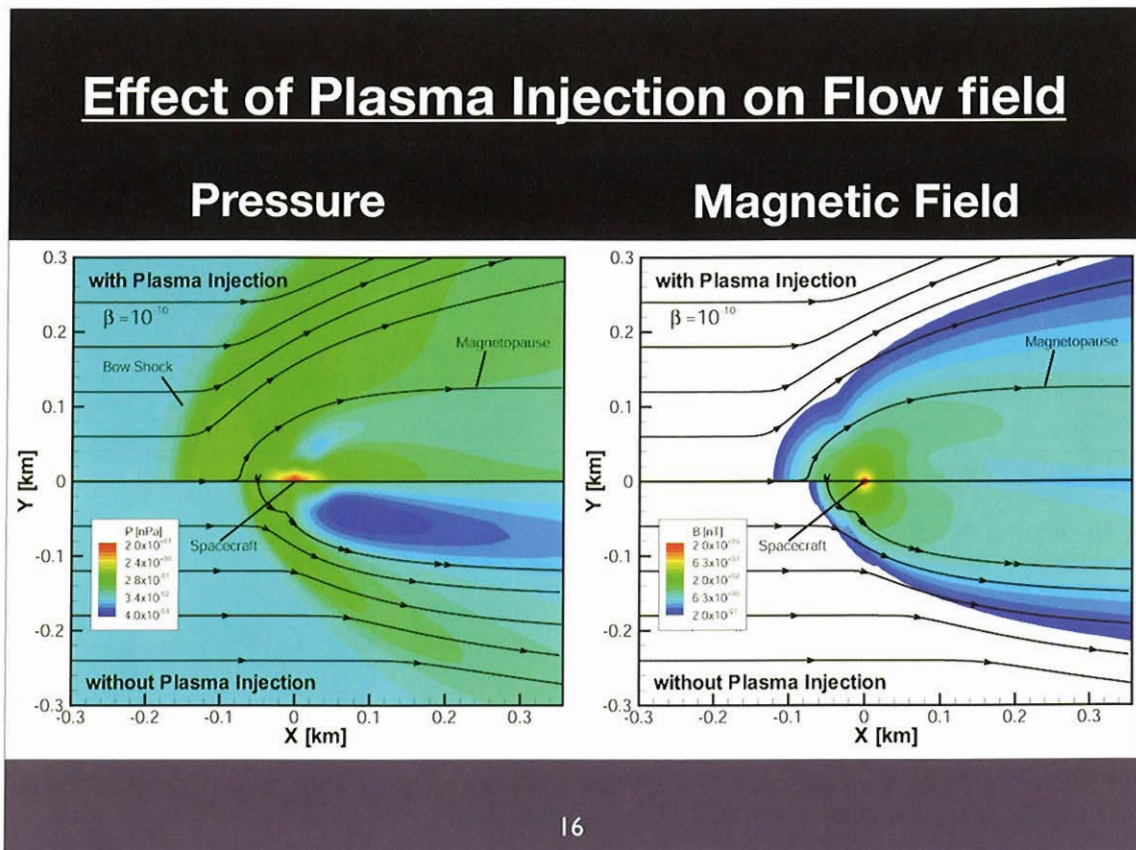
Ion	Ar <sup>+</sup>
Velocity	4.0[km/s]
Temp.	20,000[K]
Mach	1.1
Beta	10 <sup>-10</sup> ~10 <sup>0</sup>

Mag. Field at Surface : 0.02[T]

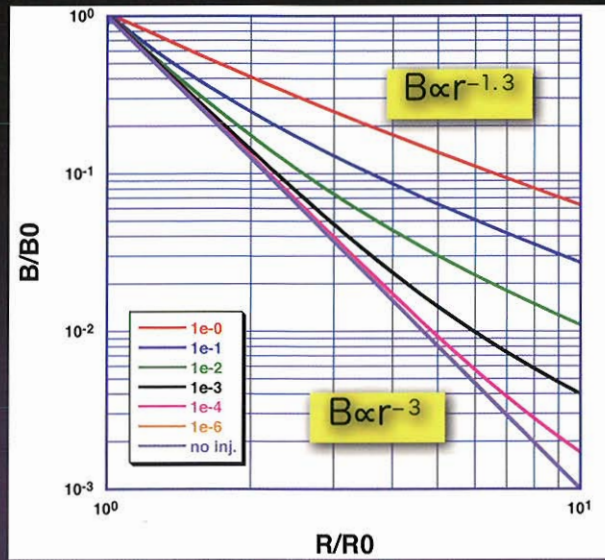
$$\beta = \frac{\text{Dynamic Pressure}}{\text{Mag. Pressure}} = \frac{\frac{1}{2}\rho u^2}{\frac{B^2}{2\mu_0}} \propto \rho$$

Beta value	10 <sup>-10</sup>	~	10 <sup>0</sup>	$\rho$ : Density $u$ : Velocity $B$ : Mag. Field $\mu_0$ : Permeability
Density [m <sup>-3</sup> ]	3.0x10 <sup>10</sup>	~	3.0x10 <sup>20</sup>	
Pressure [Pa]	1.6x10 <sup>-8</sup>	~	1.6x10 <sup>2</sup>	

15

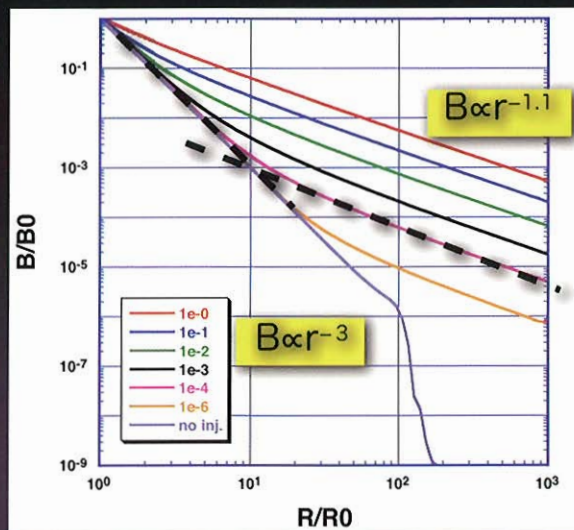


## B-Field Strength near spacecraft



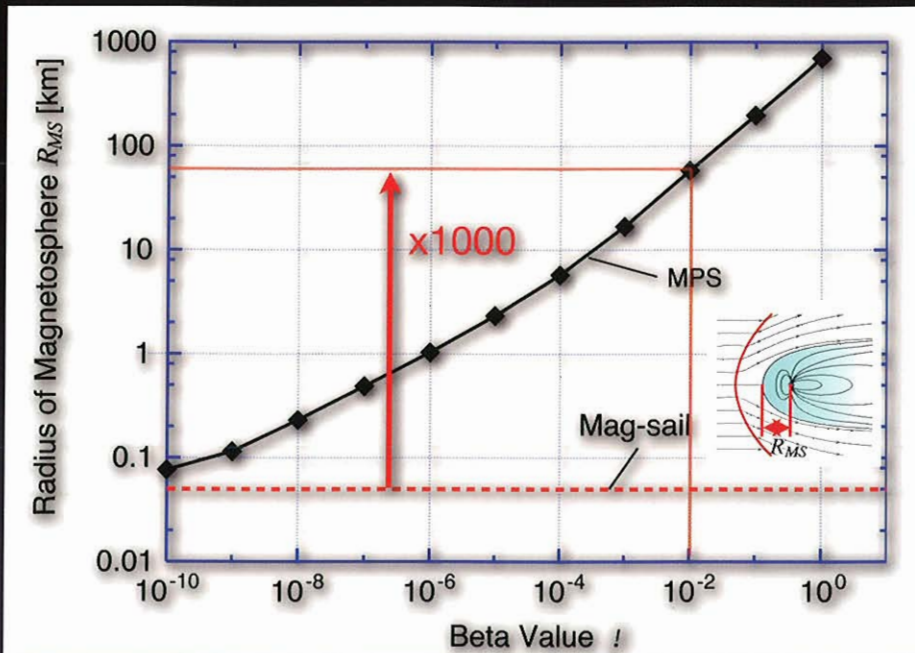
17

## B-Field Strength far from spacecraft



18

## Size of Magnetosphere



19

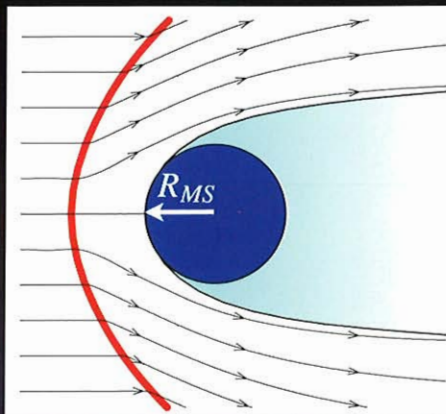
## Thrust Estimation

### Drag to the sphere

$$F = C_D \frac{1}{2} \rho_{sw} u_{sw}^2 S$$

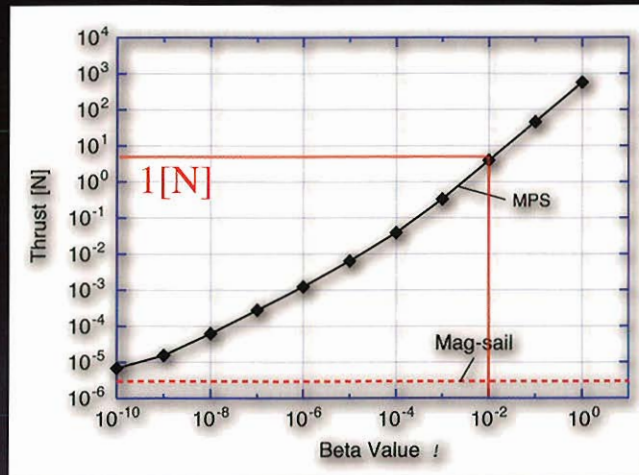
- Drag coefficient for sphere  
 $C_D = 1.0$
- Frontal Area of magnetosphere  
 $S = \pi R_{MS}^2$
- Dynamic pressure of solar wind

$$\frac{1}{2} \rho_{sw} u_{sw}^2 = 0.4 \text{ [nPa]}$$



20

## Thrust and beta value



**Thrust of 1 [N] with  $\beta=10^{-2}$  is achieved**

21

## Summary

3 dimensional MHD simulation for MPS including inflation of the magnetic field by the plasma injection is performed and the thrust of MPS is also estimated.

- Our numerical method was assessed for the case of Mag Sail.
- Magnetosphere can be inflated by the plasma injection
- The size of magnetosphere is dependent on beta value of the injected plasma.
  - ▶ Rms ( $\beta=10^{-2}$  : x1000)
  - ▶ Thrust ( $\beta=10^{-2}$  : 1[N])

22

## Numerical Simulation of Magneto Plasma Sail by using 3D Hybrid Code

Yoshihiro Kajimura, Kenji Noda, Hideki Nakashima

Department of Advanced Energy Engineering Science  
Interdisciplinary Graduate school of Engineering Sciences, Kyushu University, Japan  
[kajimura@aees.kyushu-u.ac.jp](mailto:kajimura@aees.kyushu-u.ac.jp)

We have been studying the Magneto Plasma Sail (MPS) by using 3D hybrid numerical simulation code. There are two key issues of MPS research, one is the possibility of magnetic inflation, and the other is the analysis of the interaction between the solar wind and the artificially generated magnetic field. We simulated the interaction between the solar wind and dipole magnetic field in pure-Magsail and compared with the drag coefficient obtained by using other hybrid code [1]. And we simulated the magnetic inflation by injected plasma. The simulation model is shown in Fig.1. Plasma is injected from the region located in 1.0 [m] from the center of the coil. Plasma is injected in radial direction with  $N=10^{20}[\text{m}^{-3}]$  and  $v=4.0[\text{km/s}]$ . Next we simulated the interaction between the solar wind and inflated magnetic field by the plasma injection. The simulation geometry considered here is illustrated in Figure 2. The initial magnetic field is produced at the center of the system as dipole configuration. The solar wind flows only in the positive Z direction with  $5 \times 10^6 [\text{m}^{-3}]$  density and 400 [km/s] velocity. The Ar plasma with  $5 \times 10^9 [\text{m}^{-3}]$  density and 20 [km/s] velocity is injected isotropically. We will show these simulation results and list up the difficulties of numerical simulation of MPS in each theme. And finally I will make a brief summary and talk about the Future plan.

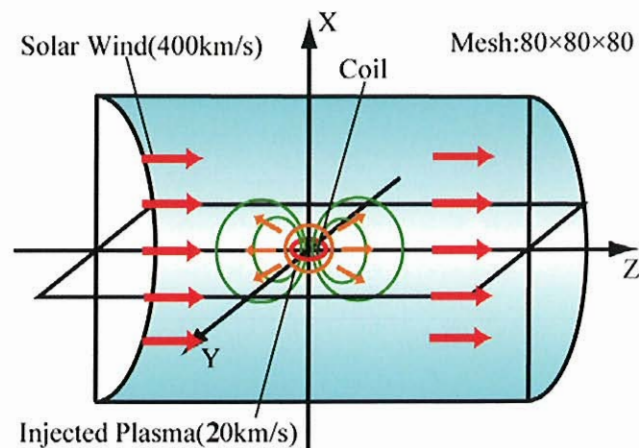
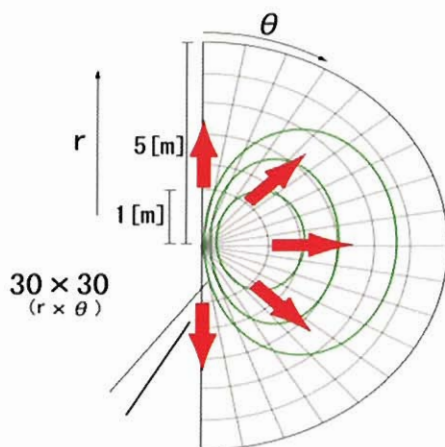


Figure.1 Simulation Model (inflation)      Figure 2. Simulation model (whole simulation)

[1] K. Fujita, "Particle Simulation of Moderately-Sized Magnetic Sails" Journal of Space Technology and Science, Vol.20, No.2, pp.26-31, 2005.



# Numerical Simulation of Magneto Plasma Sail by using 3D hybrid code

JAXA/JEDI Workshop  
Oct 2<sup>nd</sup>–3<sup>rd</sup>, 2006

Yoshihiro Kajimura, Kenji Noda, Hideki Nakashima

Department of Advanced Energy Engineering Science,  
Interdisciplinary Graduate School of Engineering Sciences,  
Kyushu University, Japan



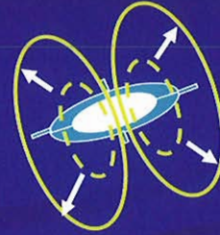
## Outline

- Key theme of MPS research
- Fundamental parameters of MPS
- Our recent simulation results of MPS
- The difficulty of MPS simulation  
(using hybrid code)
- Summary and Future plans

## Key themes of MPS research

### ■ Possibility of magnetic inflation by plasma injection

- $\beta_0 > 1$  , Magnetic Re  $\gg 1$
- How? Where? can we inject plasma for inflation effectively.
- How far? is magnetic field inflated.



### ■ Mechanism of the thrust transformation from the solar wind through the inflated magnetic field.

- Is it possible to inflate the magnetic field in the solar wind?

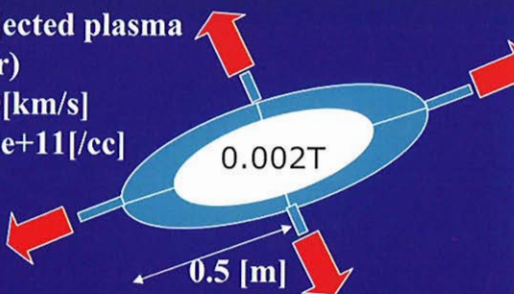


<http://www.ess.washington.edu/Space/M2P2/> by Winglee

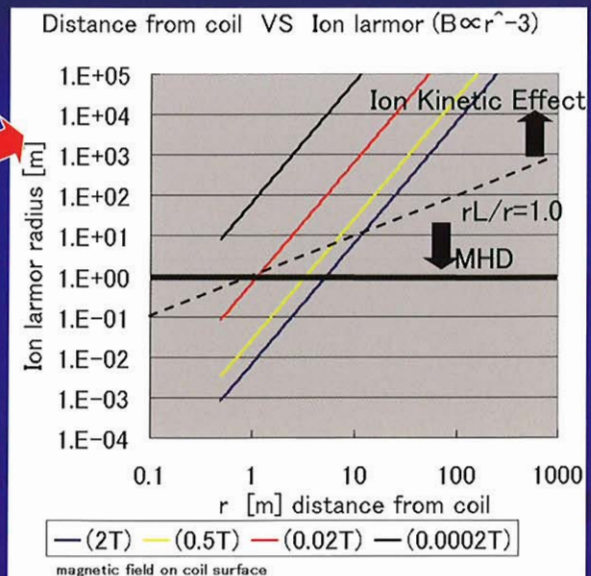
## Fundamental parameters of MPS

### ■ Magnetic inflation

Injected plasma  
(Ar)  
4.0[km/s]  
1.2e11[cc]

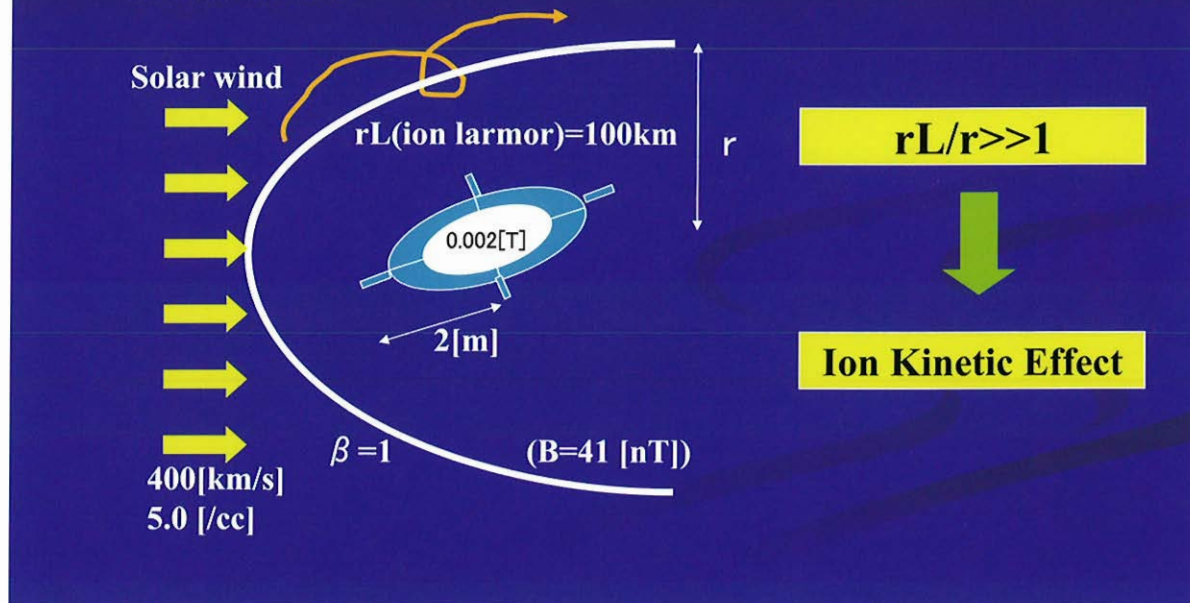


$rL$  (ion larmor) = 1 [m]



## Fundamental parameters of MPS

- Interaction between the magnetic field and solar wind



## General method of numerical simulation for plasma

- MHD
  - Plasma is treated as a fluid
  - The ion kinetic effect is ignored ( $rL \ll L$ )
- Hybrid
  - Ions are treated as particles, electrons as a fluid
  - The ion kinetic effect is taken into account. ( $rL \geq L$ )
- Full particle
  - Ions and electrons are treated as particles
  - The debye length must be used as the mesh size:
  - Injected plasma ( $[0.8 \mu\text{m}]$ )、solar wind ( $[10\text{m}]$ )

**In the MPS study,  
Ion kinetic simulations (hybrid simulation) are required**

## Our 3D Hybrid Code

• Basic equations (e: electron, i: ion)

Ion momentum equation

$$m_i \frac{d\mathbf{v}_i}{dt} = Ze(\mathbf{E} + \mathbf{v}_i \times \mathbf{B}) \quad \frac{d\mathbf{x}_i}{dt} = \mathbf{v}_i$$

Electron momentum equation

$$n_e m_e \frac{d\mathbf{v}_e}{dt} = -en_e(\mathbf{E} + \mathbf{v}_e \times \mathbf{B}) - \nabla P_e$$

Ampere's law

$$\nabla \times \mathbf{B}_p = \mu_0(\mathbf{J}_e + \mathbf{J}_i)$$

Faraday's law

$$\frac{\partial \mathbf{B}}{\partial t} = -\nabla \times \mathbf{E}$$

Current density

$$\mathbf{J}_e = -en_e \mathbf{v}_e, \mathbf{J}_i = en_i \mathbf{v}_i$$

Position of ions  $x_i^{n+1} = x_i^n + \mathbf{v}_i^{n+1/2} \Delta t$

Velocity of ions  $\mathbf{v}_i^{n+1/2} = \mathbf{A}^{-1} \mathbf{S}$

Electric field (Plasma Region)

$$\mathbf{E}^n = \frac{1}{n_i} \left\{ \frac{1}{\mu_0 Z_e} (\nabla \times \mathbf{B}_p^n) \times \mathbf{B}^n - \frac{1}{Ze} \mathbf{J}_i^n \times \mathbf{B}^n - \frac{T_e}{e} \nabla n_i^n \right\}$$

Electric field (vacuum region)

$$\nabla^2 \mathbf{E} = 0$$

CFL condition  $\Delta t < \frac{\Delta x}{V_A}$

Numerical stability condition  $\omega_{ci} \Delta t < 0.2$

Electron energy equation is not used.  
( $T_e = \text{const}$ )

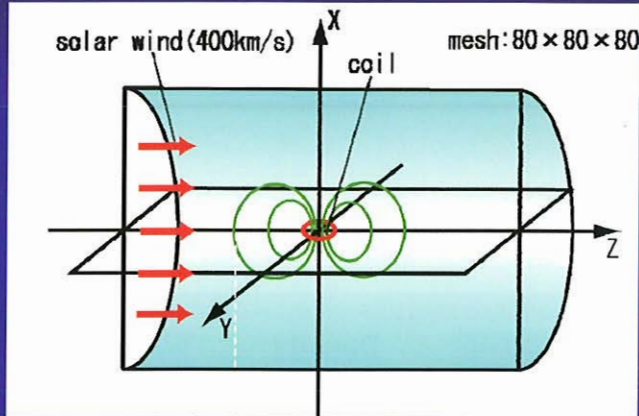
## Our recent study of MPS

- Plasma flow around Pure Magsail
- Magnetic inflation
- Interaction between the inflated magnetic field and solar wind (whole simulation)



1. Brief results
2. Difficulty in each simulation

# Plasma flow around Pure Magsail



Ion : Hydrogen  
 Ion velocity : 400km/s  
 Ion number density :  $5 \times 10^6 \text{m}^{-3}$   
 Super particle number : 2milion  
 In each cell : 15

## Drag coefficient

$$C_d = \frac{F}{\frac{1}{2} \rho V^2 S}$$

F: Thrust [N]  
 (calc from momentum)  
 $\rho$ : density of solar wind  
 V: velocity of the solar wind  
 S: The cross section of the magnetosphere =  $\pi L^2$  [m<sup>2</sup>]

# Simulation Parameters

MHD Region

case	L(m)	$r_L/L$	$\delta / \Delta x$	System Size(m)
1	8.00E+05	0.13	1	4.00E+06
2	4.00E+05	0.25	2	2.00E+06
3	2.00E+05	0.50	4	1.00E+06
4	8.00E+04	1.25	10	4.00E+05
5	4.00E+04	2.50	20	2.00E+05

$\delta$ : Skin depth

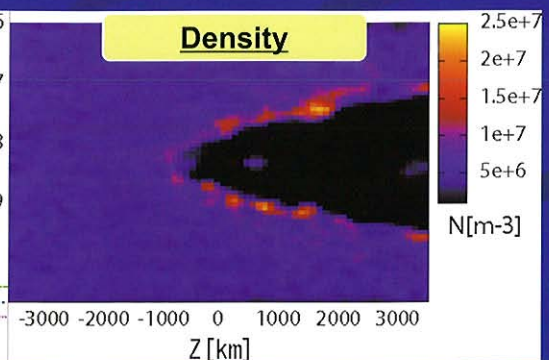
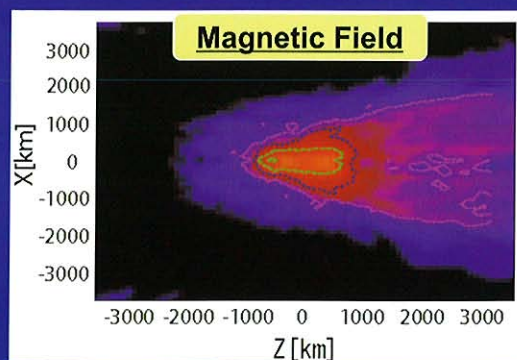
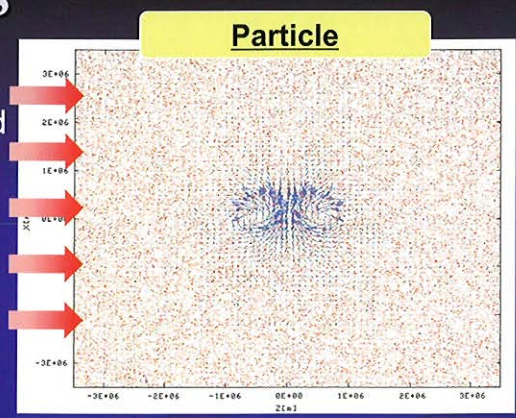
target size of MPS

Non MHD Region

# CASE1 : Results

$L=800\text{km}$   $r_L/L=0.13$

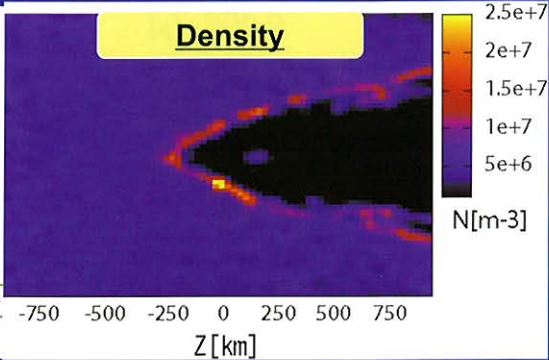
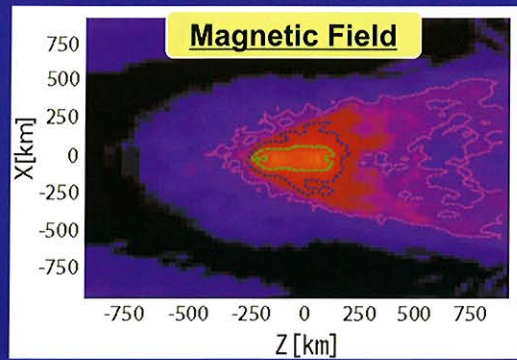
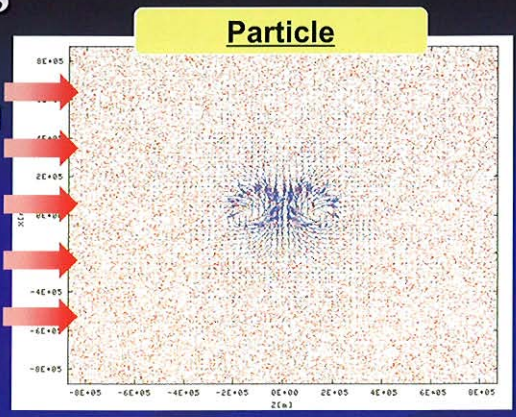
Solar Wind



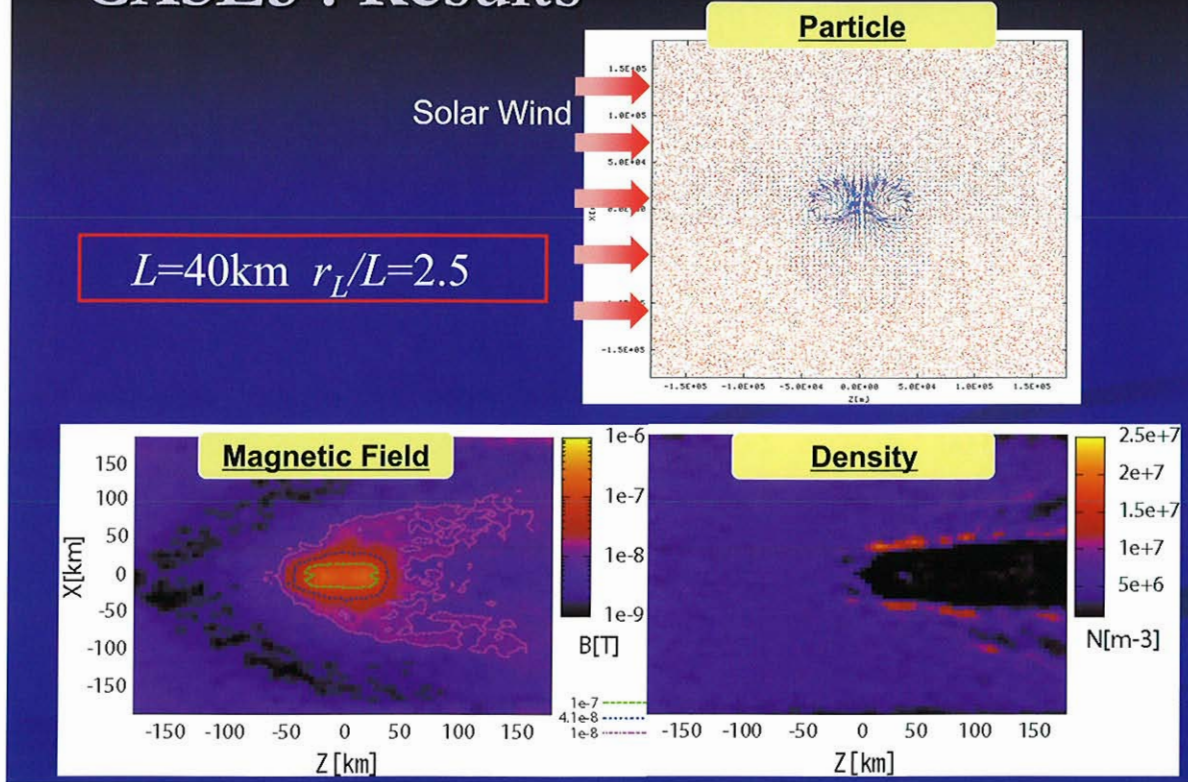
# CASE3 : Results

$L=200\text{km}$   $r_L/L=0.5$

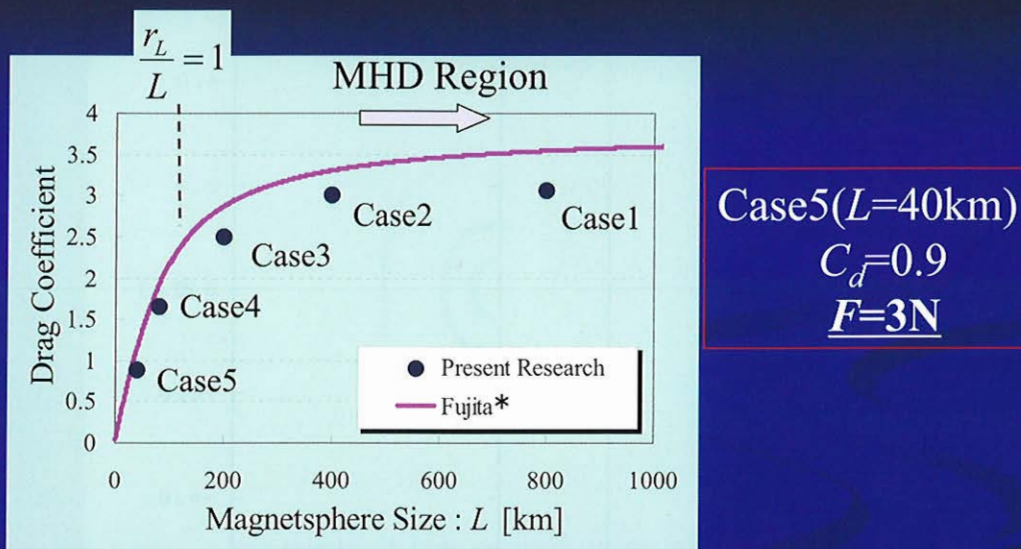
Solar Wind



# CASE5 : Results



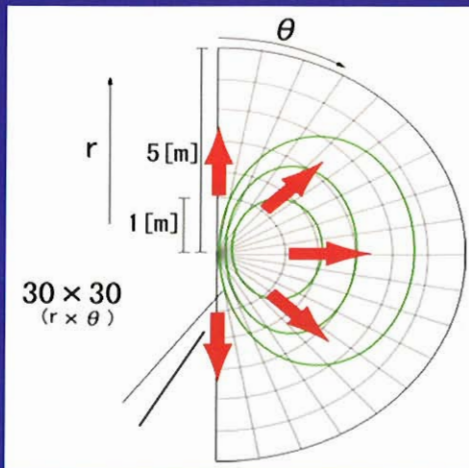
# Drag coefficient in each cases



\*Fujita, K., "Particle Simulation of Moderately-Sized Magnetic Sails,"  
 Journal of Space Technology and Science, Vol.20, No.2, pp.26-31, (2005).

## Magnetic inflation

### ■ 2D spherical coordinates grid



Injected Plasma : Ar

$$N_{in} = 3.0 \times 10^{20} \text{ [m}^{-3}\text{]}$$

$$v_{in} = 4.0 \times 10^3 \text{ [m/s]}$$

$$T_i = 0.5 \text{ [eV]}$$

$$T_e = 4.0 \text{ [eV]}$$

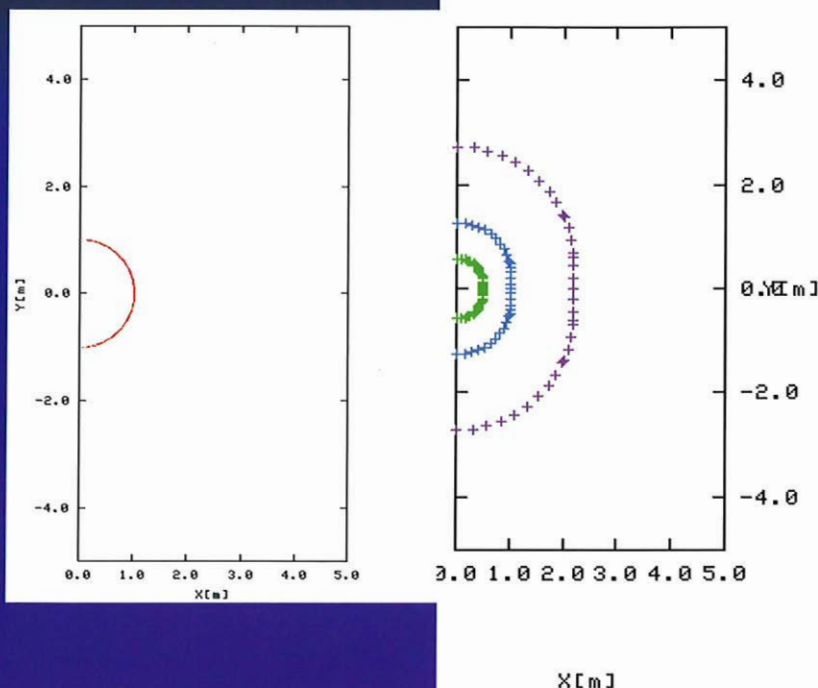
$$B_{r=rp} = 0.02 \text{ [T]}$$

$$R_{r=rp} = 0.084 \text{ [m]}$$

$$\beta_{in} = 1$$

## Magnetic inflation

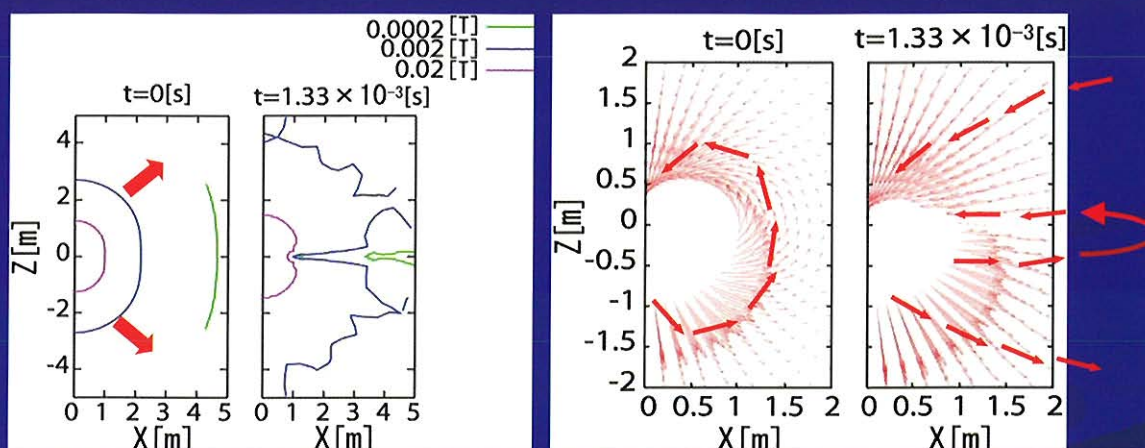
### ■ Simulation results





## Magnetic inflation

### ■ Simulation results



Compared with the original dipole magnetic field of  $B \propto r^{-3}$  ( $\theta = 0$ ) after the plasma injected, it gradually decreases at a rate of  $B \propto r^{-2.1}$ .

## Difficulty of simulation (Inflation)

- We need to perform simulations in a larger region as we want to confirm how far the magnetic field is inflated.
- However, in such large field, density of plasma will be low and calculations by using hybrid code will be more difficult.
  - This is because in our hybrid code, the plasma region and vacuum region are clearly separated and in each region. The calculation method of the electric field is quite different. In the vacuum region, the Laplace's Equation is used.

# Our 3D Hybrid Code

• Basic equations (e: electron, i: ion)

**Ion momentum equation**

$$m_i \frac{dv_i}{dt} = Ze(\mathbf{E} + \mathbf{v}_i \times \mathbf{B}) \quad \frac{dx_i}{dt} = \mathbf{v}_i$$

**Electron momentum equation**

$$n_e m_e \frac{dv_e}{dt} = -en_e(\mathbf{E} + \mathbf{v}_e \times \mathbf{B}) - \nabla P_e$$

**Ampere's law**

$$\nabla \times \mathbf{B}_p = \mu_0(\mathbf{J}_e + \mathbf{J}_i)$$

**Faraday's law**

$$\frac{\partial \mathbf{B}}{\partial t} = -\nabla \times \mathbf{E}$$

**Current density**

$$\mathbf{J}_e = -en_e \mathbf{v}_e, \mathbf{J}_i = en_i \mathbf{v}_i$$

**Position of ions**  $x_i^{n+1} = x_i^n + \mathbf{v}_i^{n+1/2} \Delta t$

**Velocity of ions**  $\mathbf{v}_i^{n+1/2} = \mathbf{A}^{-1} \mathbf{S}$

**Electric field (Plasma Region)**

$$\mathbf{E}^n = \frac{1}{n_i} \left\{ \frac{1}{\mu_0 Z_e} (\nabla \times \mathbf{B}_p^n) \times \mathbf{B}^n - \frac{1}{Ze} \mathbf{J}_i^n \times \mathbf{B}^n - \frac{T_e}{e} \nabla n_i^n \right\}$$

**Electric field (vacuum region)**

$$\nabla^2 \mathbf{E} = 0$$

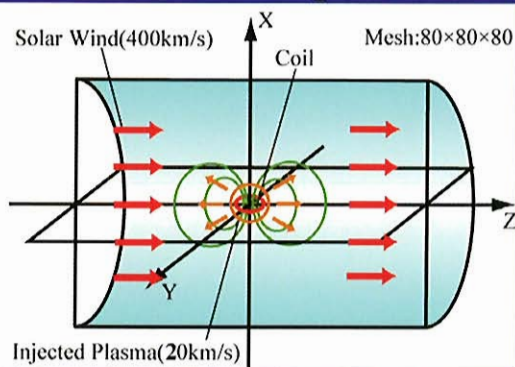
**CFL condition**  $\Delta t < \frac{\Delta x}{V_A}$

**Numerical stability condition**  $\omega_{ci} \Delta t < 0.2$

**Electron energy equation is not used.**  
( $T_e = \text{const}$ )

# Whole simulation

- Simulation model
- Simulation parameters

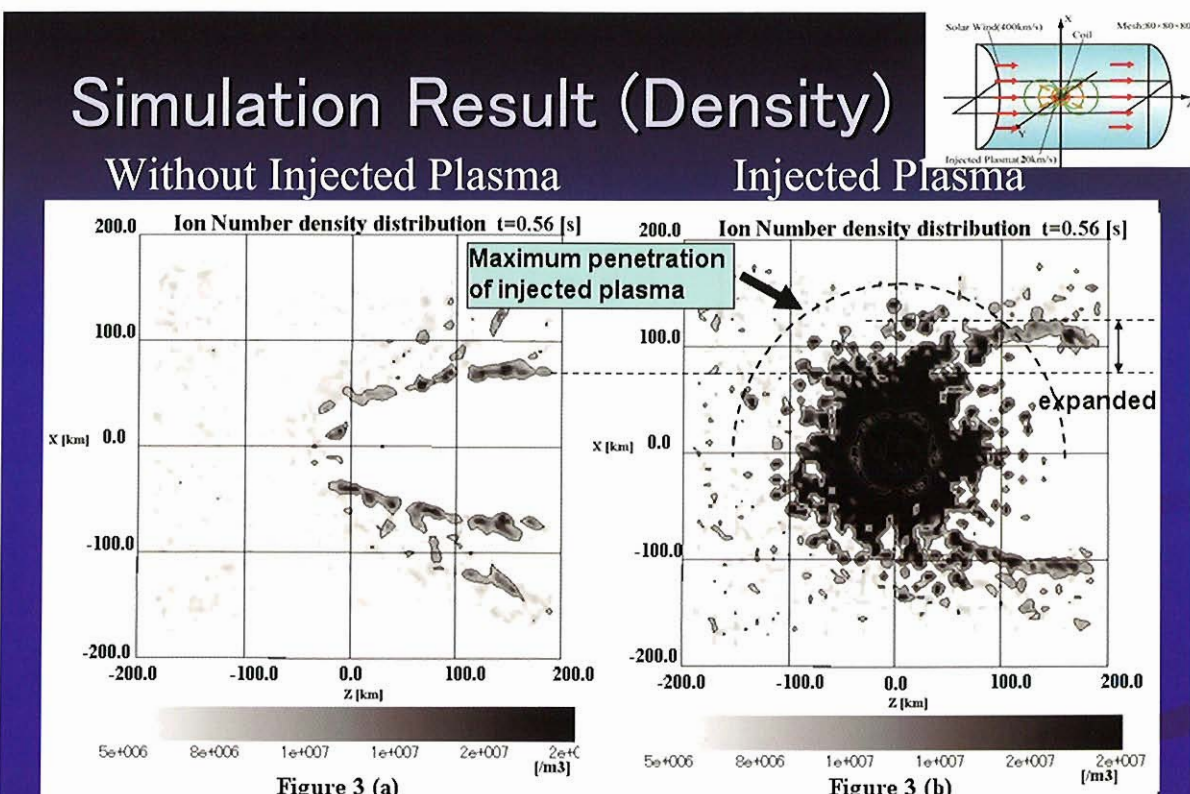
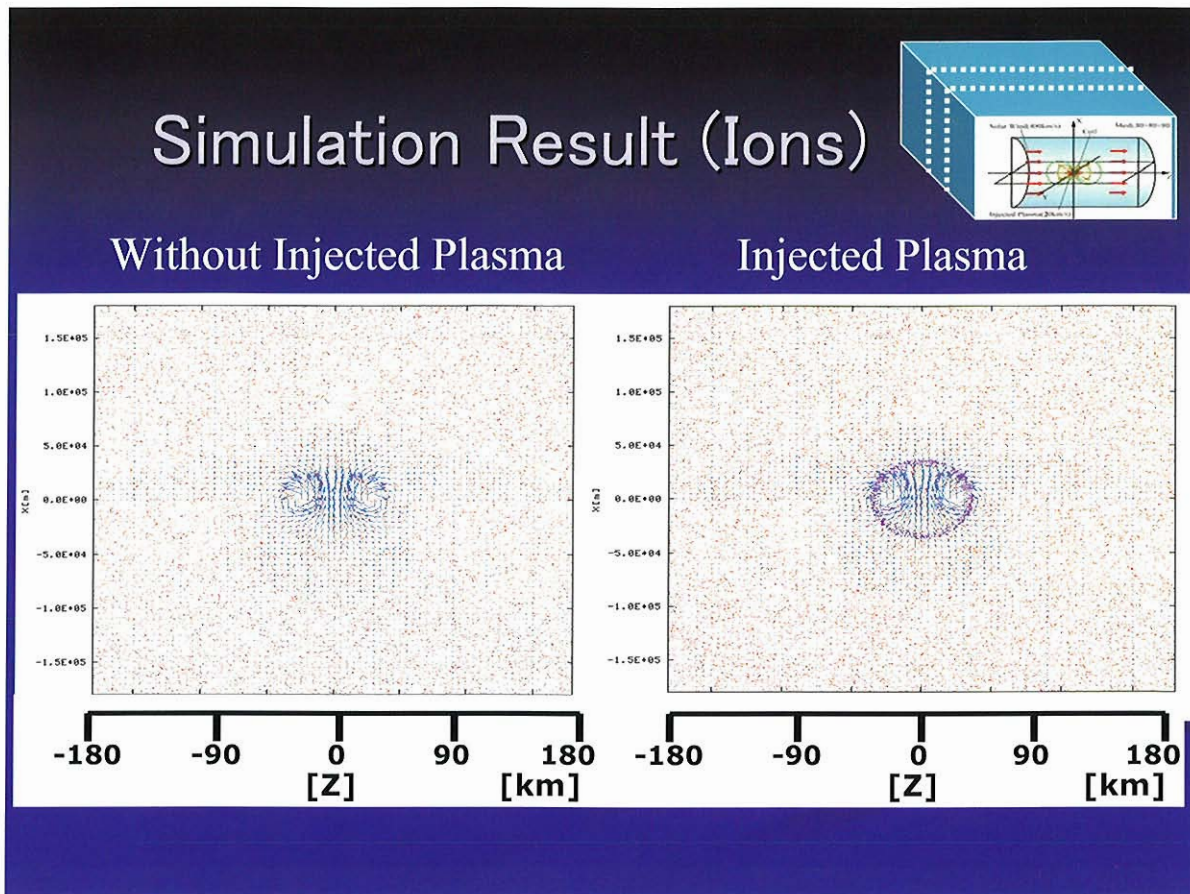


**$rL(\text{solar wind})/L \gg 1$**

**Injected Plasma  $\beta = 1.0$**

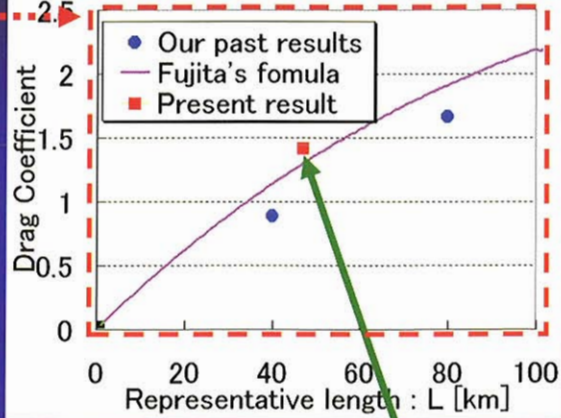
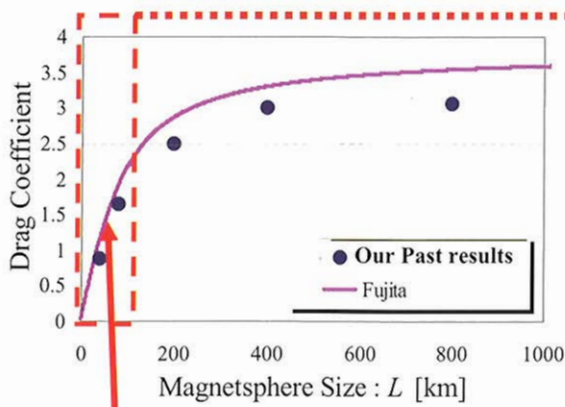
**$rL(\text{Injected Plasma})/L \sim 1.0$**

- Ions (solar Wind) : hydrogen
- Ions (Injected Plasma) : Ar
- Mesh numbers :  $80 \times 80 \times 80$
- Mesh size [km] :  $\Delta x = 5$
- Delta T [s] :  $\Delta t = 1.2 \times 10^{-5}$   
(near the coil)  $(0.2 \omega_{ci}^{-1} t)$
- \*  $\omega_{ci}$  : ion cyclotron frequency
- Time steps : 50,000
- Time : 0.6 [s]
- Particle number : 3,000,000
- In each cell : 6



The magnetosphere size of injected plasma is about two times larger than the case of without injected plasma.

## Thrust Estimation (Without Injected Plasma)



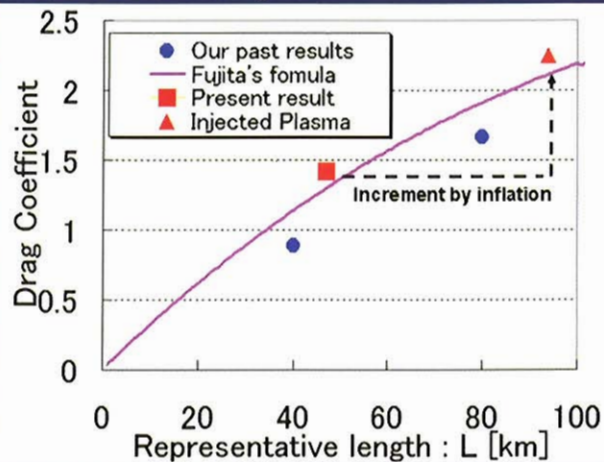
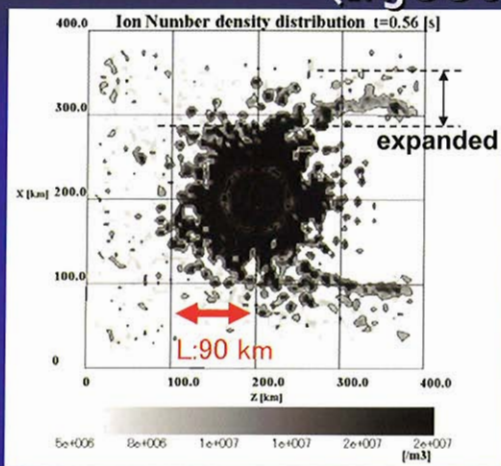
$$C_d = \frac{3.4}{R_L} \exp\left(-\frac{0.22}{R_L^2}\right)$$

$$R_L \geq 1 : R_L = rL1 / L$$

The magnetosphere size of without injected plasma is 45 km. And calculated drag coefficient is 1.4. This is good agreement with the formula derived from Fujita.

Fujita, K., "Particle Simulation of Moderately-Sized Magnetic Sails," Journal of Space Technology and Science, Vol.20, No.2, pp.26-31, (2005).

## Thrust Estimation (Injected Plasma)



The magnetosphere size with injected plasma is about twice the size than without injected plasma.

The magnetosphere size with Injected plasma is around 90 km.

The calculated drag coefficient obtained from the simulation is 2.3.

This also agrees with the results from Fujita's formula.

## Discussion

- We had not been sure whether if MPS could really obtain the thrust through the interaction between the inflated magnetic field and solar wind.
- In this whole simulation, we confirmed that MPS could obtain the thrust from inflated magnetic field, and this thrust value also can be calculated by the Fujita's formula.
- We need to resolve the issue :how large can MPS inflate the magnetic field in the solar wind.

## Difficulty of simulation (whole simulation)

- Coil radius ( $\sim$ m) and required magnetosphere ( $\sim$ km), so we have to treat the very wide region.
  - Density 5[/cc] (solar wind) and  $10^{14}$ [/cc] (injected plasma), so we have to treat the ions which have a big differences of density. (it needs some techniques)
  - Velocity 400 [km/s] (solar wind) and 4 [km/s] (injected plasma) so we have to treat the ions which have a big differences of velocity. (small delta T)
- We need huge cost for simulation.....

## Future Plan

- If we try to simulate under the actual scaling parameters, we have to use a much smaller mesh and time steps. It is necessary to develop a code suitable for parallel processing.
- Furthermore, in order to use a mesh variable in size of kilometers rather than meters, we are now developing code using spherical polar coordinates for whole simulation.

END

宇宙航空研究開発機構特別資料 JAXA-SP-06-014

---

発行 平成 19 年 2 月 1 日

編集・発行 宇宙航空研究開発機構

〒182-8522 東京都調布市深大寺東町 7-44-1

URL : <http://www.jaxa.jp/>

印刷・製本 (有) ノースアイランド

---

本書及び内容についてのお問い合わせは、下記にお願いいたします。

宇宙航空研究開発機構 情報システム部 研究開発情報センター

〒305-8505 茨城県つくば市千現 2-1-1

TEL : 029-868-2079 FAX : 029-868-2956

---

© 2007 宇宙航空研究開発機構

※ 本書の一部または全部を無断複写・転載・電子媒体等に加工することを禁じます。

